

년
월

석
박
사
학
위
논
문

2013년 8월
석사학위 논문

A study on the development of energy saving device for the twin screw car ferry

2축 프로펠러를 가진 57m급
차도선의 연료절감 부가물 개발에 관한 연구

성
명

조선대학교 대학원

선박해양공학과

임연지

A study on the development
of energy saving device
for the twin screw car ferry

2축 프로펠러를 가진 57m급
차도선의 연료절감 부가물 개발에 관한 연구

2013년 8월 23일

조선대학교 대학원

선박해양공학과

임연지

A study on the development of energy saving device for the twin screw car ferry

2축 프로펠러를 가진 57m급
차도선의 연료절감 부가물 개발에 관한 연구

지도교수 이 귀 주

이 논문을 석사학위신청 논문으로 제출함

2013년 4월

조선대학교 대학원

선박해양공학과

임 연 지

임연지의 석사학위논문을 인준함

위원장	Chalmers 대학교 교수	<u>Carl-Erik Janson(인)</u>
위원	조선대학교 교수	<u>이 귀 주 (인)</u>
위원	FlowTech 연구소 소장	<u>Leif Broberg (인)</u>

2013년 5 월

조선대학교 대학원

Contents

List of Tables

List of Figures

ABSTRACT

I. Introduction

II. Design of Hull form and Appendages

III. Development of Energy Saving Device

IV. Theoretical Calculation

A. FLOWSOLVERS

B. Potential flow solver

1. Boundary layer method

2. RANS solver

C. MODELLING OF THE PROPELLER

D. validation

1. Resistance Calculation Result

2. Self Propulsion Calculation Result

V. Model Test

A. Test facility

B. Hull model

C. Propeller model

D. Extrapolation by ITTC78 and modified ITTC78
method

E. Result of model test

VI. Check the seakeeping performance

References

Contents

List of Tables	III
List of Figures	IV
ABSTRACT	1
I. Introduction.....	2
II. Design of Hull form and Appendages ...	3
III. Development of Energy Saving Device ..	7
IV. Theoretical Calculation.....	11
A. FLOWSOLVERS	12
B. Potentialflowsolver	12
1.Boundarylayermethod.....	13
2.RANSsolver.....	13
C.MODELLINGOFTHEPROPELLER	
D.validation	13
1. Resistance Calculation Result.....	14
2. Self Propulsion Calculation Result.....	15

V. Model Test	41
A. Test facility	41
B. Hull model	42
C. Propeller model	42
D. Extrapolation by ITTC78 and modified ITTC78 method	44
E. Result of model test	45
VI. Check the seakeeping performance	51
VII. Conclusions	72
References	73

List of Tables

Table 2-1	Main dimension of ship·····	3
Table 3-1	The config of energy saving device·····	9
Table 4-1	Comparison of resistance components·····	14
Table 4-2	Comparison of propulsion coefficient·····	15
Table 5-1	Main dimension of ship and model·····	42
Table 5-2	Main characteristics model propeller·····	43
Table 5-3	Comparison of the results of self-propulsion tests·····	46
Table 6-1	Dimension of ship·····	53
Table 6-2	Input of RAO-response·····	55

List of Figures

Fig. 2-1	Lines of car ferry·····	4
Fig. 2-2	modeling of Hull ·····	4
Fig. 2-3	3D model of Bracket Fin1(BF1)·····	5
Fig. 2-4	3D model of Bracket Fin2(BF2)·····	5
Fig. 2-5	3D model of Bracket Fin1+Long stator(BF1+LS)·····	6
Fig. 2-6	3D model of Long stator(LS)·····	6
Fig. 3-1	Pre-swirl stator·····	7
Fig. 3-2	Strut Fin·····	8
Fig. 4-1	Four Different Configuration of Energy Saving Device·····	12
Fig. 4-2	Resistance components vs F_n ·····	14
Fig. 4-3	F_n vs propulsion coefficients·····	15
Fig. 4-4(a)	Comparison of potential flow streamlines (Bare Hull, side bow view)·····	16
Fig. 4-4(b)	Comparison of potential flow streamlines (BF1, side bow view)·····	16
Fig. 4-4(c)	Comparison of potential flow streamlines (BF2, side bow view)·····	16
Fig. 4-4(d)	Comparison of potential flow streamlines (BF1+LS, side bow view)·····	17
Fig. 4-4(e)	Comparison of potential flow streamlines (LS, side bow view···	17
Fig. 4-5(a)	Comparison of Stream line(Bare Hull, bottom stern view)·····	17
Fig. 4-5(b)	Comparison of Stream line(BF1, bottom stern view)·····	18
Fig. 4-5(c)	Comparison of Stream line(BF2, bottom stern view)·····	18
Fig. 4-5(d)	Comparison of Stream line(BF1+LS, bottom stern view)·····	18
Fig. 4-5(e)	Comparison of Stream line(LS, bottom stern view)·····	19
Fig. 4-6(a)	Comparison of Stream line(Bare Hull, persp. stern view)·····	19
Fig. 4-6(b)	Comparison of Stream line(BF1, persp. stern view)·····	19
Fig. 4-6(c)	Comparison of Stream line(BF2, persp. stern view)·····	20

Fig. 4-6(d) Comparison of Stream line(BF1+LS, persp. stern view)·····	20
Fig. 4-6(e) Comparison of Stream line(LS, persp. stern view)·····	20
Fig. 4-7(a) Stern flow direction(Bare Hull, stern view)·····	21
Fig. 4-7(b) Stern flow direction(BF1, stern view)·····	21
Fig. 4-7(c) Stern flow direction(BF2, stern view)·····	21
Fig. 4-7(d) Stern flow direction(BF1+LS, stern view)·····	22
Fig. 4-7(e) Stern flow direction(LS, stern view)·····	22
Fig. 4-8(a) Comparison of the V_R / V_O (Bare Hull)·····	22
Fig. 4-8(b) Comparison of the V_R / V_O (BF1)·····	23
Fig. 4-8(c) Comparison of the V_R / V_O (BF2)·····	23
Fig. 4-8(d) Comparison of the V_R / V_O (BF1+LS)·····	23
Fig. 4-8(e) Comparison of the V_R / V_O (LS)·····	24
Fig. 4-9(a) Comparison of the V_T / V_O (Bare Hull)·····	24
Fig. 4-9(b) Comparison of the V_T / V_O (BF1)·····	24
Fig. 4-9(c) Comparison of the V_T / V_O (BF2)·····	25
Fig. 4-9(d) Comparison of the V_T / V_O (BF1+LS)·····	25
Fig. 4-9(e) Comparison of the V_T / V_O (LS)·····	25
Fig. 4-10(a) Comparison of the V_{TR} / V_O (Bare Hull)·····	26
Fig. 4-10(b) Comparison of the V_{TR} / V_O (BF1)·····	26
Fig. 4-10(c) Comparison of the V_{TR} / V_O (BF2)·····	26
Fig. 4-10(d) Comparison of the V_{TR} / V_O (BF1+LS)·····	27
Fig. 4-10(e) Comparison of the V_{TR} / V_O (LS)·····	27
Fig. 4-11(a) Comparison of the wakefraction (Bare Hull)·····	27
Fig. 4-11(b) Comparison of the wakefraction (BF1)·····	28
Fig. 4-11(c) Comparison of the wakefraction (BF2)·····	28
Fig. 4-11(d) Comparison of the wakefraction (BF1+LS)·····	28
Fig. 4-11(e) Comparison of the wakefraction (LS)·····	29
Fig. 4-12(a) Comparison of the vtr (Bare Hull)·····	29

Fig. 4-12(b) Comparison of the vtr (BF1)·····	29
Fig. 4-12(c) Comparison of the vtr (BF2)·····	30
Fig. 4-12(d) Comparison of the vtr (BF1+LS)·····	30
Fig. 4-12(e) Comparison of the vtr (LS)·····	30
Fig. 4-13(a) Comparison of the wake (Bare Hull)·····	31
Fig. 4-13(b) Comparison of the wake (BF1)·····	31
Fig. 4-13(c) Comparison of the wake (BF2)·····	31
Fig. 4-13(d) Comparison of the wake (BF1+LS)·····	32
Fig. 4-13(e) Comparison of the wake (LS)·····	32
Fig. 4-14(a) Comparison of Wake in $U_{x=3}$ (Bare Hull)·····	32
Fig. 4-14(b) Comparison of Wake in $U_{x=3}$ (BF1)·····	33
Fig. 4-14(c) Comparison of Wake in $U_{x=3}$ (BF2)·····	33
Fig. 4-14(d) Comparison of Wake in $U_{x=3}$ (BF1+LS)·····	33
Fig. 4-14(e) Comparison of Wake in $U_{x=3}$ (LS)·····	34
Fig. 4-15(a) Comparison of Wake in $U_{x=4}$ (Bare Hull)·····	34
Fig. 4-15(b) Comparison of Wake in $U_{x=4}$ (BF1)·····	34
Fig. 4-15(c) Comparison of Wake in $U_{x=4}$ (BF2)·····	35
Fig. 4-15(d) Comparison of Wake in $U_{x=4}$ (BF1+LS)·····	35
Fig. 4-15(e) Comparison of Wake in $U_{x=4}$ (LS)·····	35
Fig. 4-16(a) Comparison of Wake in $U_{x=5}$ (Bare Hull)·····	36
Fig. 4-16(b) Comparison of Wake in $U_{x=5}$ (BF1)·····	36
Fig. 4-16(c) Comparison of Wake in $U_{x=5}$ (BF2)·····	36
Fig. 4-16(d) Comparison of Wake in $U_{x=5}$ (BF1+LS)·····	37
Fig. 4-16(e) Comparison of Wake in $U_{x=5}$ (LS)·····	37
Fig. 5-1 Photo of Towing Tank of Hiroshima Univ.·····	38
Fig. 5-2 Hull model·····	39
Fig. 5-3 Propeller model·····	40
Fig. 5-4 Photographs of mdel test·····	43

Fig. 5-5	Calibration of rps vs F_n	43
Fig. 5-6	Model wake(w_m) vs for with and without BF1.....	44
Fig. 5-7	t_m vs F_n for Without BF1 and With BF1	44
Fig. 5-8	η_r vs F_n for Without BF1 and With BF1 condition.....	44
Fig. 5-9	1-t vs F_n for Without BF1 and With BF1 condition.....	45
Fig. 5-10	1-w vs F_n for Without BF1 and With BF1 condition.....	45
Fig. 5-11	η_H vs F_n for Without BF1 and With BF1 condition.....	45
Fig. 5-12	η_o vs F_n for Without BF1 and With BF1 condition.....	46
Fig. 5-13	η_D vs F_n for Without BF1 and With BF1 condition.....	46
Fig. 5-14	η_r vs F_n for Without BF2 and With BF2 condition.....	46
Fig. 5-15	1-t vs F_n for Without BF2 and With BF2 condition.....	47
Fig. 5-16	1-w vs F_n for Without BF2 and With BF2 condition.....	47
Fig. 6-1	Calculation result of Loading Condition.....	50
Fig. 6-2	Matrixes of ship.....	51
Fig. 6-3	Calculated RAO.....	53
Fig. 6-4	Sea condition.....	59
Fig. 6-5	Motion of ship.....	63

ABSTRACT

A study on the development of energy saving device for the twin screw car ferry

Lim, Yeon Ji

Advisor : Prof. Lee Kwi-joo, Ph.D.

Department of Naval Architecture

& Ocean Engineering,

Graduate School of Chosun University

본 논문에서는 스트럿으로 지지된 2축 프로펠러를 가진 57m급 차도선의 연료절감 부가물개발에 관한 결과를 다루었다. 본 차도선은 실제 운항 중인 선박이며 이의 선미부 스트럿에 새로운 Pre-swirl타입의 새로운 연료절감 부가물인 BF1, BF2, BF1+LS, LS의 형상을 좌현과 우현에 대칭으로 부착하여 프로펠러 회전방향으로 인해 비효율적으로 흐르는 유동을 통제하는 역할을 하게 하였다. 이는 기존의 Pre-swirl Stator와 비교했을 때 프로펠러 반경의 반절길이의 수평 Fin과 부착하는 Fin의 수를 줄여 선미 부의 하중을 감소 시킬 것이며 제작비용이 절감되고 유지보수가 용이할 것으로 예상된다. 서로 다른 형태의 네 가지 다른 디자인은 쉽플로우를 이용한 CFD이론계산에 의해 질적 분석이 수행되었고 그 중 두 가지 경우에 대하여 예인수조에서의 모형시험이 수행되었다. 선미부에 부착 된 Fin은 프로펠러에 흐름을 유도하고 wake peak를 감소하여 프로펠러면에서의 wake를 균일하게 유도하였다. 한 방향으로만 회전하는 프로펠러로 인해 좌현과 우현의 수행이 다르게 되고 비대칭 압력분포는 선체에 악영향을 미치게 되나 후류 패턴을 바꾸어 프로펠러와 선미사이의 손실 에너지를 감소시키는 역할을 하게 하였다. 기존의 stator와 비교하여 짧은 길이의 Fin으로 기존의 것과 같은 효과를 나타낼 수 있으며 예인수조시험 결과는 계획속도의 만재상태에서 2%의 동력을 얻을 수 있다는 결론을 얻었다.

I. Introduction

Recently the whole world is working for environmental protection and energy saving. The world has been implemented the Kyoto Protocol 2008 to 2012. Although Korea excluded from the Kyoto Protocol since 1990 according to the Economic growth increase in greenhouse gas emissions were more than twice. As a result, Korea was implemented until 2020 Green Growth law and Korea's greenhouse gas reduction target is 4% as contrast in 2005.

International Maritime Organization were discussed ship fuel regulations on 22 March 2010. According to the Fuel economy regulations (EEDI, Energy Design Index) a new technology of vessels will lead to a new eco-friendly technology. Ship operation causes many kinds of environmental pollution. International Maritime Organization (IMO) has strengthened the regulation according to environmental pollution from vessels. Eco-friendly technology, ship design, various new technologies for the reduction of fuel should be investigated aggressively.

The more energy it consumes and energy saving technologies are essential for developments of green ships. Solution to this problem is, in the early stage, to design a hull form having not only the minimum resistance but also the optimum propulsive efficiency. However, the hull forms of general ships bear long term experience of operations which is not expected to be improved radically. Thus, it is considered more appropriate to attach energy saving devices rather than to improve the hull form directly. In this thesis, appendages attached a ship has been studied. Through model tests in the towing tank, the conditions are sought in which the appendages can reduce the ship resistance. The effects of the appendages upon the wake distributions at a propeller plane are also investigated to clarify the effectiveness of them on the equalizations of the distributions, which are closely related to the ship propulsive efficiencies. It is found that appendage attached vertically to the ship stern can accelerate flow in the region, resulting equalization of the wake distribution. The results of CFD have been compared with the

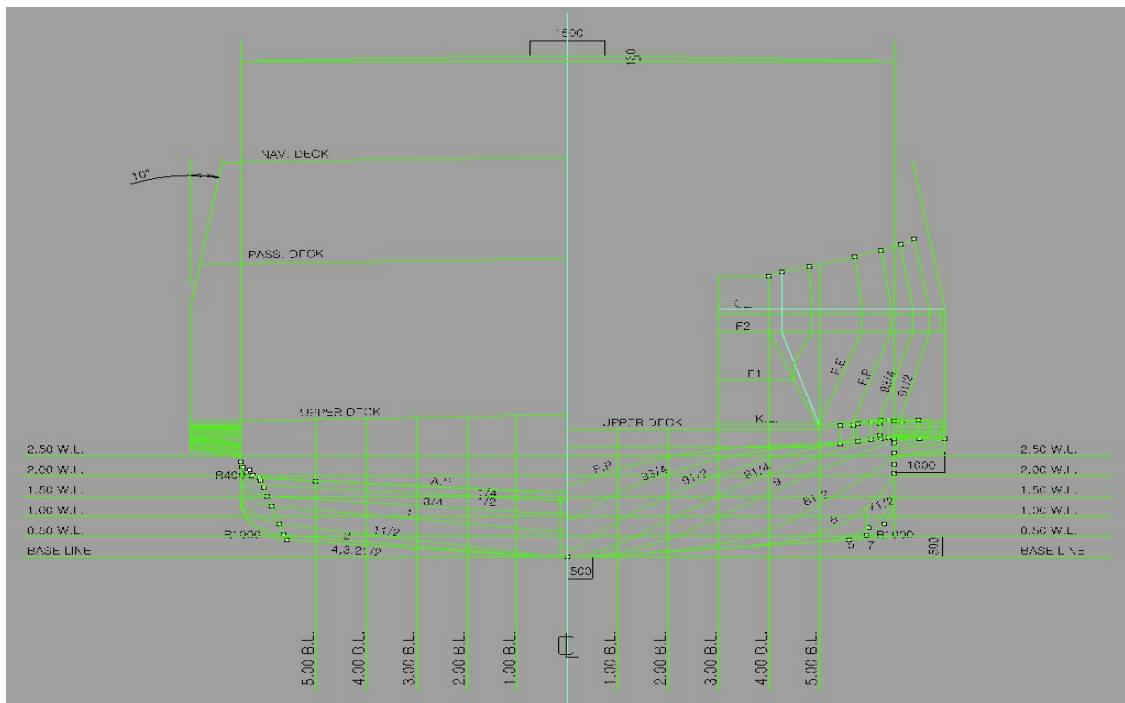
experimental results, to validate the efficiency of appendage. To apply the results developed to ship design, effects to the resistance characteristics and propulsive performances of the ship should be carefully investigated. Furthermore, the developed tools from each specific projects should be closely linked, verified and enhanced, if to be applicable practically.

II. Design of Hull form and Appendages

The main Particulars of ship which has been used in this thesis is shown in Table 2-1

Table 2-1 Main dimension of ship

	Ship
Length between perpendiculars	57m
Length at load water line	60.23m
Breadth	13m
Depth	2.9m
Design Draft	1.8m



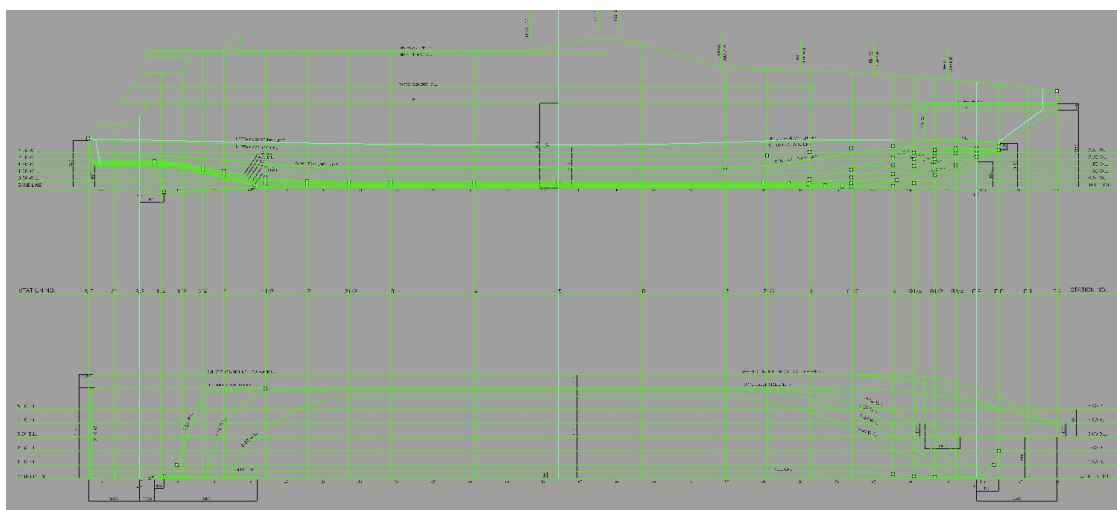


Fig. 2-1 Lines of car ferry

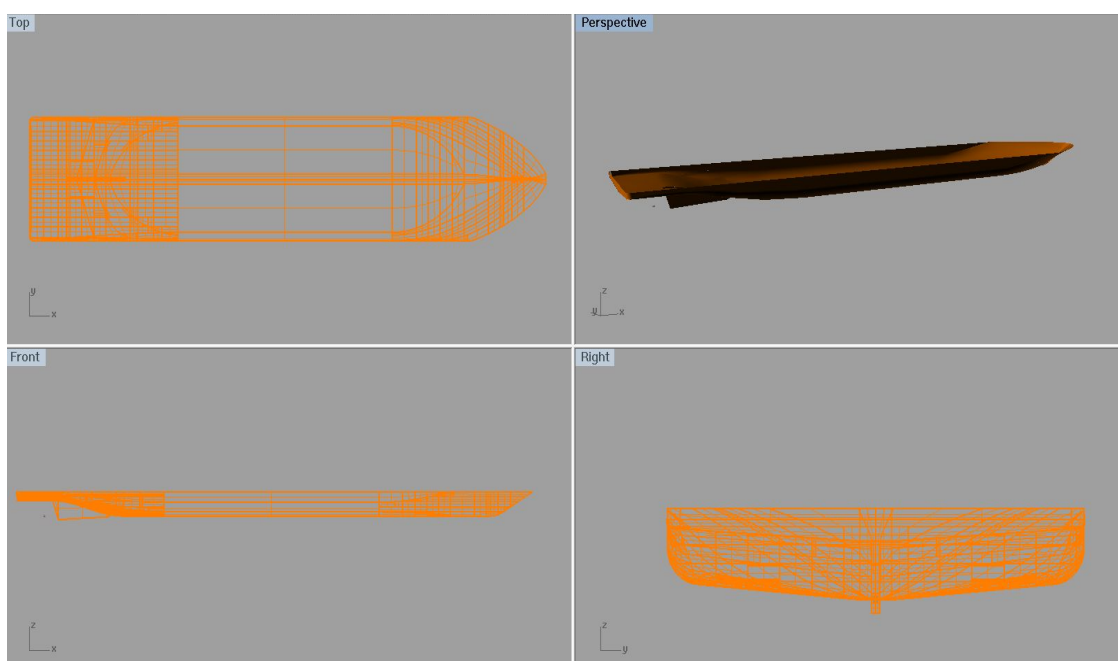


Fig. 2-2 modeling of Hull

BF1 has been attached on the right side of the Y-shaped strut with a 650mm length of the plate, 450 * 200mm size, with a 100° angle from the central axis of the shaft of the stator is attached. 3D design are confirmed in Fig. 2-3~2-6

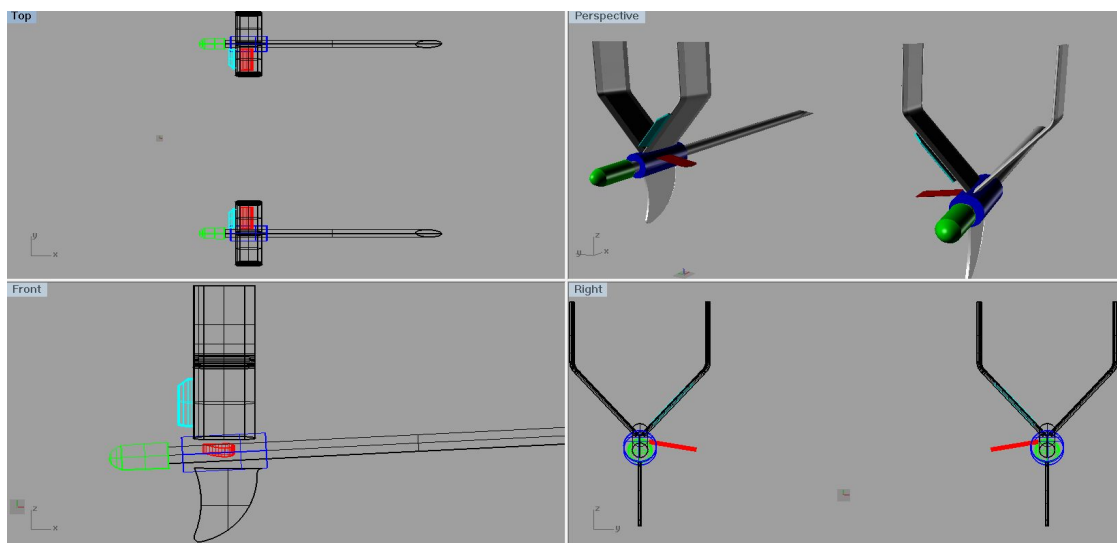


Fig. 2-3 3D model of Bracket Fin1(BF1)

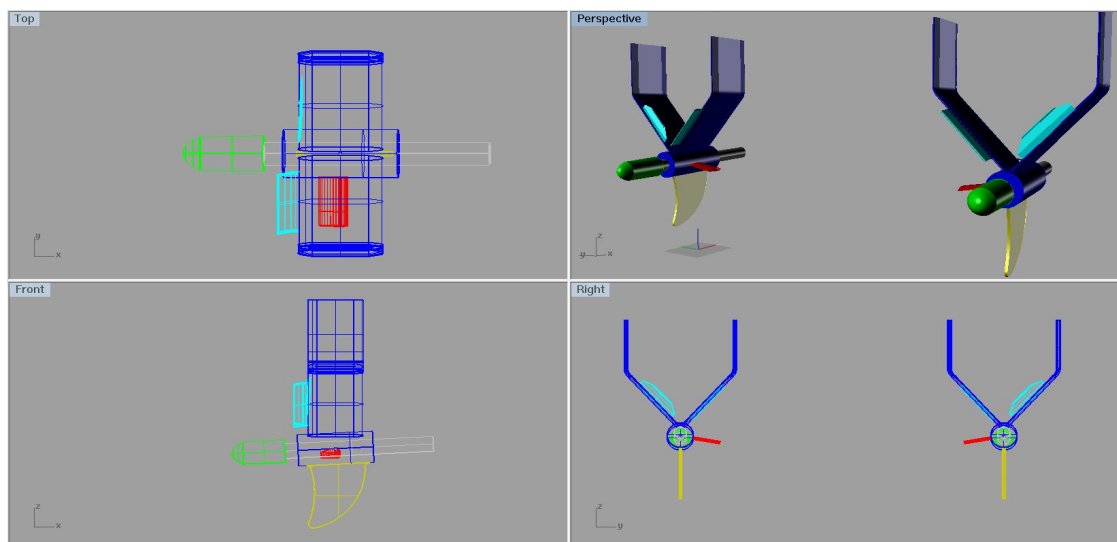


Fig. 2-4 3D model of Bracket Fin2(BF2)

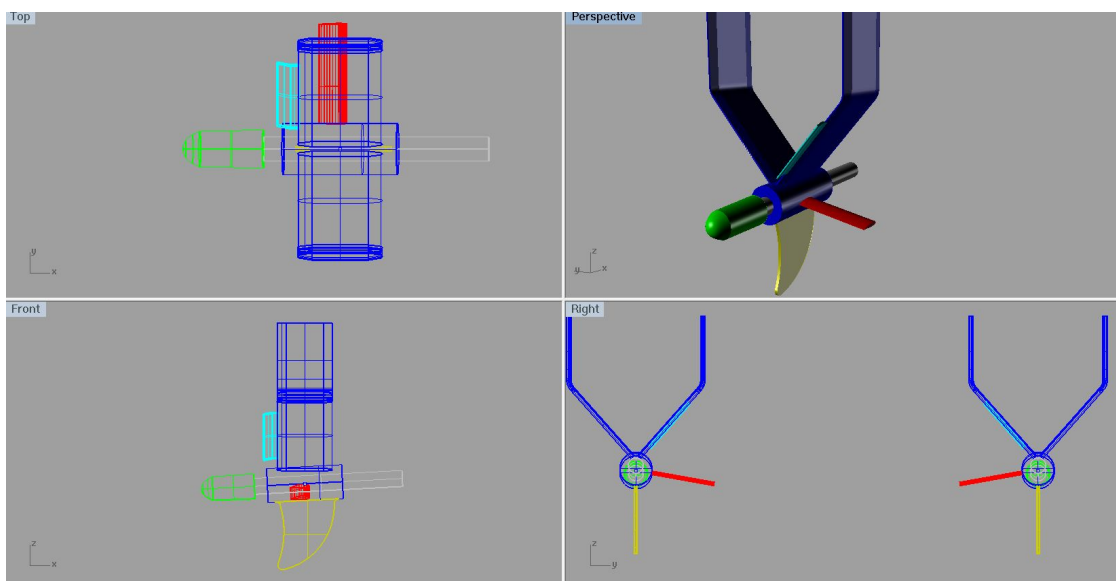


Fig. 2-5 3D model of Bracket Fin1+Long stator(BF1+LS)

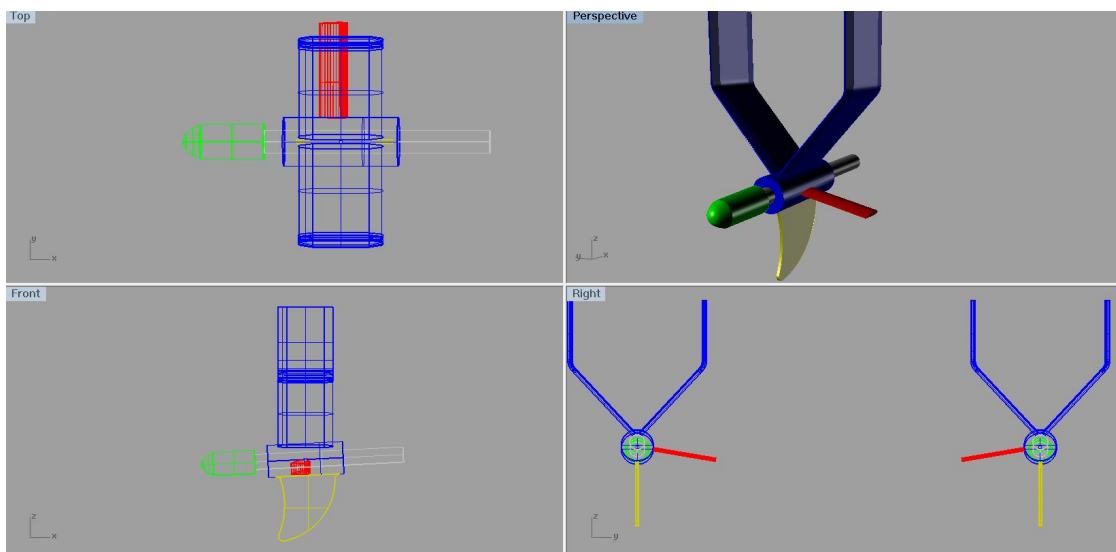


Fig. 2-6 3D model of Long stator(LS)

III. Development of Energy Saving Device

Despite of continuous efforts of scientists and engineers in finding the better hull form, the performance improvement by hull form improvement itself has its limitations in many cases.

So, the extensive activities on the development of energy saving devices are still on their progress and utilized in the actual ships (Lee et al., 1992).

One of the most applicable to energy saving in ships will be pre-swirl stator for which variations are shown in following Fig. 3-1



Fig. 3-1 Pre-swirl stator

Conventional pre-swirl stator consists of several fins which have almost the same span length as the propeller radius and are fixed radially on the stern frame in front of the propeller.

The setting angles of the conventional horizontal fins were fixed to control mainly the flow near the fin tip. In this case, the fin did not control properly the flow field near the fin root by the presence of longitudinal vortex due to the ship hull, rather deteriorated the propulsive efficiency. By adopting the horizontal fins of almost half-length of propeller radius, it may contribute to can control the flow field only near the stern frame and then get almost equal effect to the conventional fin. Furthermore, the bent plate on the edge of strut generate the counter flow to the propeller turning direction. That is, as shown in Fig.3-2, this new pre-swirl type energy-saving device consists of two fins. This device is named “Strut Fin”, which also can enhance the safety for a drift obstacle such as wood or timber, and reduce manufacturing cost.



Fig. 3-2 Strut Fin

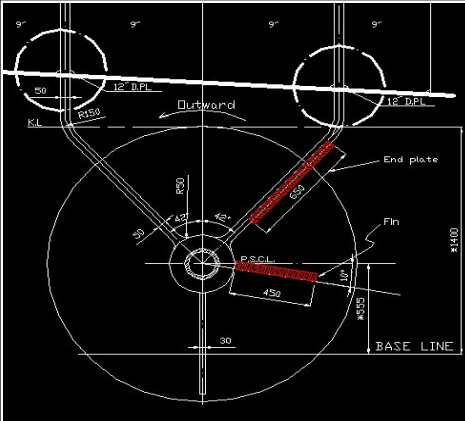
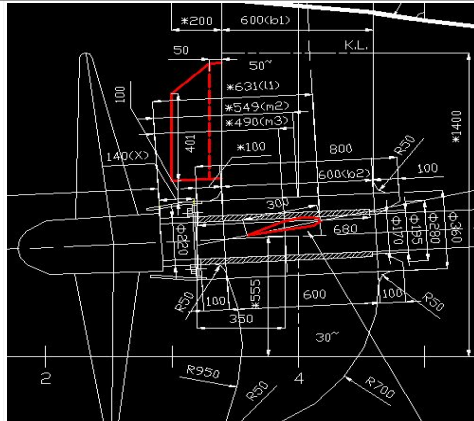
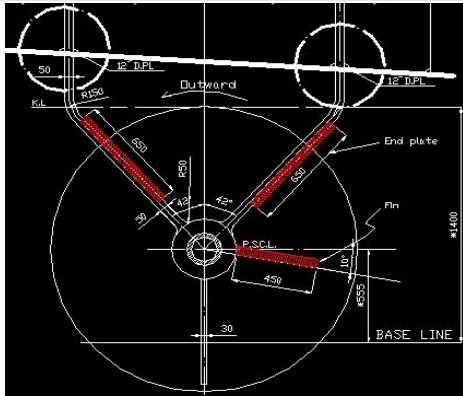
Against the stern flow mechanism, the design of the stern fin generally plays a role as flow guiding device making a wake field near the upper part of the propeller plane uniform by both deflecting flow toward propeller and reducing the wake peak at propeller top position.

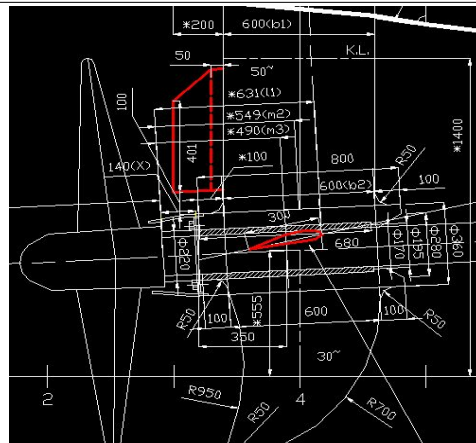
When the propeller rotates in one specific direction, its performances on port and starboard side are different and the pressure center shifts to the side where the propeller blades move downwards.

This in turn leads to a asymmetric pressure distribution on the hull in front of the propeller, which influences the boundary layers on port and starboard side differently. The idea in the design of Strut Fin is to reflect the stern vortices which move upwards in the region the propeller rotates downwards. This reflecting may reduce the wake near propeller tip and contribute to the equalization of wake field, thus may lead to a positive gain in propulsion efficiency. In case of a clockwise turning more separation occurs on port side above the propeller shaft where the propeller blades move upwards. The flow becomes turbulent and is even partly deflected in the opposite direction. From this point of view developed appendage might contribute towards the reflection of vortex flow which moves upwards in the region where propeller blades move downwards, by which the increase of propulsive efficiency might be attained.

The dimensions of full scale energy saving device are presented in Table. 3-1

Table 3-1 The config of energy saving device

BF1	 <p>Technical drawing of the End plate for BF1. It shows a circular base with a central hole. Two red lines represent the End plate, extending from the center at an angle of 42° from the vertical. Dimensions include a radius of 12 DPL, a length of 0.65m, and a breadth of 0.2m. The origin is at (1.65, 1.68, 1.5).</p>	 <p>Technical drawing of the Fin for BF1. It shows a rectangular base with a central hole. A red line represents the Fin, extending from the center at an angle of 100° from the vertical. Dimensions include a length of 0.45m, a breadth of 0.3m, and a radius of 12 DPL. The origin is at (2, 2.25, 0.545).</p>	
	<p><End plate> Length : 0.65m Breadth : 0.2m The Z-axis of rotation : 42° Origin : (1.65, 1.68, 1.5)</p>	<p><Fin> Length : 0.45m Breadth : 0.3m The Z-axis of rotation : 100° Origin : (2, 2.25, 0.545)</p>	
BF2	 <p>Technical drawing of the End plate and End plate 2 for BF2. It shows a circular base with a central hole. Two red lines represent the End plate and End plate 2, extending from the center at angles of 42° and -42° from the vertical. Dimensions include a radius of 12 DPL, a length of 0.65m, and a breadth of 0.2m. The origin is at (1.65, 1.68, 1.5).</p>		
	<p><End plate> Length : 0.65m Breadth : 0.2m The Z-axis of rotation : 42° Origin : (1.65, 1.68, 1.5)</p>	<p><End plate 2> Length : 0.65m Breadth : 0.2m The Z-axis of rotation : -42° The X-axis of rotation : 80° Origin : (1.68, 2.7, 1.5)</p>	<p><Fin> Length : 0.45m Breadth : 0.3m The Z-axis of rotation : 100° Origin : (2, 2.25, 0.545)</p>

 $\langle \text{Fin} \rangle$

Length : 0.45m

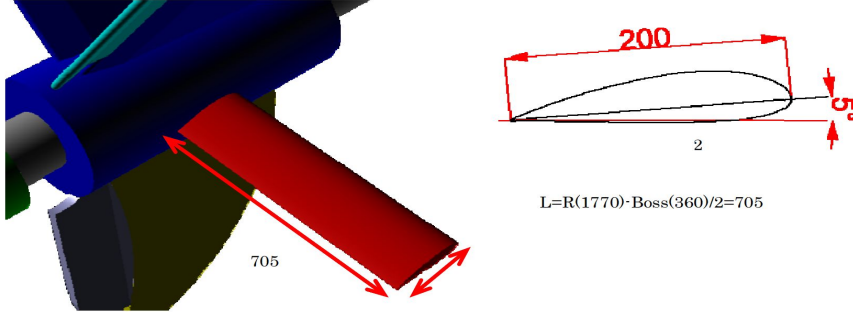
Breadth : 0.3m

The Z-axis of rotation : 100°

Origin : (2, 2.25, 0.545)



$$L=R(1770) \cdot \text{Boss}(360)/2=705$$

LS	 <p><LS> Length : 0.705m Breadth : 0.2m The Z-axis of rotation : 100° Origin : (2, 2.25, 0.545)</p>
----	-----------------------------------------------------------------------------------------------------------------------------------------------------------------------------------------------------------------

IV. Theoretical Calculation

Computational Fluid Dynamics (CFD) is widely used in the ship design process. In particular during the initial design stage CFD has become an important tool. It enables the designer to evaluate a larger number of hull alternatives and thereby a better optimized and reliable design before the final validation. It is true that not only for new buildings but also for existing ships and retro fitting of ship energy saving devices. The tough competition on the shipbuilding market creates high demands on short lead times and competitive designs. This must be met by developments of effective CFD tools and integration with CAD(MEPD, 2009).

SHIPFLOW has developed steadily since the first version was released by FLOWTECH in 1992. . This program is optimized for ship hydrodynamics design. Grids for the RANS solvers as well as meshes for XPAN are created automatically from the hull shape. Various types of hull shapes can be handled, such as monohulls, twin skeg hulls, multihulls, sailing yachts etc. In addition to this SHIPFLOW uses an efficient overlapping grid technique for use with appendages. Resistance and

propulsion data are presented in the naval architects way and the solvers are adapted for hull geometries.

CFD code makes cost down for the evaluation and prediction of performance of ship. Comparative theoretical calculation has been performed by CFD code of Shipflow for four different designs of Strut Fin as shown in Fig. 4-1

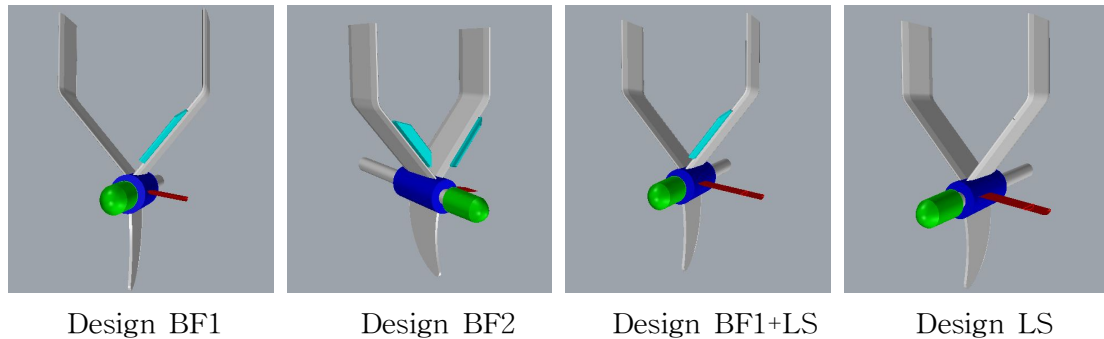


Fig. 4-1 Four Different Configuration of Energy Saving Device

A.FLOWSOLVERS

Computations are performed with SHIPFLOW developed at FLOWTECH International AB. There are three kinds of flow solvers in SHIPFLOW. XCHAP is a RANS solver for steady incompressible flow, XPAN a potential flow solver and XBOUND is an integral method for thin boundary layers. The solvers can be used separately or in combination depending on the needs.

The zonal approach is an efficient technique for many applications. The methods are in this case applied in a sequence. The free surface and the dynamic trim are first computed by XPAN, thereafter the boundary layer on the fore body by XBOUND and finally the flow around the stern and in the wake by XCHAP. Alternatively, the more general global approach can be used where the complete flow domain is computed by XCHAP.

B.Potentialflowsolver

The potential flow method XPAN is a non-linear Rankine source panel method [4]. It uses higher order panels and singularity distributions and a non-linear free surface boundary conditions.

The method can handle lift and induced drag by adding dipoles to the lifting surfaces and trailing wake. A Kutta condition is applied to find the strength of the

bound circulation.

Dynamic sinkage and trim are computed during the iterative procedure for the non-linear free surface boundary condition. During each iteration the ship is repositioned and the panellization of the hull and free surface is regenerated.

1. Boundary layer method

XBOUND is a first order integral method [5]. It computes the boundary layer along potential flow streamlines. The flow can be laminar or turbulent. The method includes a model for the transition from laminar to turbulent flow.

2. RANS solver

XCHAP solves the steady incompressible Reynolds Average Navier-Stokes equations. There are two available turbulence models the k- ω SST [6] and the Explicit Algebraic Stress Model EASM [7,8]. The EASM takes the non-isotropy into account using algebraic expressions for the Reynolds stresses containing non-linear terms in the mean strain and rotation rates. The model is a good compromise between performance and the ability to predict the important vortex flow in the stern wake and is therefore the standard model in the program. No wall functions are used and the equations are integrated down to the wall.

C.MODELLING OF THE PROPELLER

To simulate the effect of the propeller, body forces are introduced in a cylindrical component grid in the overlapping grid. When the flow passes through the propeller its linear and angular momentum increases as if it had passed a propeller of infinite number of blades. The forces vary in space but are independent of time and therefore approximating a propeller induced steady flow.

D.validation

A validation of the method is presented with comparisons of resistance, open water test and self propulsion simulations at model scale.

The resistance was computed using the coarse approach in SHIPFLOW. The wave resistance was computed by the potential flow module XPAN.

The open water characteristics are required in order to make the full scale extrapolation using the modified-ITTC78 procedure. SHIPFLOW can automatically compute an open water The speed of the propeller was automatically adjusted during the self propulsion simulation such that the propeller thrust balanced the

resistance of the hull corrected for the towing force. The towing force was computed according to the modified-ITTC78 procedure and include the model-ship correlation and roughness allowance. simulation for a sequence of advance ratios.

1. Resistance Calculation Result

k and ct compared to barehull were all large value except BF1+LS.

Resistance calculation results are compared in Table. 2 and in Fig. 4-1

Table 4-1 Comparison of resistance components

	Bare hull	BF1	BF2	BF1+LS	LS
k	0.201	0.202	0.222	0.200	0.204
Cw	1.046×10^{-3}	1.046×10^{-3}	1.046×10^{-3}	1.046×10^{-3}	1.046×10^{-3}
Ct	5.266×10^{-3}	5.270×10^{-3}	5.341×10^{-3}	5.263×10^{-3}	5.279×10^{-3}

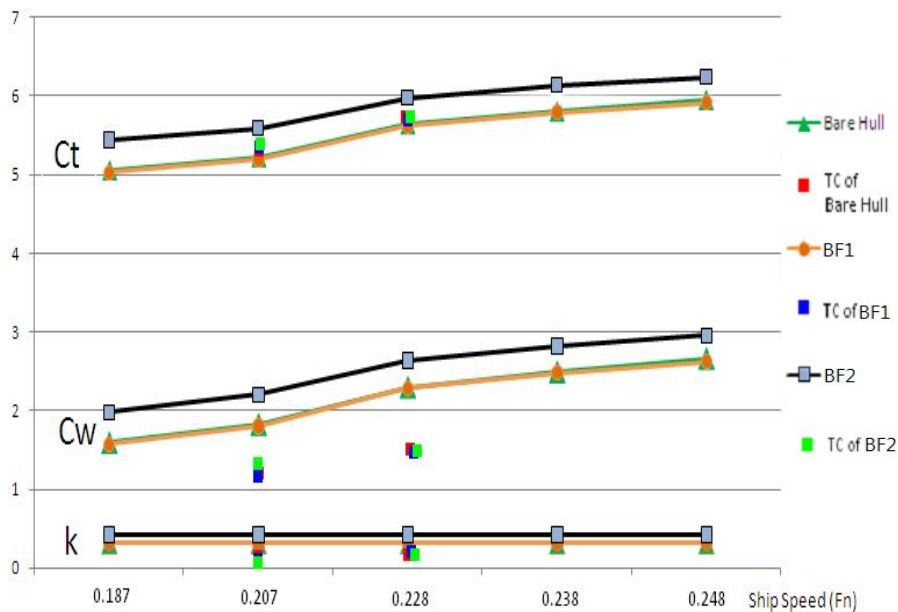


Fig. 4-2 Resistance components vs Fn

2. Self Propulsion Calculation Result

1-w compared to barehull were all large value. In case of 1-t, compared to barehull were all small value except BF2. BF1 BF1 + LS, and LS compared to barehull η_H was highly calculated. BF1 case of η_R and η_D , the results were both high compared to barehull. η_R had the greatest results in the value of the BF2 and η_D had the greatest results in the value of the BF1.

Self propulsion calculation results are summarized in Table. 4-2 and in Fig. 4-3

Table 4-2 Comparison of propulsion coefficient

	1-w	1-t	η_H	η_O	η_R	η_D
Bare hull	0.819	0.894	1.093	0.721	1.020	0.804
BF1	0.814	0.905	1.111	0.721	1.026	0.821
BF2	0.808	0.877	1.085	0.721	1.040	0.811
BF1+LS	0.817	0.904	1.107	0.721	1.026	0.818
LS	0.818	0.905	1.106	0.721	1.026	0.818

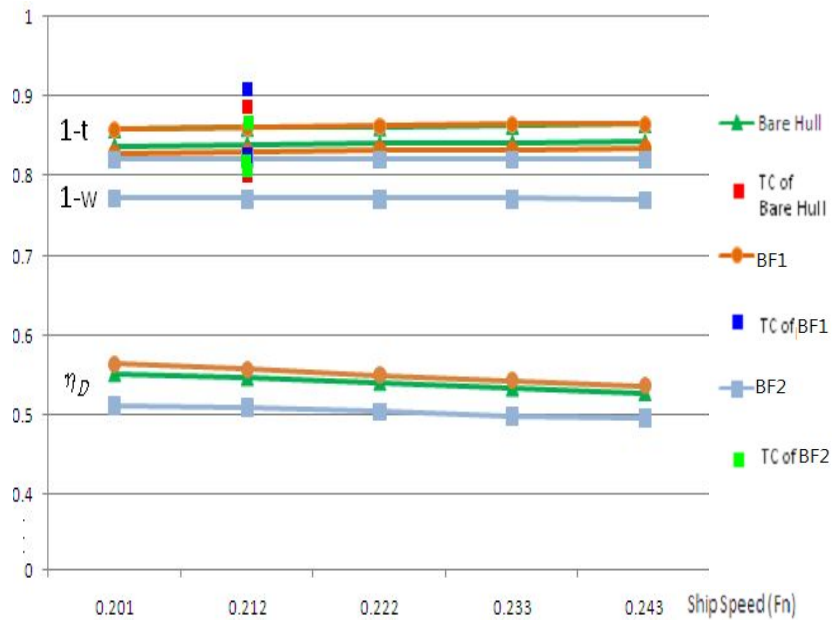


Fig. 4-3 Fn vs propulsion coefficients

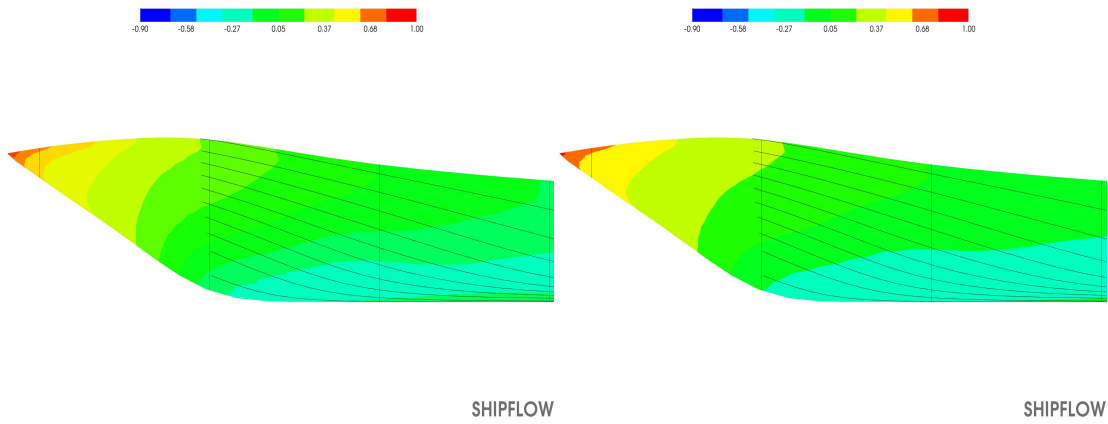


Fig. 4-4(a) Comparison of potential flow streamlines (Bare Hull, side bow view)

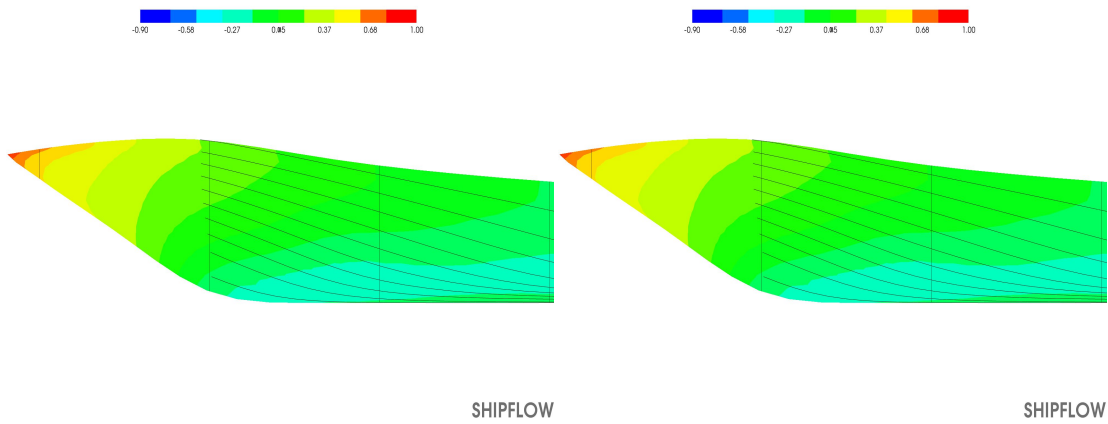


Fig. 4-4(b) Comparison of potential flow streamlines (BF1, side bow view)

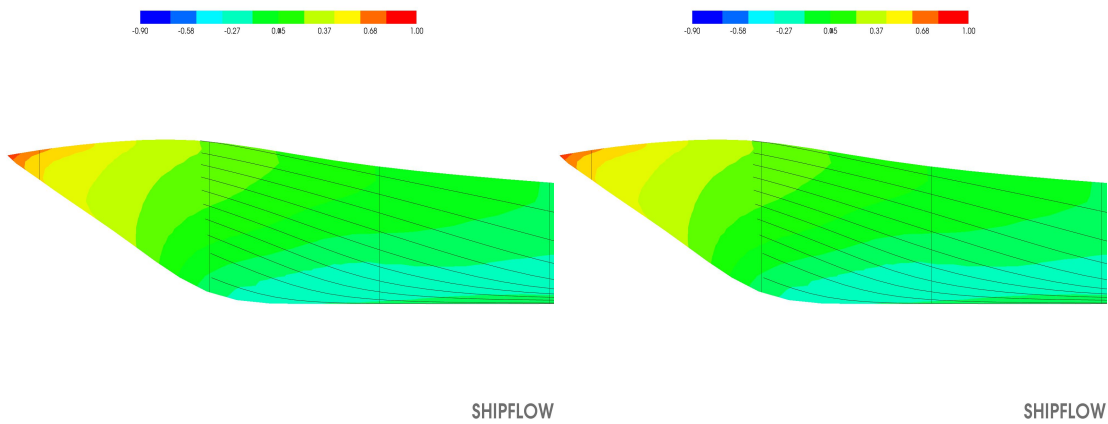


Fig. 4-4(c) Comparison of potential flow streamlines (BF2, side bow view)

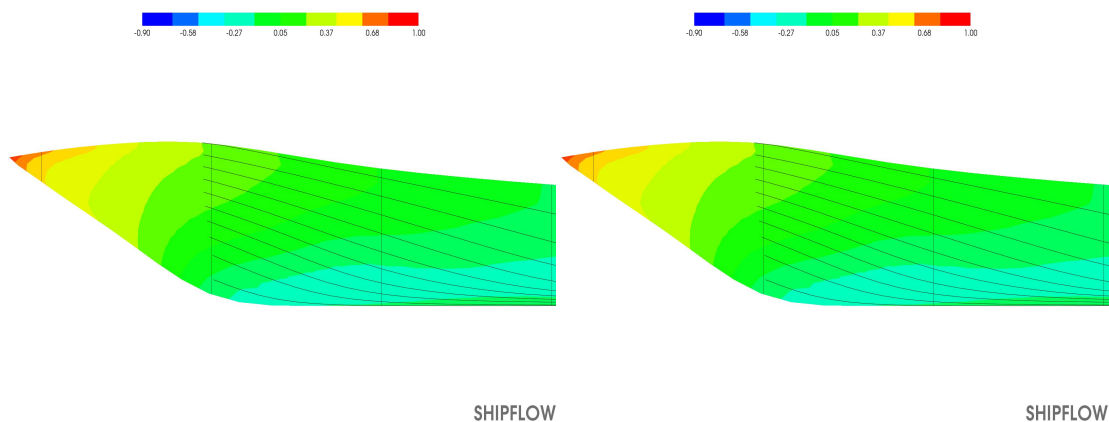


Fig. 4-4(d) Comparison of potential flow streamlines (BF1+LS, side bow view)

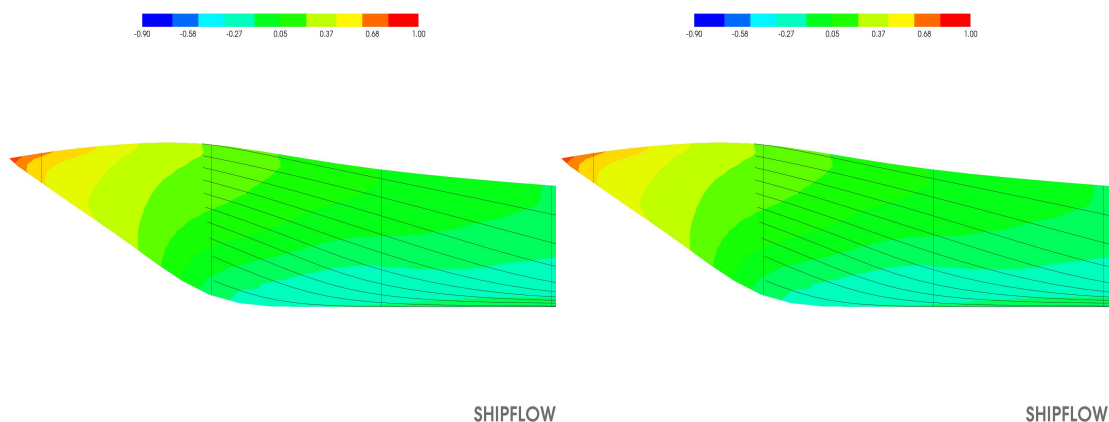


Fig. 4-4(e) Comparison of potential flow streamlines (LS, side bow view)

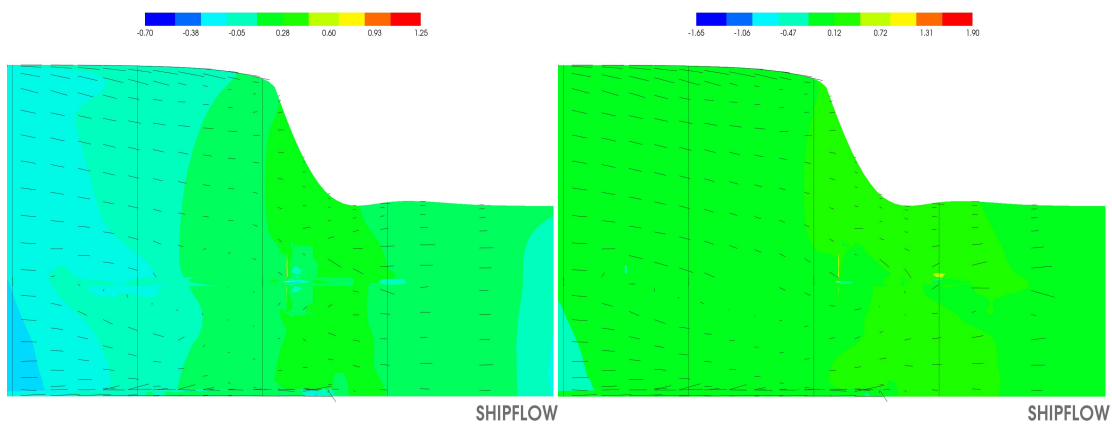


Fig. 4-5(a) Comparison of Stream line(Bare Hull, bottom stern view)

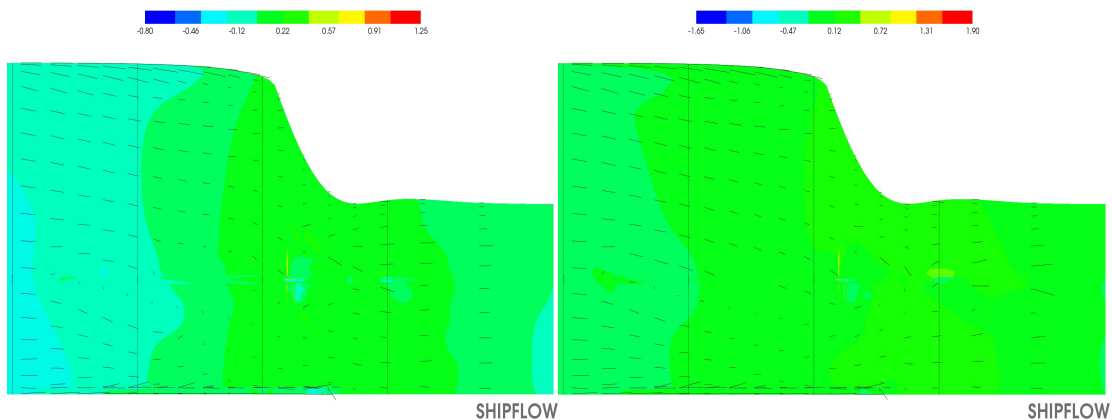


Fig. 4-5(b) Comparison of Stream line(BF1, bottom stern view)

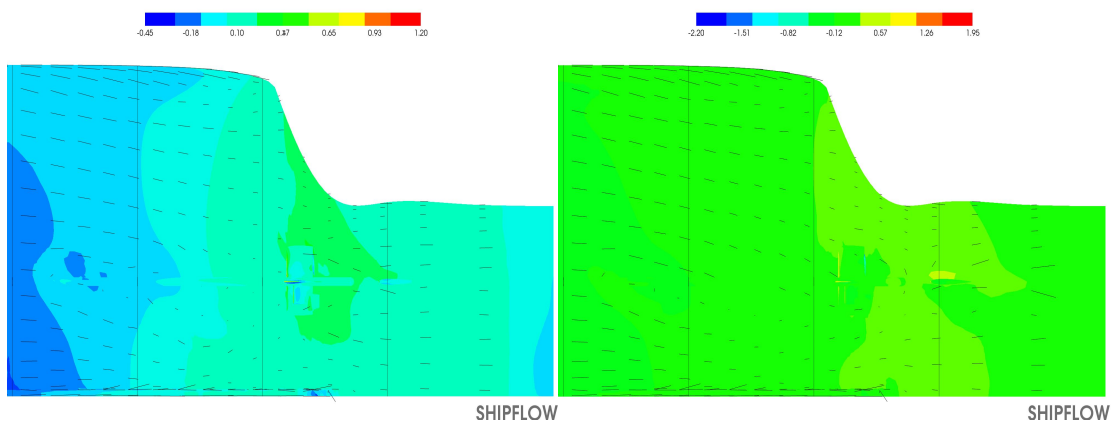


Fig. 4-5(c) Comparison of Stream line(BF2, bottom stern view)

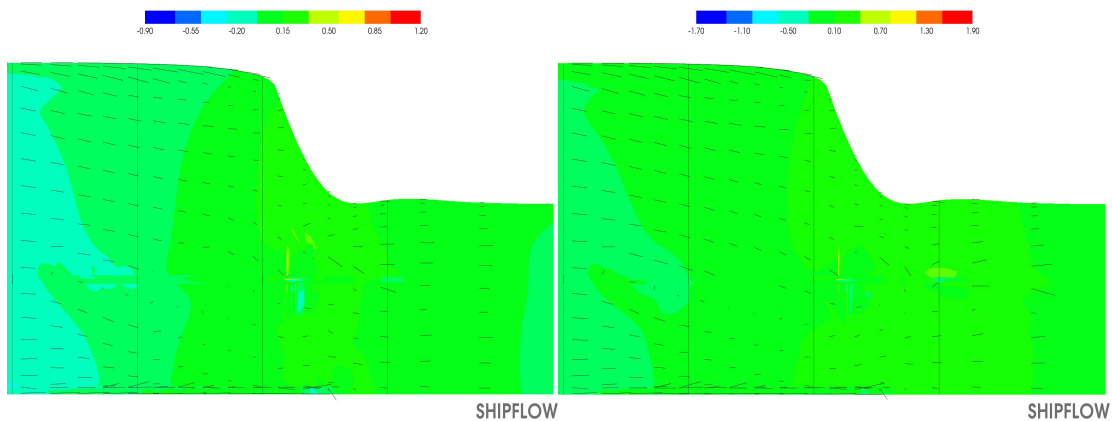


Fig. 4-5(d) Comparison of Stream line(BF1+LS, bottom stern view)

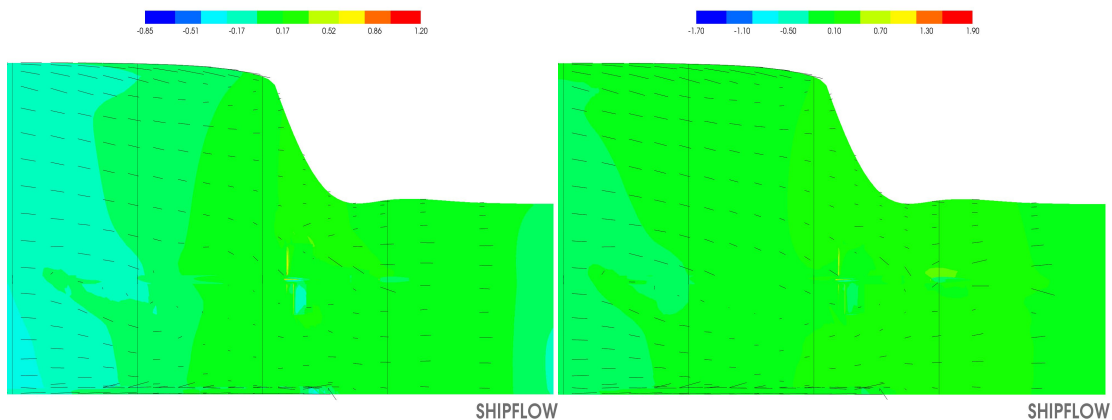


Fig. 4-5(e) Comparison of Stream line(LS, bottom stern view)

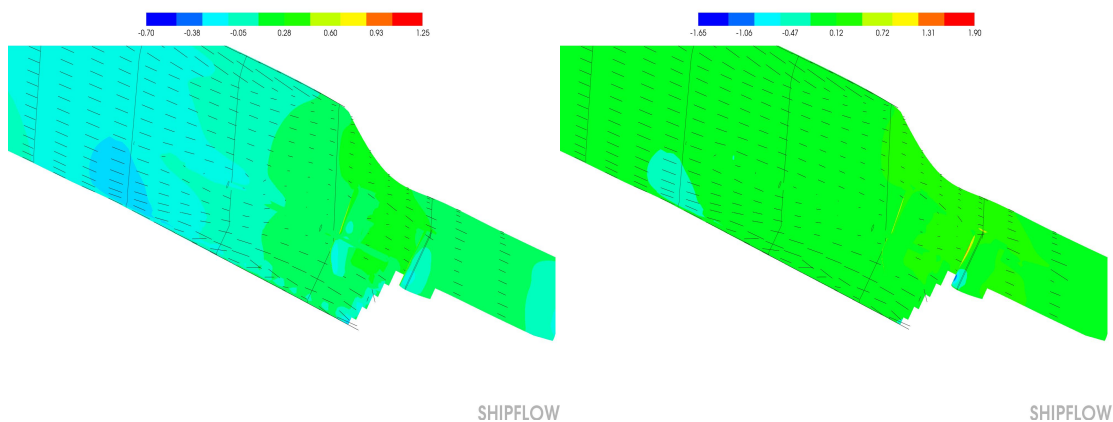


Fig. 4-6(a) Comparison of Stream line(Bare Hull, persp. stern view)

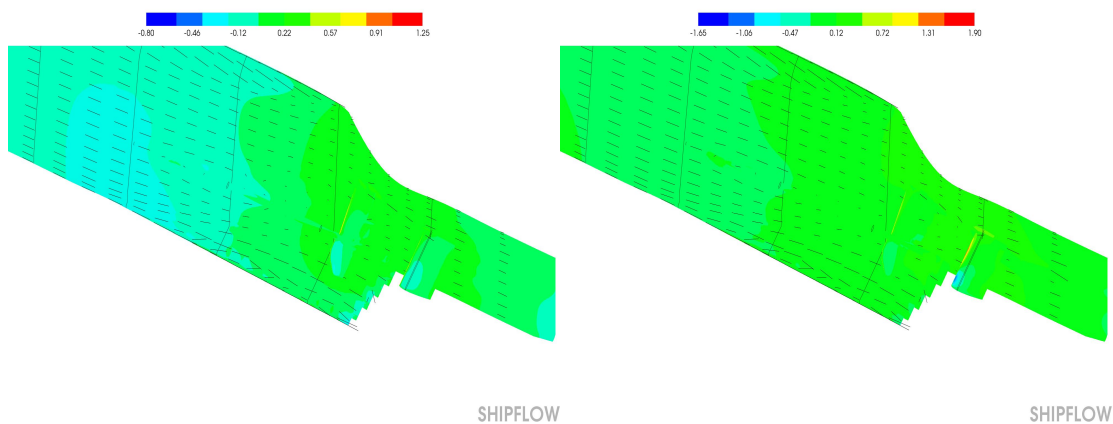
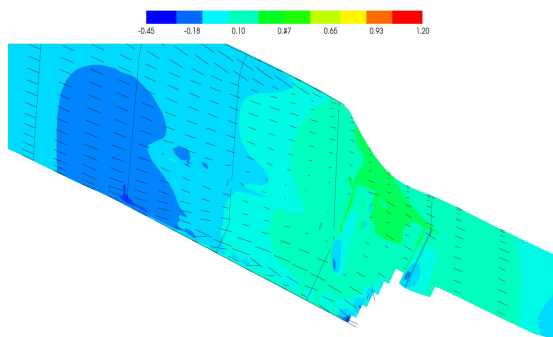
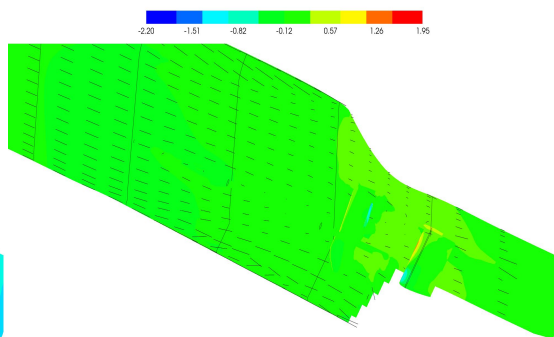


Fig. 4-6(b) Comparison of Stream line(BF1, persp. stern view)

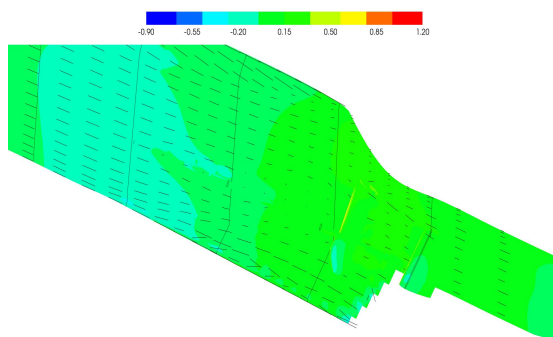


SHIPFLOW

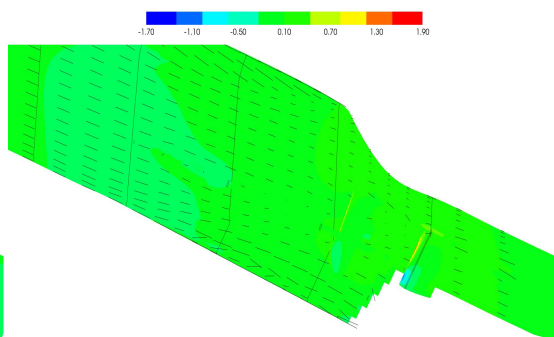


SHIPFLOW

Fig. 4-6(c) Comparison of Stream line(BF2, persp. stern view)

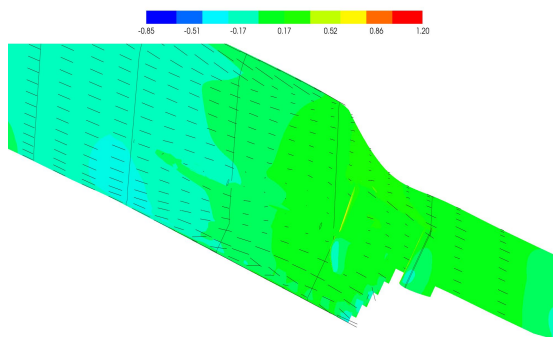


SHIPFLOW

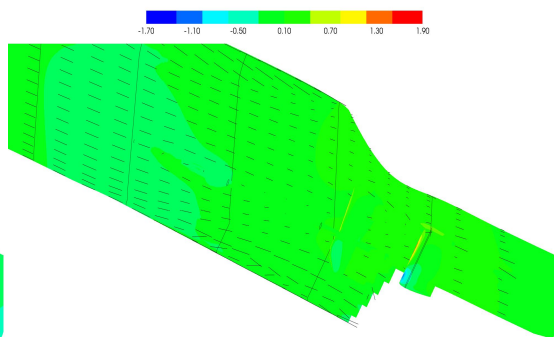


SHIPFLOW

Fig. 4-6(d) Comparison of Stream line(BF1+LS, persp. stern view)



SHIPFLOW



SHIPFLOW

Fig. 4-6(e) Comparison of Stream line(LS, persp. stern view)

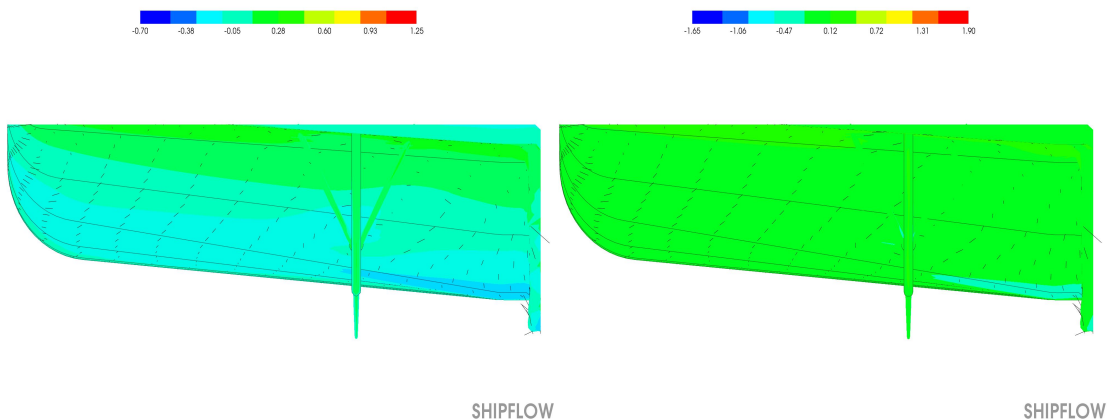


Fig. 4-7(a) Stern flow direction(Bare Hull, stern view)

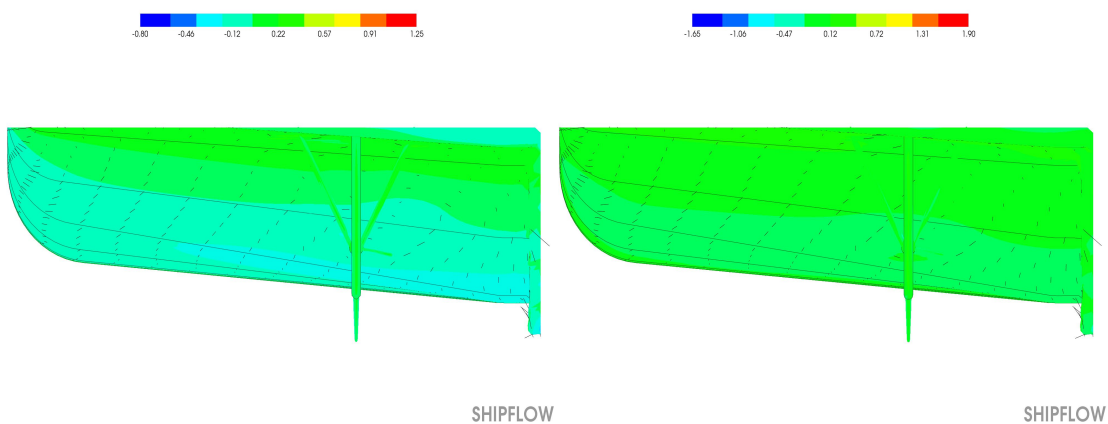


Fig. 4-7(b) Stern flow direction(BF1, stern view)

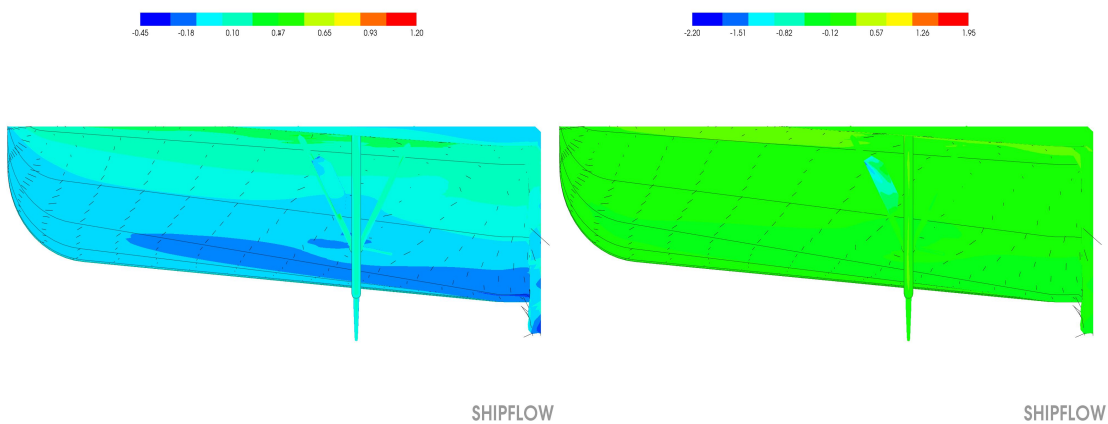


Fig. 4-7(c) Stern flow direction(BF2, stern view)

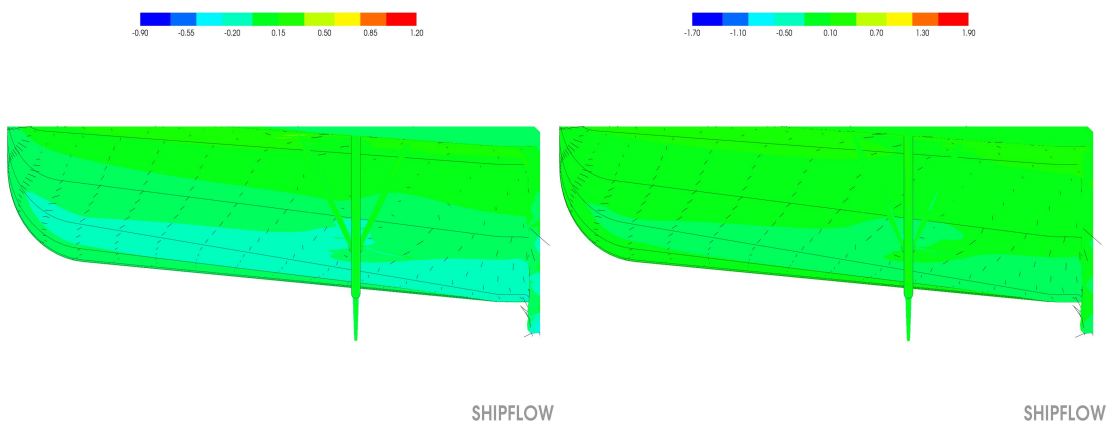


Fig. 4-7(d) Stern flow direction(BF1+LS, stern view)

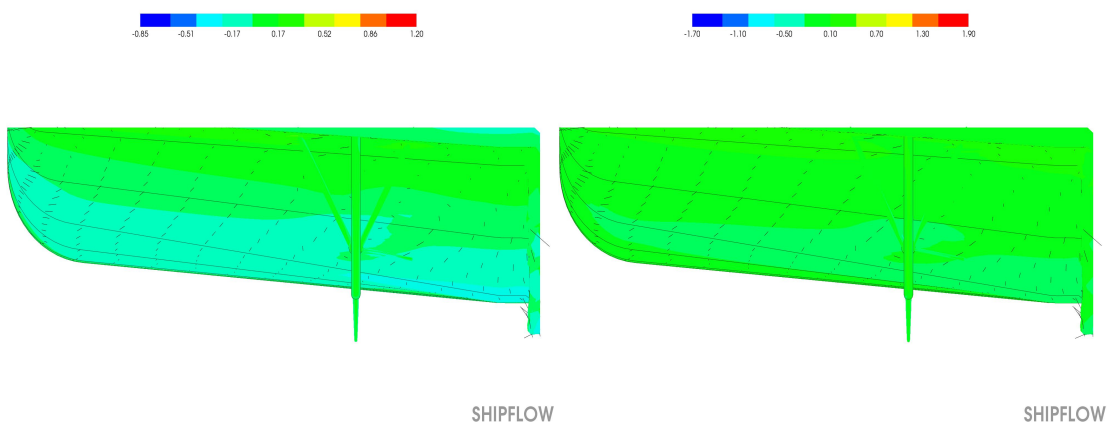


Fig. 4-7(e) Stern flow direction(LS, stern view)

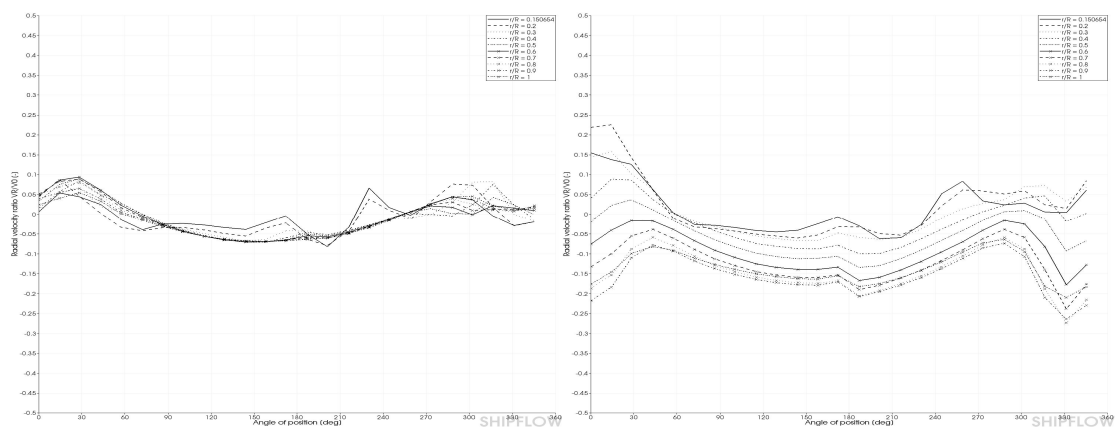


Fig. 4-8(a) Comparison of the V_R / V_O (Bare Hull)

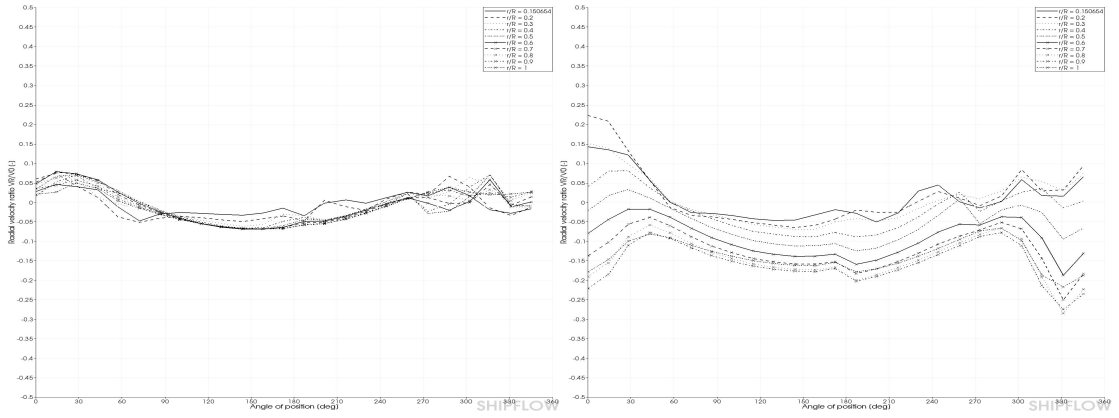


Fig. 4-8(b) Comparison of the V_R / V_O (BF1)

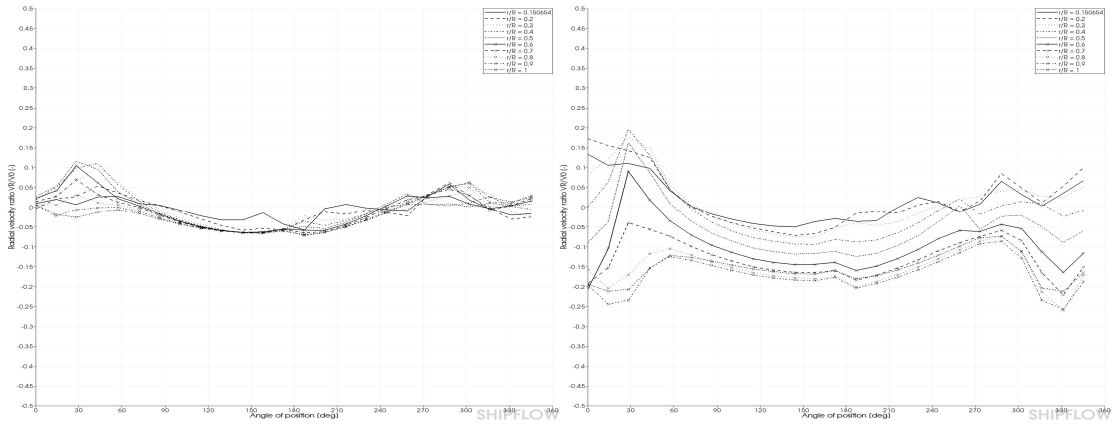


Fig. 4-8(c) Comparison of the V_R / V_O (BF2)

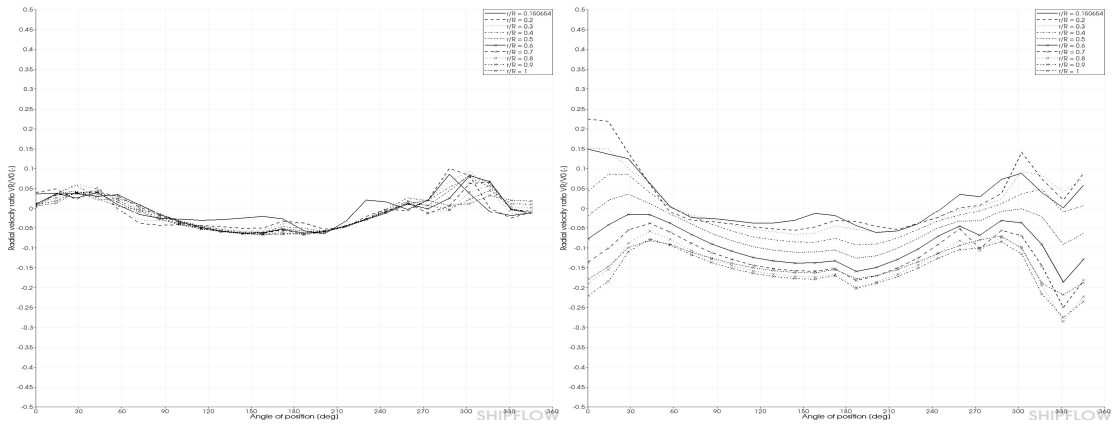


Fig. 4-8(d) Comparison of the V_R / V_O (BF1+LS)

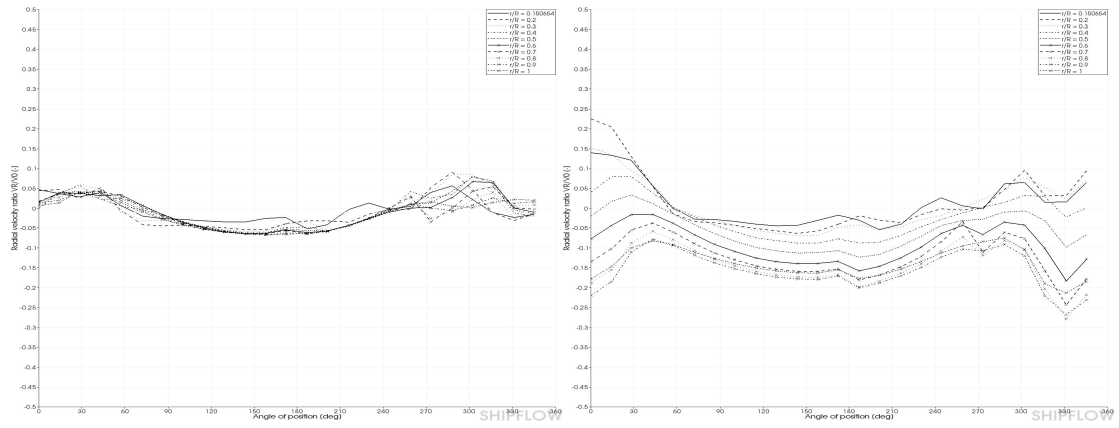


Fig. 4-8(e) Comparison of the V_R / V_O (LS)

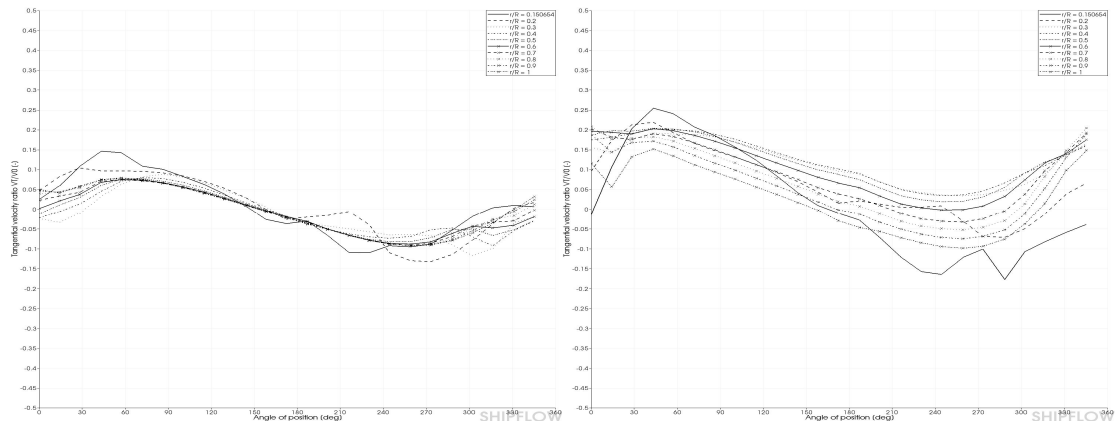


Fig. 4-9(a) Comparison of the V_T / V_O (Bare Hull)

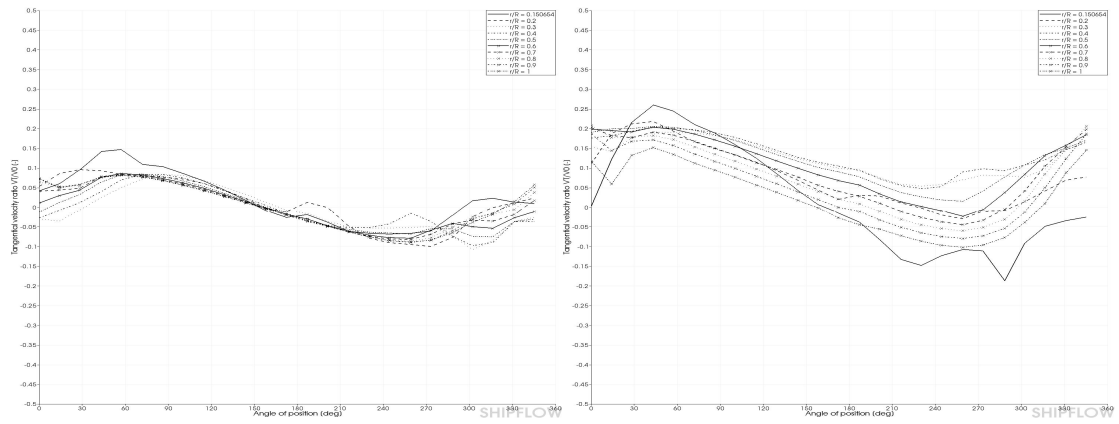


Fig. 4-9(b) Comparison of the V_T / V_O (BF1)

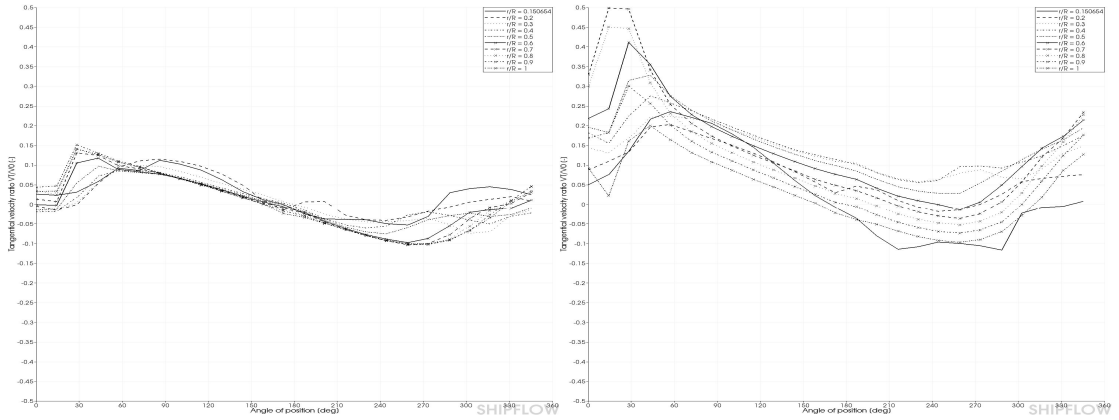


Fig. 4-9(c) Comparison of the V_T/V_O (BF2)

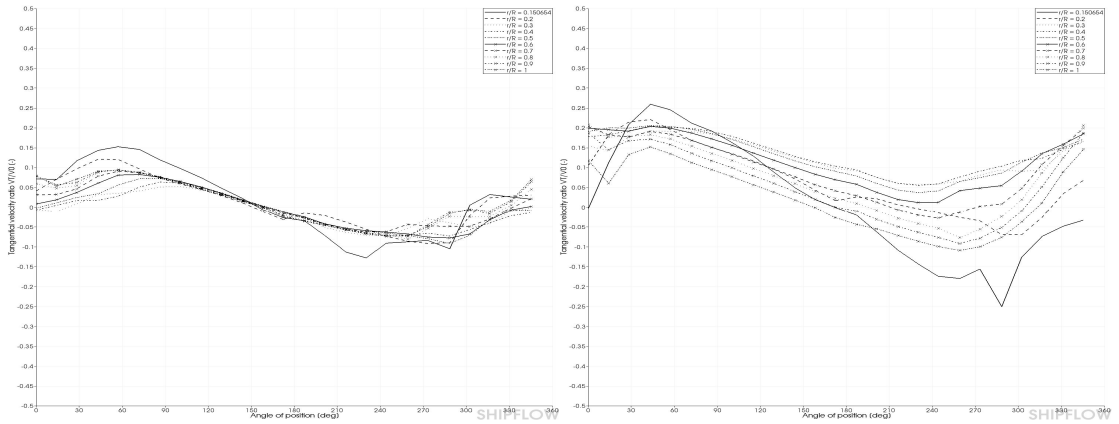


Fig. 4-9(d) Comparison of the V_T/V_O (BF1+LS)

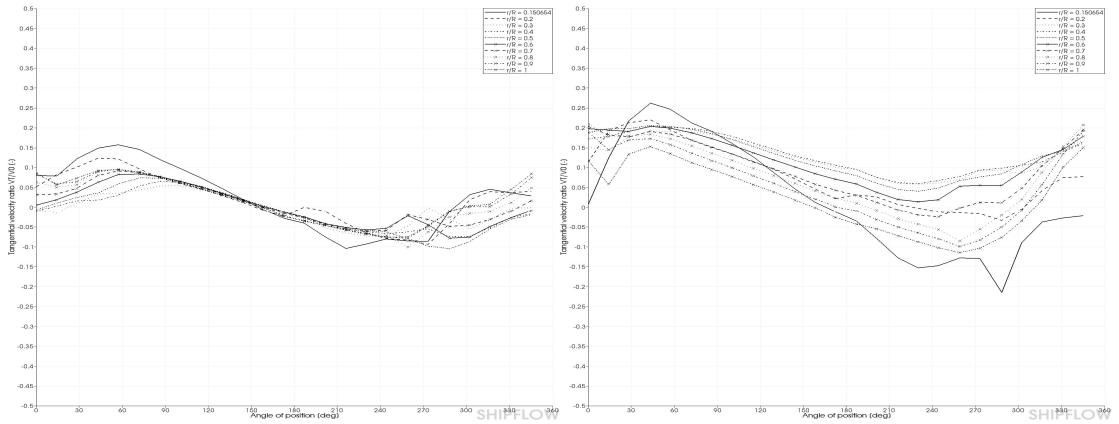


Fig. 4-9(e) Comparison of the V_T/V_O (LS)

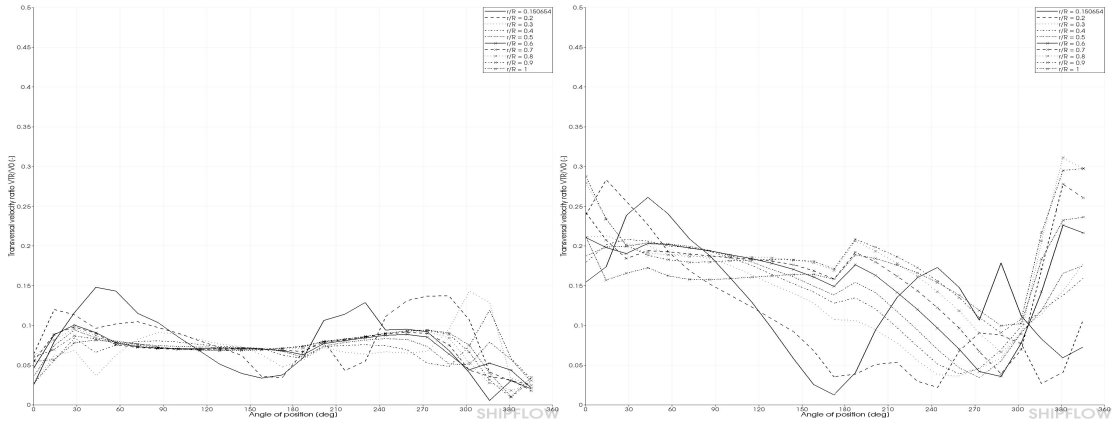


Fig. 4-10(a) Comparison of the V_{TR}/V_O (Bare Hull)

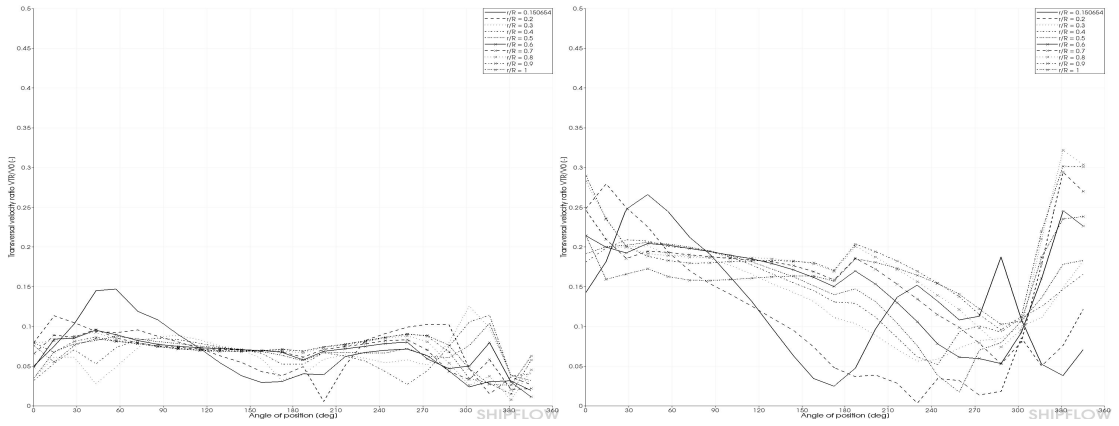


Fig. 4-10(b) Comparison of the V_{TR}/V_O (BF1)

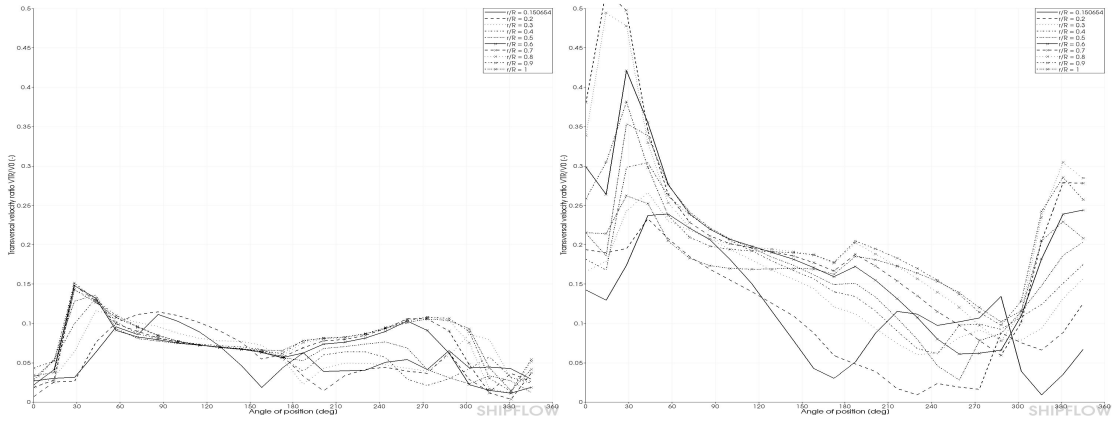


Fig. 4-10(c) Comparison of the V_{TR}/V_O (BF2)

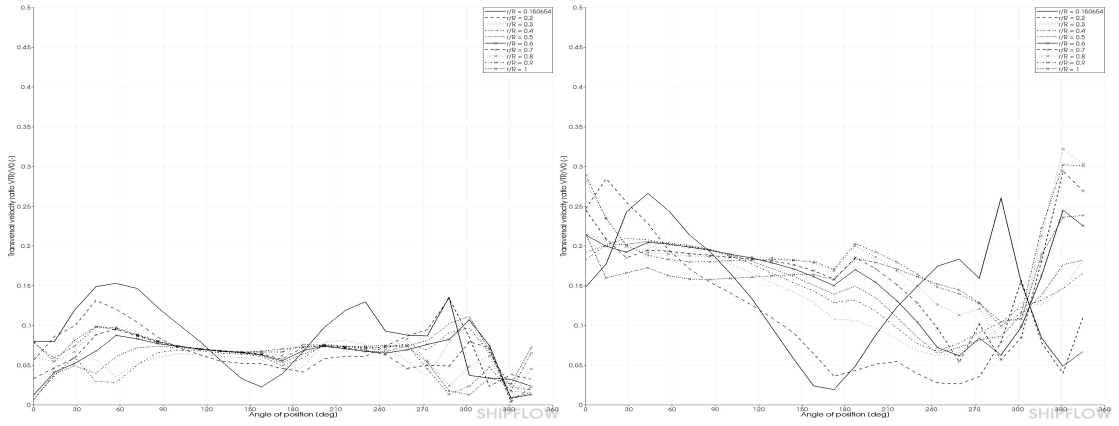


Fig. 4-10(d) Comparison of the V_{TR}/V_O (BF1+LS)

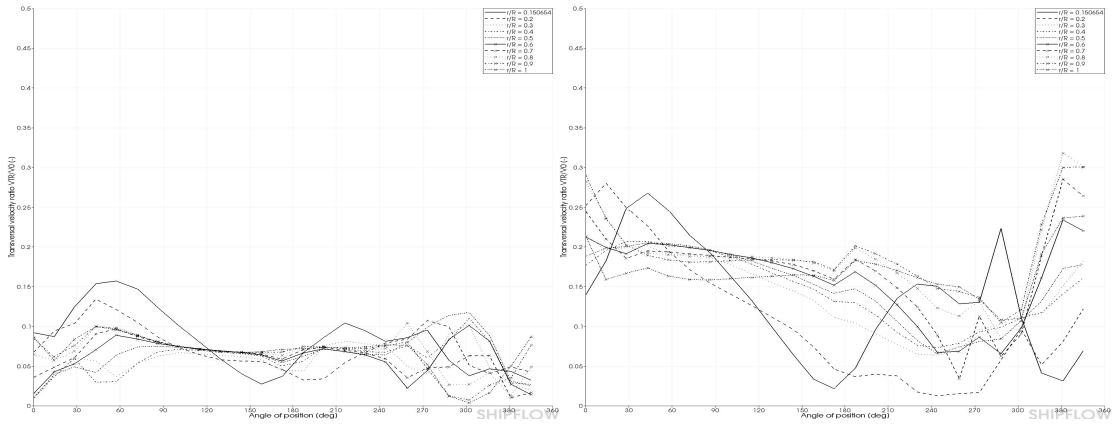


Fig. 4-10(e) Comparison of the V_{TR}/V_O (LS)

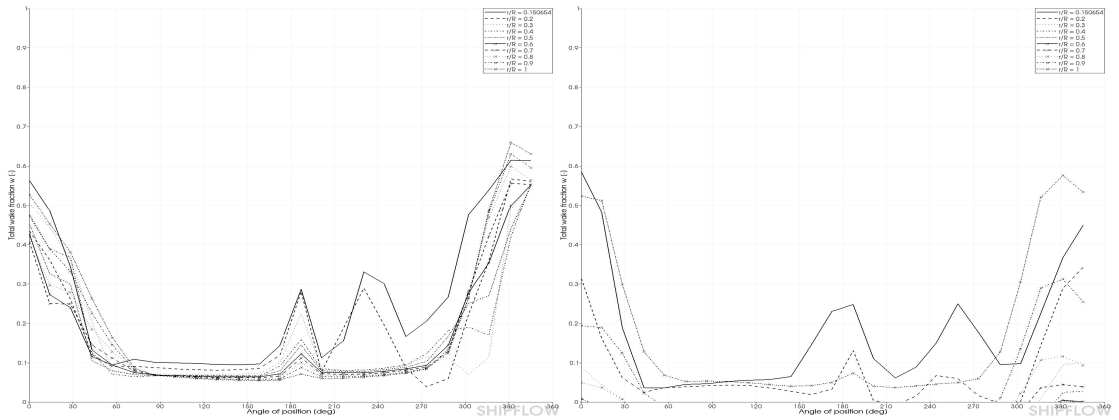


Fig. 4-11(a) Comparison of the wakefraction (Bare Hull)

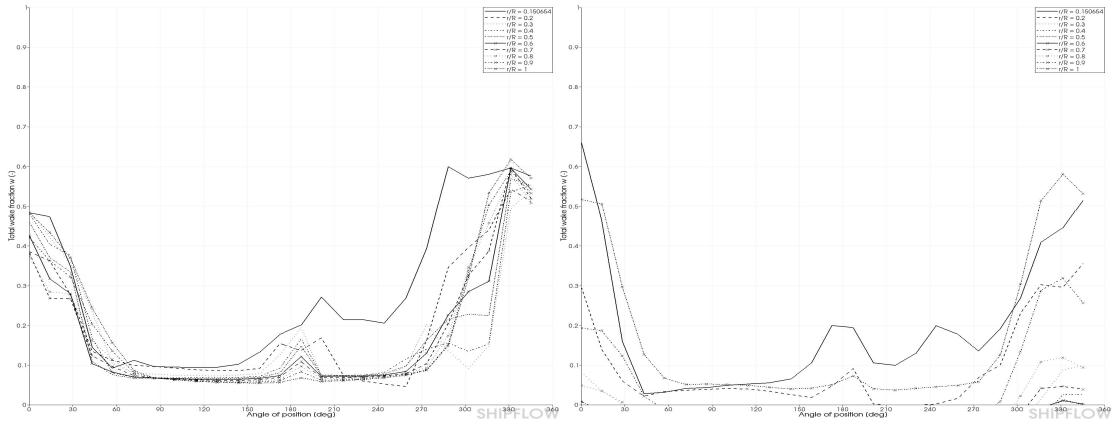


Fig. 4-11(b) Comparison of the wakefraction (BF1)

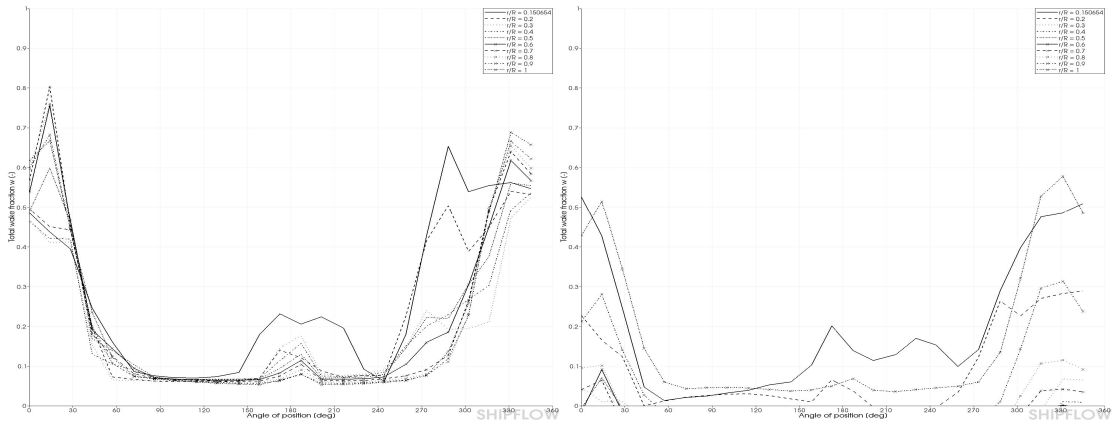


Fig. 4-11(c) Comparison of the wakefraction (BF2)

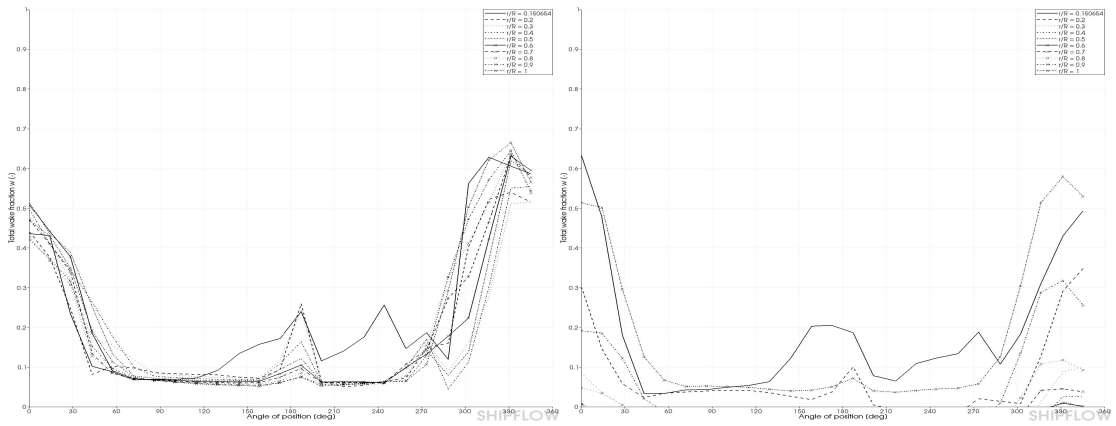


Fig. 4-11(d) Comparison of the wakefraction (BF1+LS)

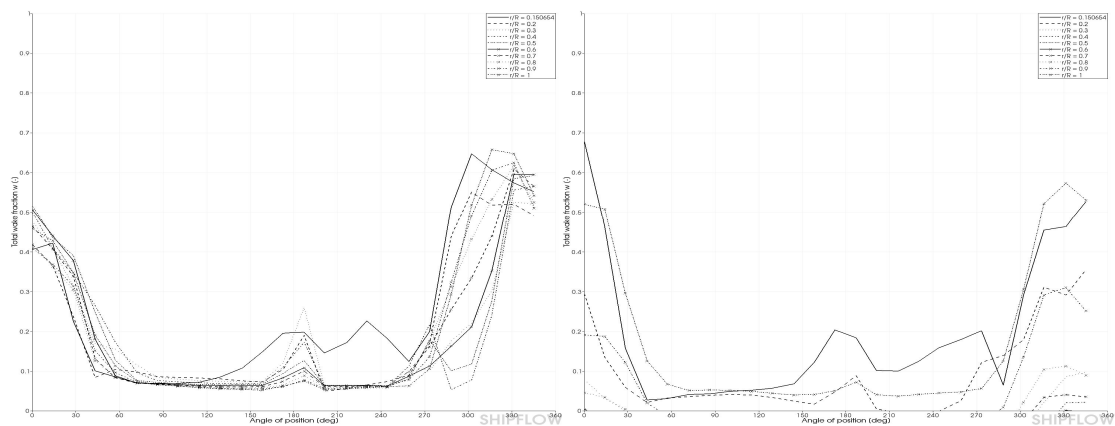


Fig. 4-11(e) Comparison of the wakefraction (LS)

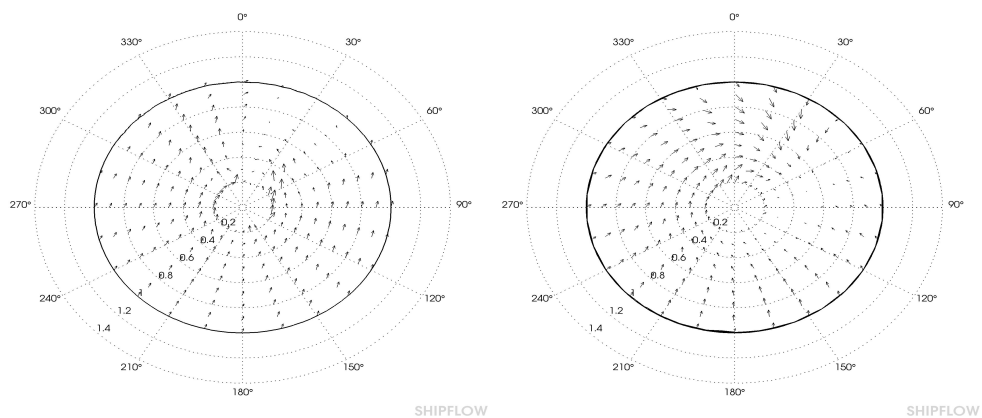


Fig. 4-12(a) Comparison of the vtr (Bare Hull)

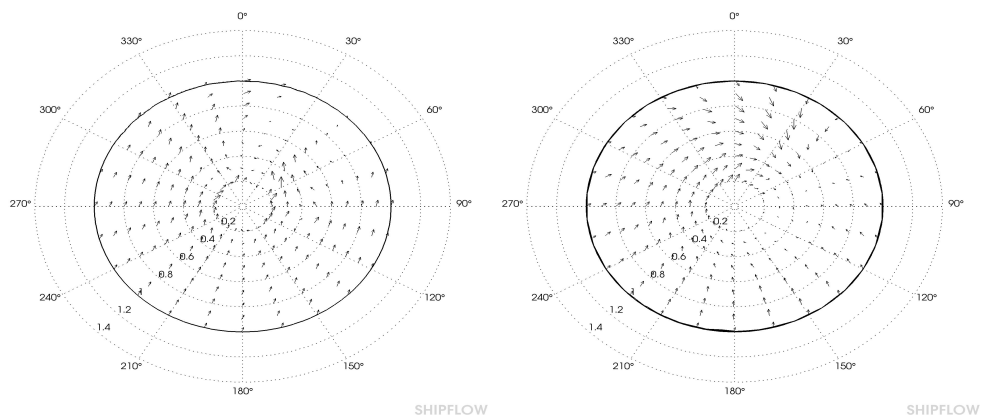


Fig. 4-12(b) Comparison of the vtr (BF1)

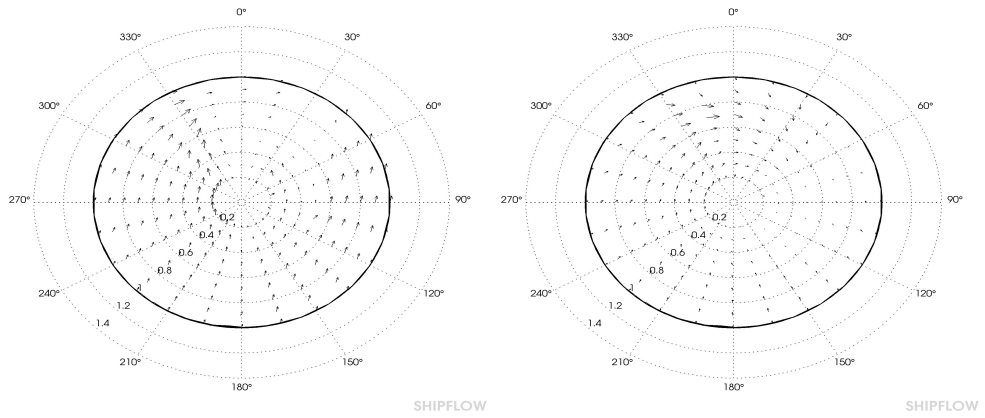


Fig. 4-12(c) Comparison of the vtr (BF2)

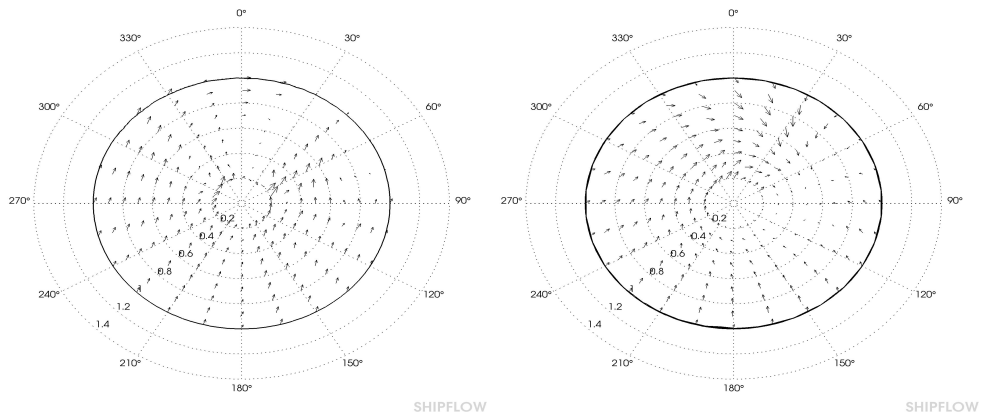


Fig. 4-12(d) Comparison of the vtr (BF1+LS)

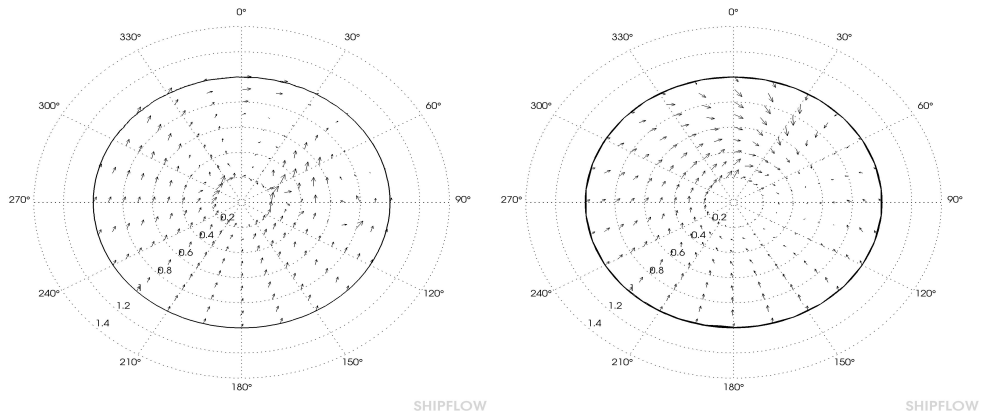


Fig. 4-12(e) Comparison of the vtr (LS)

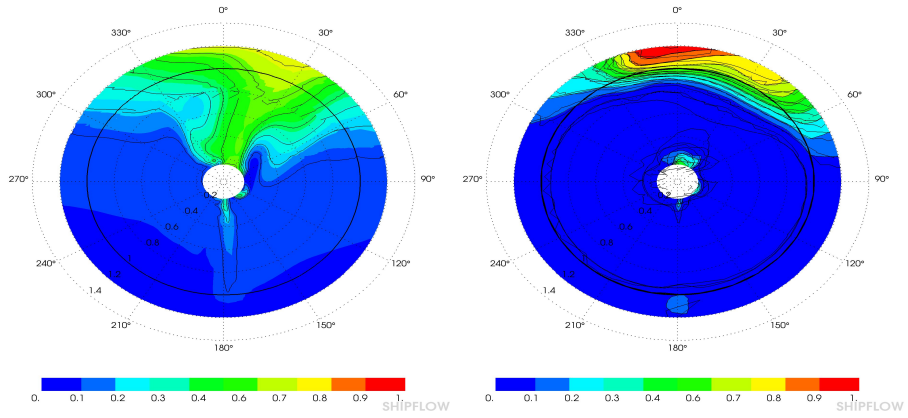


Fig. 4-13(a) Comparison of the wake (Bare Hull)

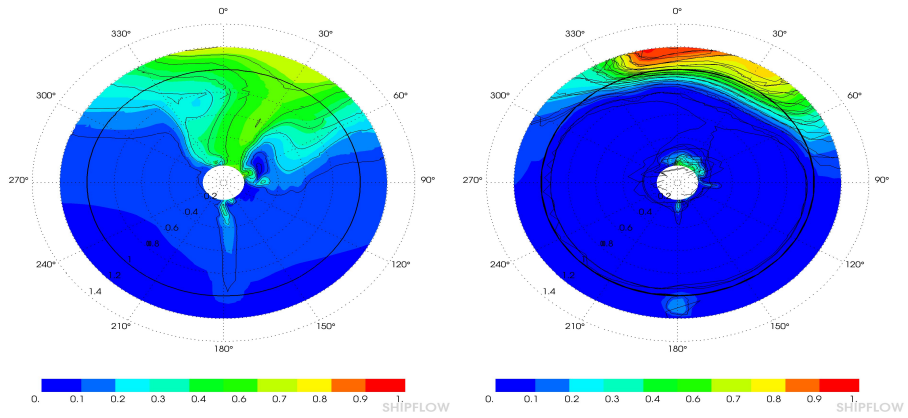


Fig. 4-13(b) Comparison of the wake (BF1)

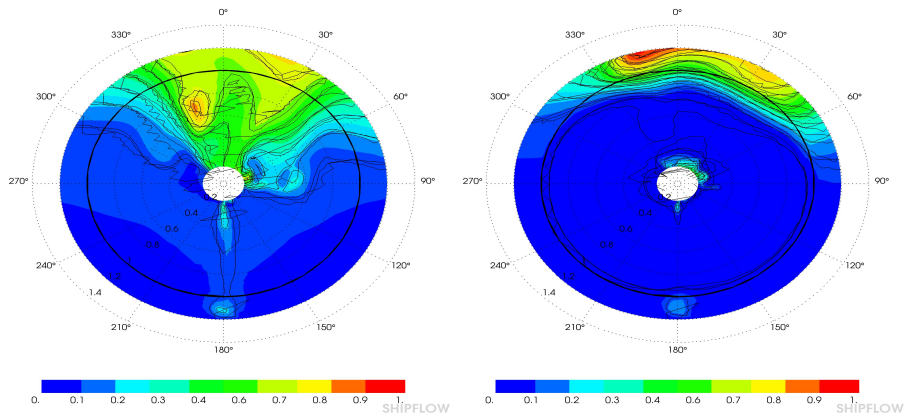


Fig. 4-13(c) Comparison of the wake (BF2)

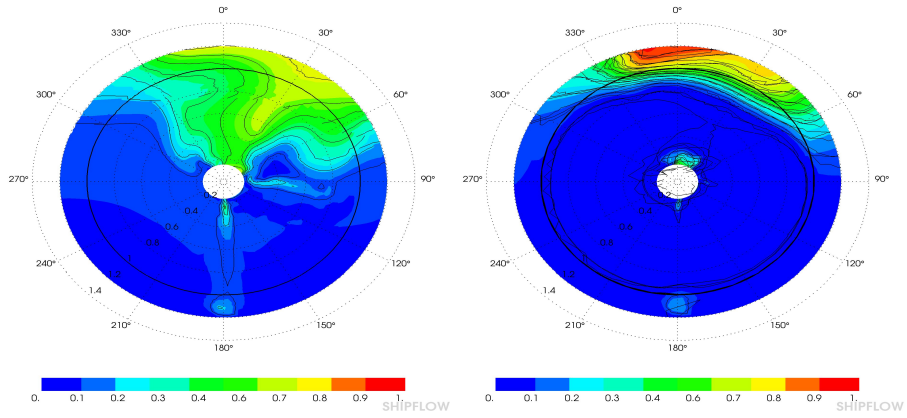


Fig. 4-13(d) Comparison of the wake (BF1+LS)

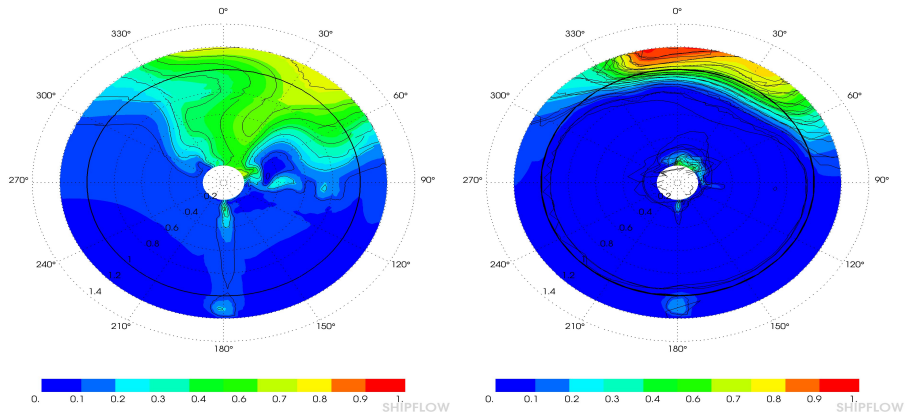


Fig. 4-13(e) Comparison of the wake (LS)

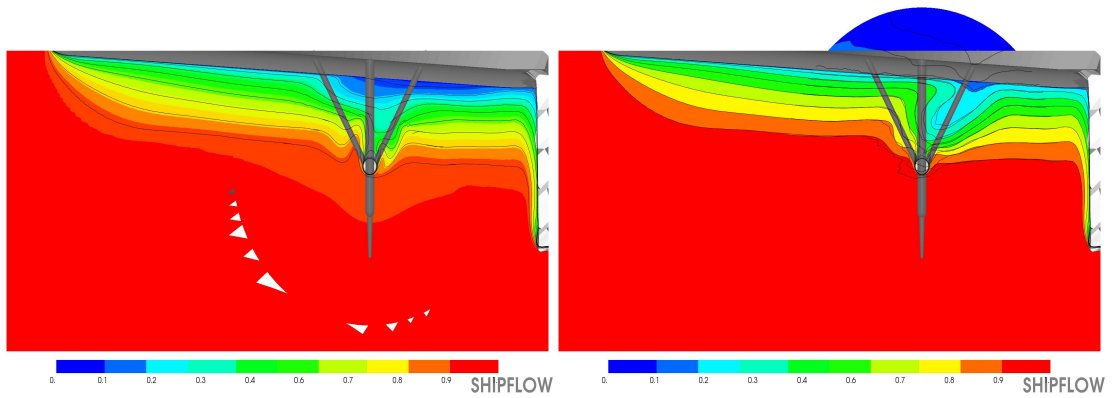


Fig. 4-14(a) Comparison of Wake in $U_x=3$ (Bare Hull)

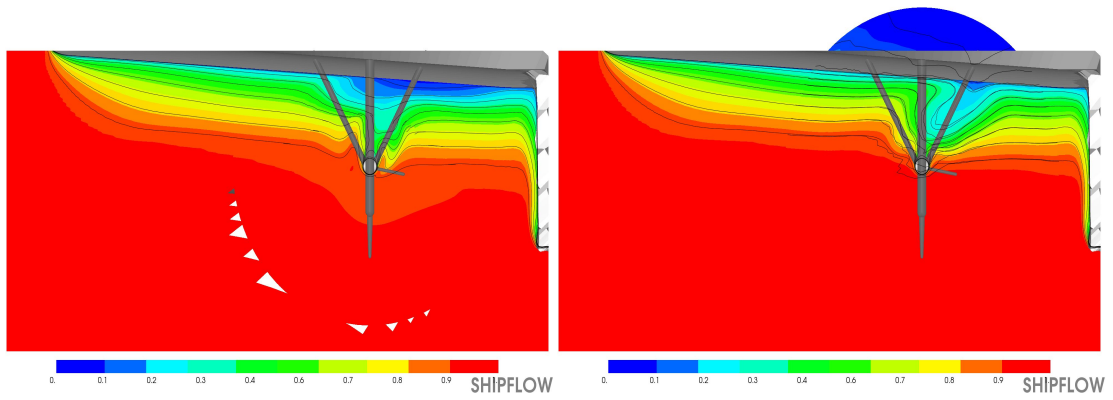


Fig. 4-14(b) Comparison of Wake in $U_{x=3}$ (BF1)

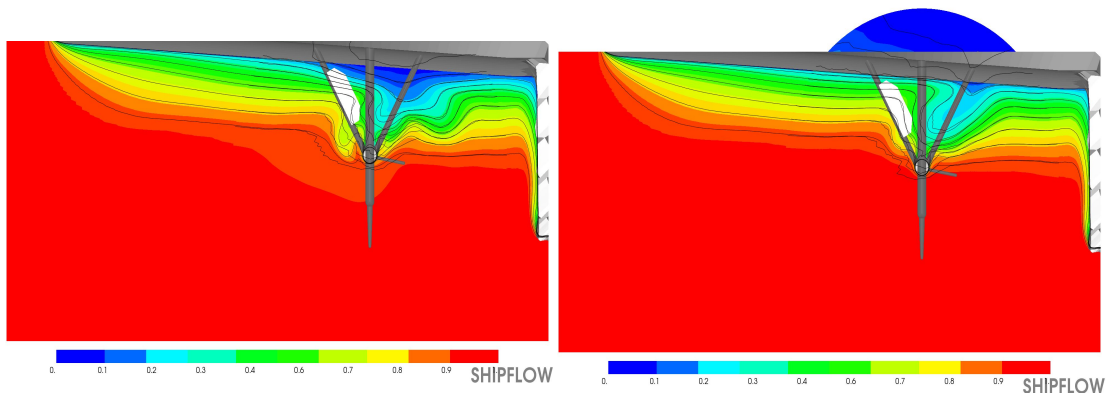


Fig. 4-14(c) Comparison of Wake in $U_{x=3}$ (BF2)

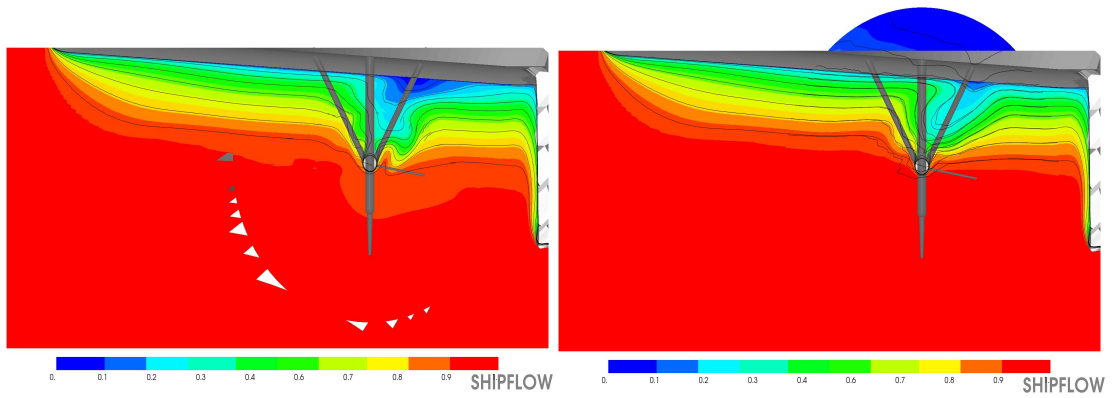


Fig. 4-14(d) Comparison of Wake in $U_{x=3}$ (BF1+LS)

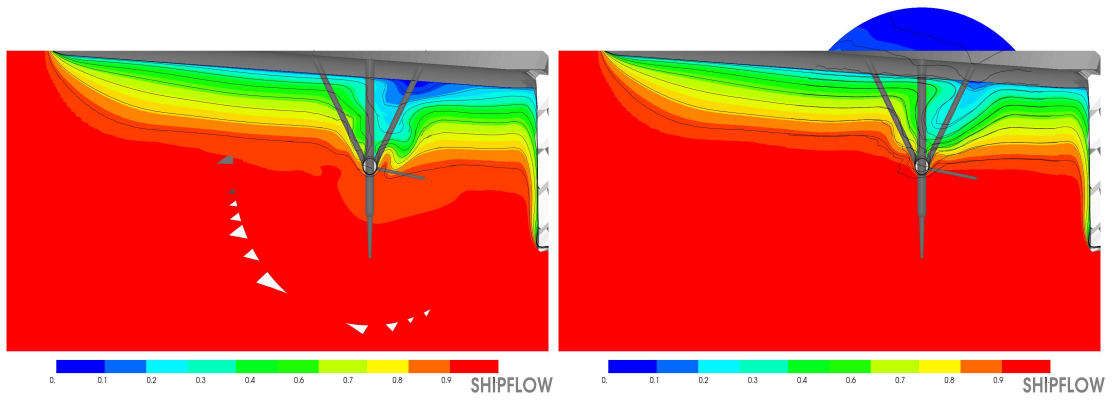


Fig. 4-14(e) Comparison of Wake in $U_x = 3$ (LS)

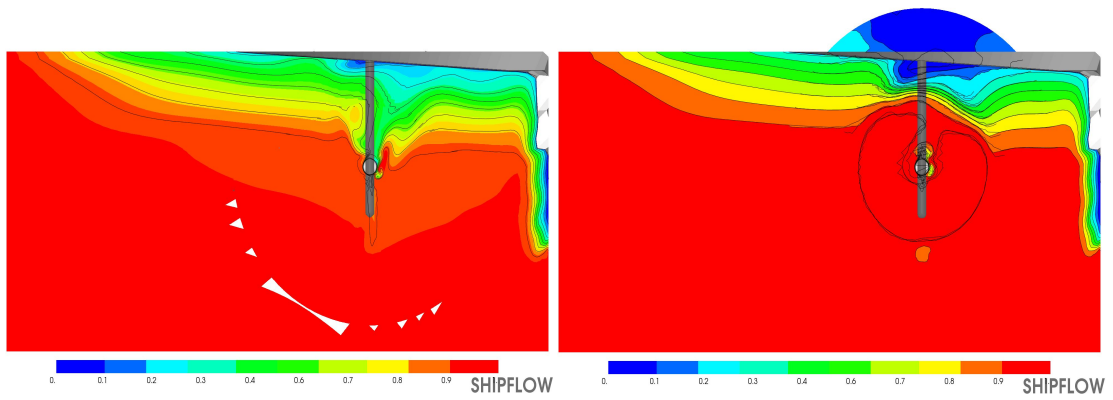


Fig. 4-15(a) Comparison of Wake in $U_x = 4$ (Bare Hull)

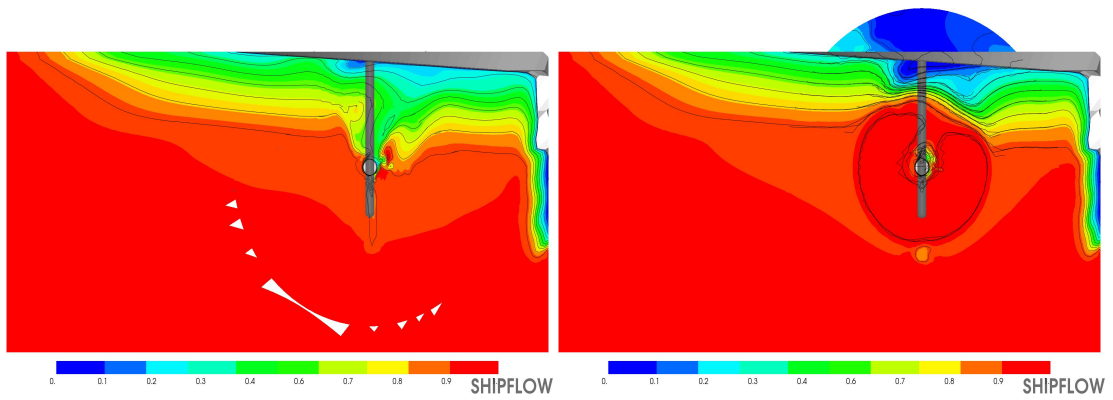


Fig. 4-15(b) Comparison of Wake in $U_x = 4$ (BF1)

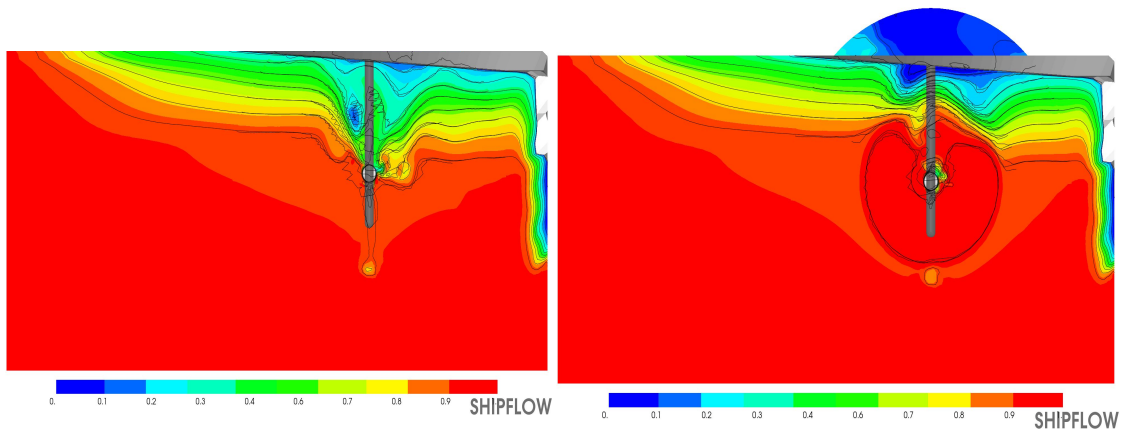


Fig. 4-15(c) Comparison of Wake in $U_x = 4$ (BF2)

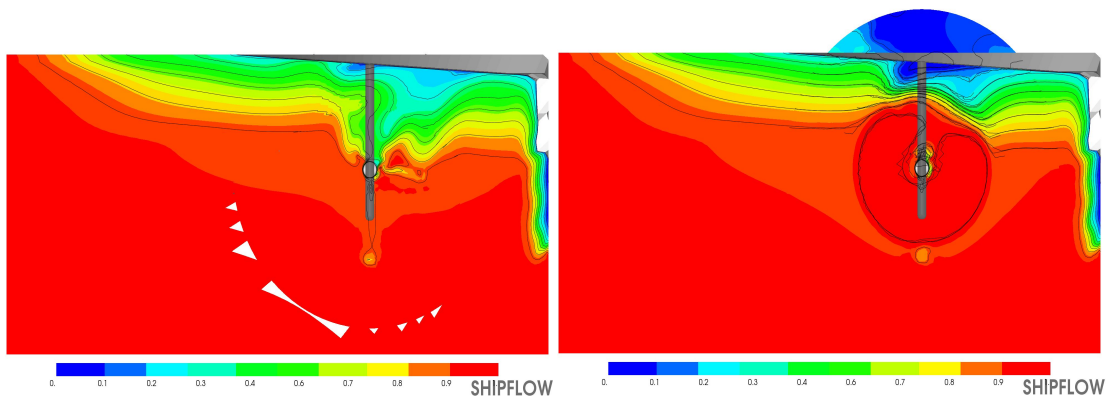


Fig. 4-15(d) Comparison of Wake in $U_x = 4$ (BF1+LS)

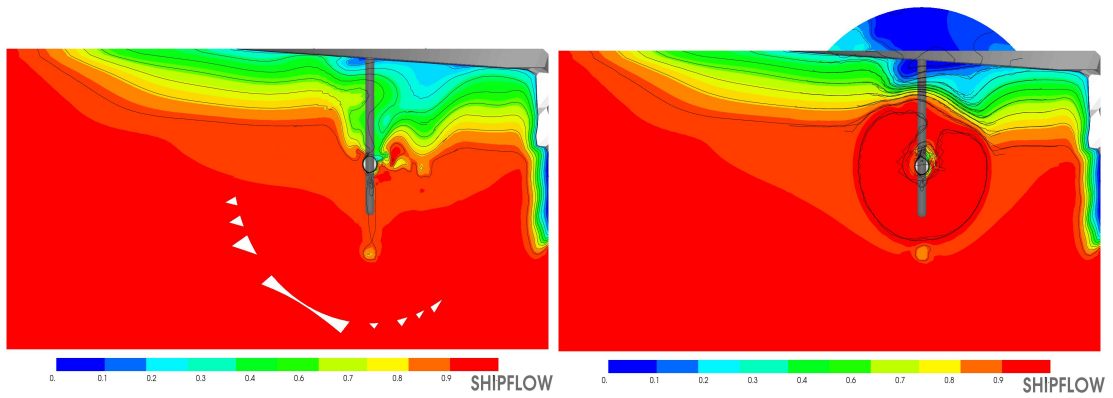


Fig. 4-15(e) Comparison of Wake in $U_x = 4$ (LS)

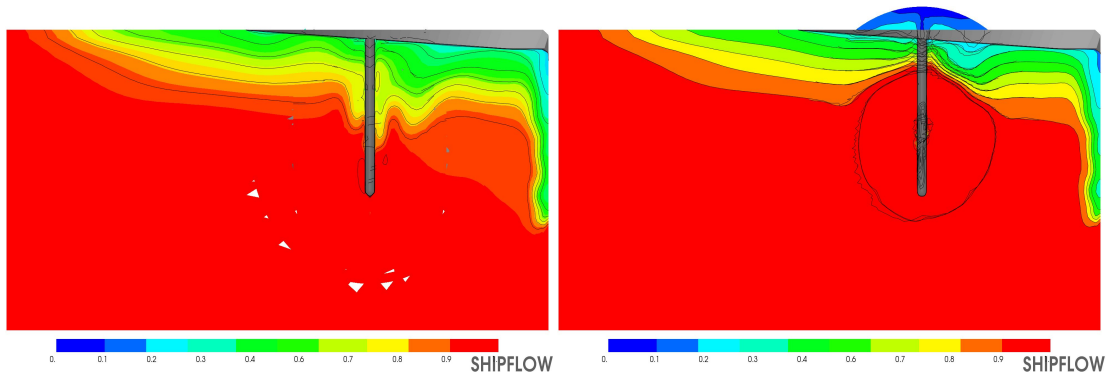


Fig. 4-16(a) Comparison of Wake in $U_x = 5$ (Bare Hull)

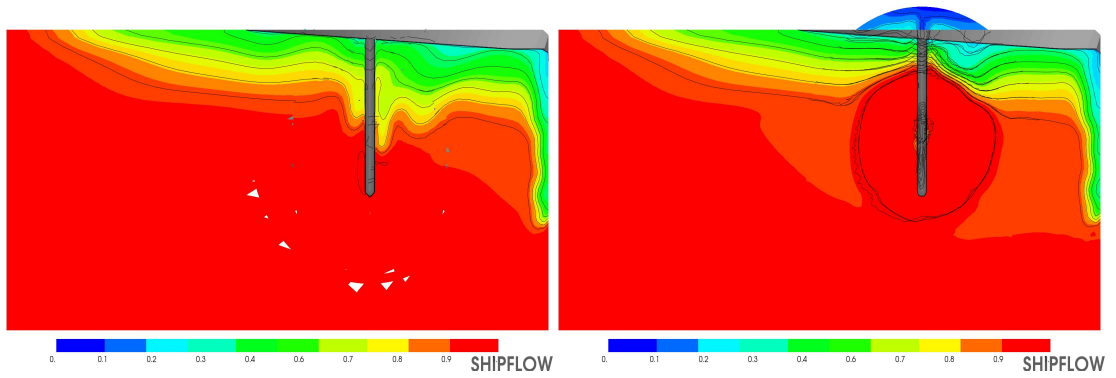


Fig. 4-16(b) Comparison of Wake in $U_x = 5$ (BF1)

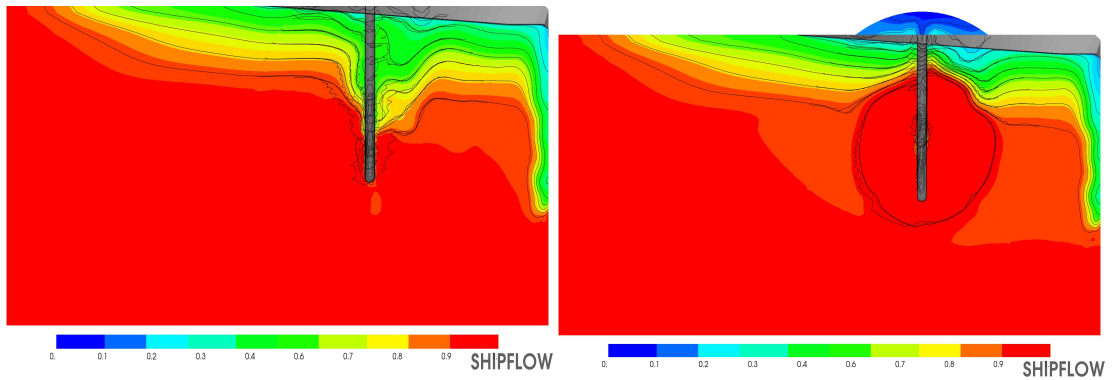


Fig. 4-16(c) Comparison of Wake in $U_x = 5$ (BF2)

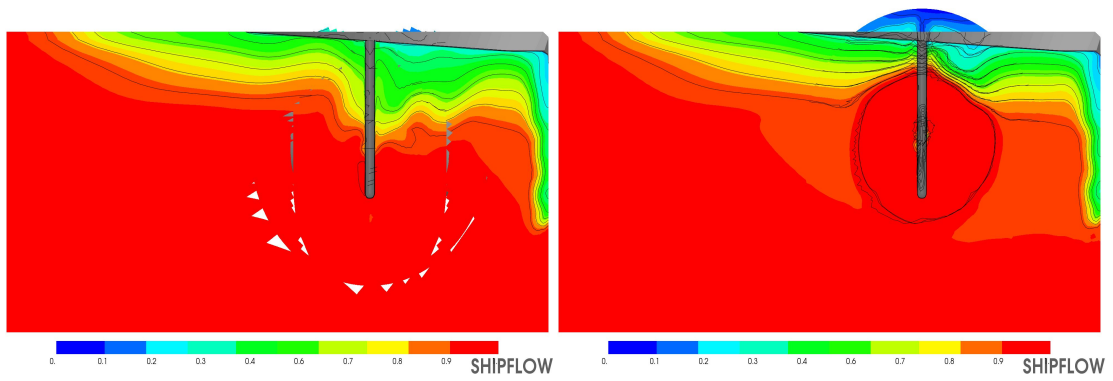


Fig. 4-16(d) Comparison of Wake in $U_{x=5}$ (BF1+LS)

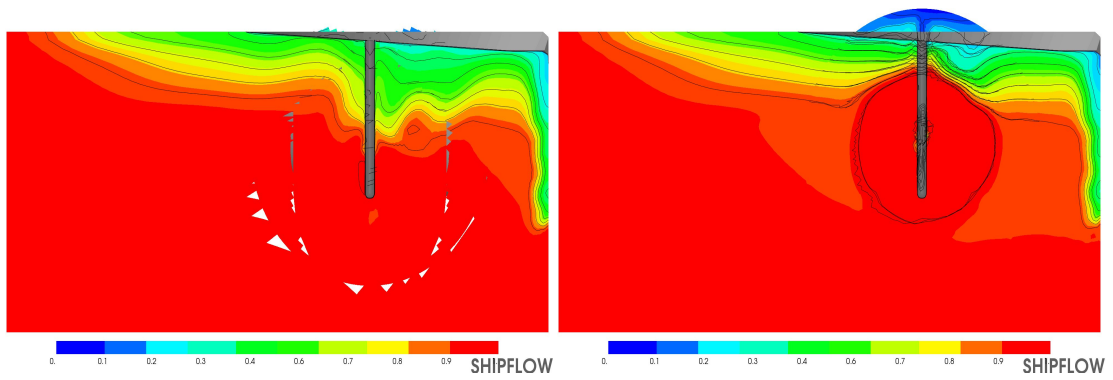


Fig. 4-16(e) Comparison of Wake in $U_{x=5}$ (LS)

V. Model Test

A. Test facility

- Model tests are carried out in the towing tank of Hiroshima Univ.

The towing tank has the following main particulars:

Basin	L X B X D	100×8(partly10)×3.5m
Carriage	Speed	3m/s



Fig. 5-1 Photo of Towing Tank of Hiroshima Univ.

B. Hull model

The dimensions of full scale ship and model are presented in Table. 5-1.

Table 5-1 Main dimension of ship and model

	scale	17
	ship	model
Loa	69	4.059
Lpp	57	3.353
Bmax	15	0.882
Bmould	13	0.765
Depth	2.9	0.171
draft	1.8	0.106

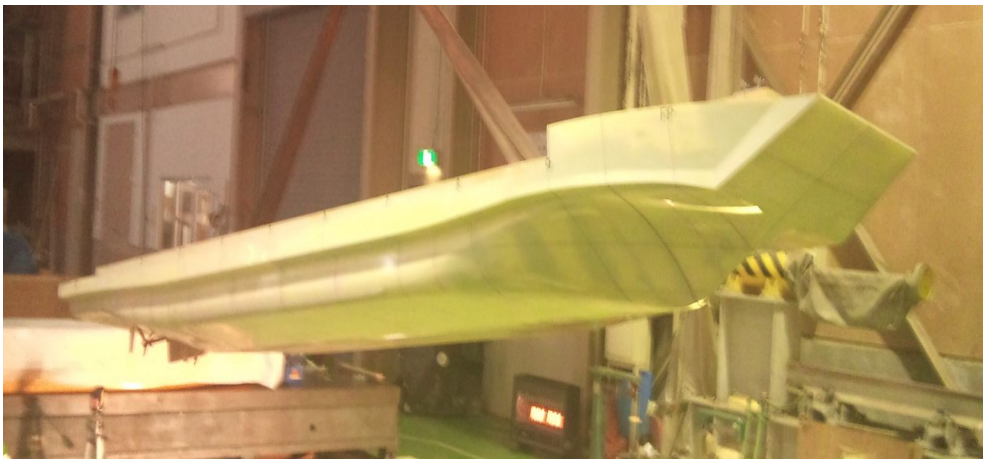


Fig. 5-2 Hull model

C. Propeller model

– Manufactured propeller models are outward turning twin screw, four bladed propeller with characteristics as shown in Table. 5-2.

Table 5-2 Main characteristics model propeller

Characteristic	Value
Diameter model scale	0.1 m
Diameter full scale	1.7 m
Pitch ratio P/D at $r/R = 0.75$	0.7
Blade area ratio AD/A_0	0.7



Fig. 5-3 Propeller model

D. Extrapolation by ITTC78 and modified ITTC78 method

In case of without the complex appendage mounted the predictions were made according to the 1978 ITTC extrapolation method.

With the complex appendage mounted a somewhat modified wake scaling was used. The method has been discussed at the meeting in 1999 ITTC and tentatively accepted for the case of evaluation of pre-swirl stator concepts. The wake scaling presumes that tests with the same propeller but without the stator have been performed as well. The difference between model effective wake with stator and the model wake without stator is considered as a potential wake created by the stator.

The hull potential wake and the frictional wake are scaled as for the model with -out stator according to the ITTC - 78 method, to which the stator potential part is added. The amount 0.04 represents the potential wake created by the rudder at the location of the propeller.

Thus is in the modified ITTC 1978 extrapolation the full scale wake.

$$W_{Tsw} = (t_{wo} + 0.04) + (W_{Tmwo} - (t_{wo} + 0.04)) \\ * [(1+k)C_{Fs} + \Delta C_{Fs} / (1+k)C_{Fm}] + [W_{Tmw} - W_{Tmwo}]$$

where,

"W" stands for "with complex appendage"

"wo" stands for "without complex appendage"

"m" stands for "model"

"s" stands for "ship scale"

"T" stands for "thrust identity"

The form factor is based on the case without complex appendage.

E. Result of model test

Model test has been performed in the towing tank with a 3.35m length model which scale is 1/17.

The full scale wake is calculated from the model wake W_{TM} , and the thrust deduction t :

$$W_{TS} = (t + 0.04) + (W_{TM} - t - 0.04) \times \frac{C_{Fs} + C_A}{C_{FMc}} \quad (1)$$

In the formula, the factor 0.04 is used to take account for rudder effect. If full scale wake

W_{TS} is greater than model wake W_{TM} , following formula is used.

$$W_{TM} = W_{TS} \quad (2)$$

Stator angle of attack and position had been decided based upon the CFD calculation results inflow angle and direction of flow at stator position. Self propulsion tests results are analysis by modified ITTC 78 prediction method. The results of the propulsion test are summarized in Table. 5-3 for the speed of 9.5 Knots. And the photographs of model test are presented in Fig. 5-4.



< 9 Knots >



< 10 Knots >

Fig. 5-4 Photographs of model test

Table 5-3 Comparison of the results of self-propulsion tests

	Bare hull ¹⁾ F_n	BF1	BF2
Trust deduction fraction(t)	0.141	0.141	0.179
Ship wake fraction(w)	0.176	0.185	0.228
Hull efficiency(η_H)	1.024	1.036	1.064
Relative rotative efficiency(η_R)	0.983	0.983	0.963
η_D	0.550	0.560	0.513

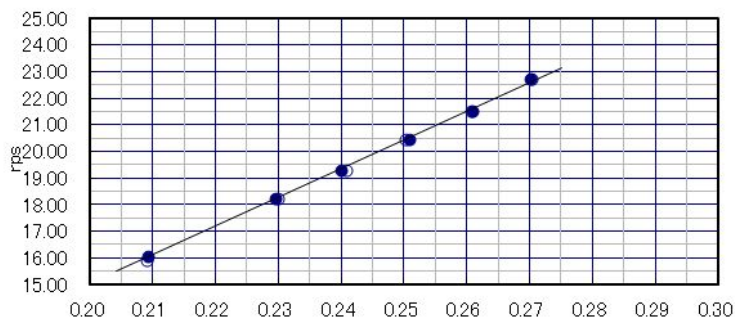


Fig. 5-5 Calibration of rps vs F_n

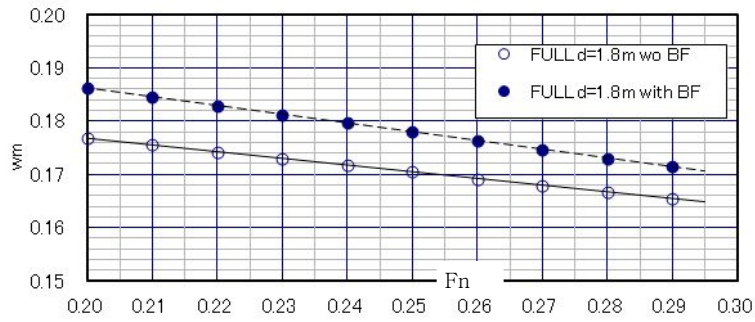


Fig. 5-6 Model wake(w_m) vs F_n for with and without BF1

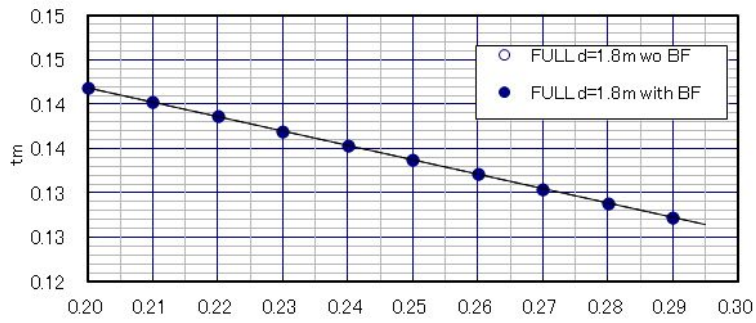


Fig. 5-7 t_m vs F_n for Without BF1 and With BF1 condition

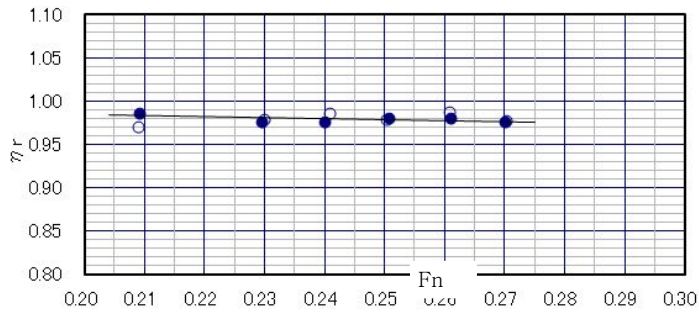


Fig. 5-8 η_r vs F_n for Without BF1 and With BF1 condition

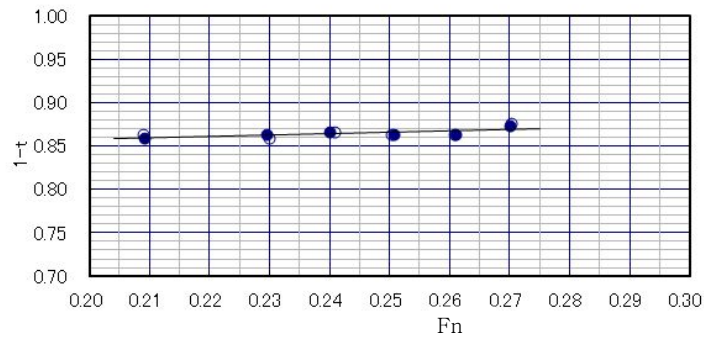


Fig. 5-9 $1-t$ vs F_n for Without BF1 and With BF1 condition

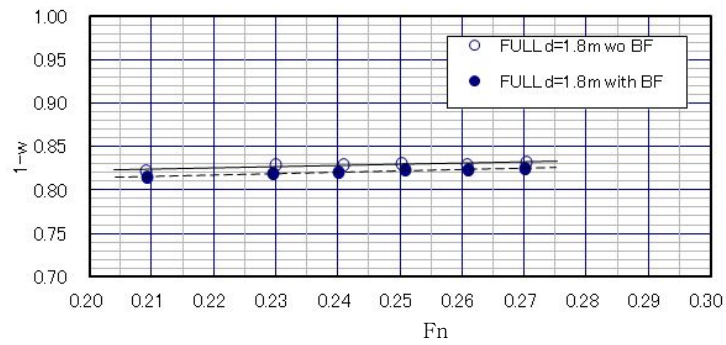


Fig. 5-10 $1-w$ vs F_n for Without BF1 and With BF1 condition

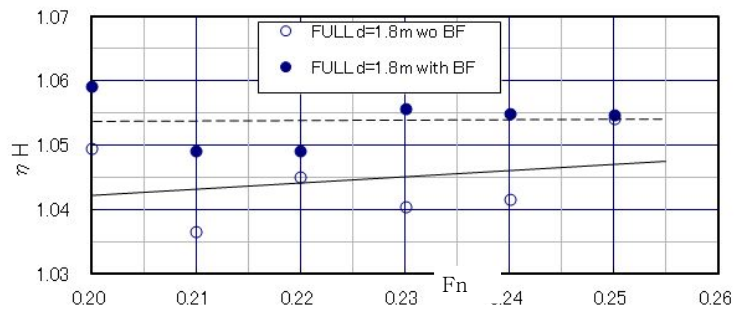


Fig. 5-11 η_H vs F_n for Without BF1 and With BF1 condition

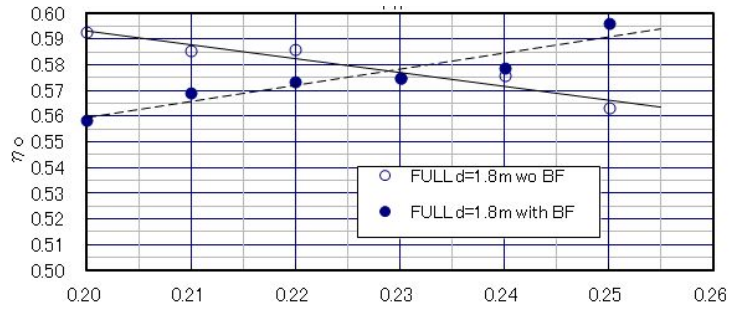


Fig. 5-12 η_o vs F_n for Without BF1 and With BF1 condition

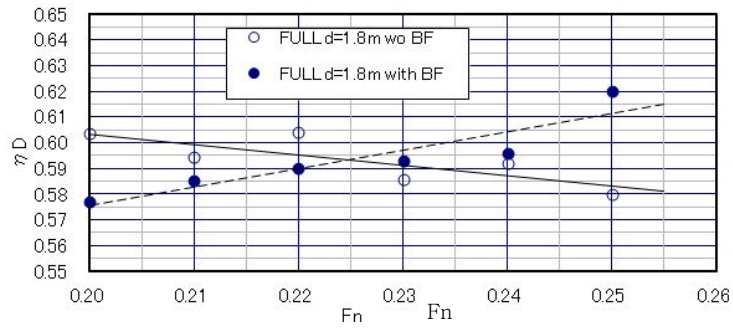


Fig. 5-13 η_D vs F_n for Without BF1 and With BF1 condition

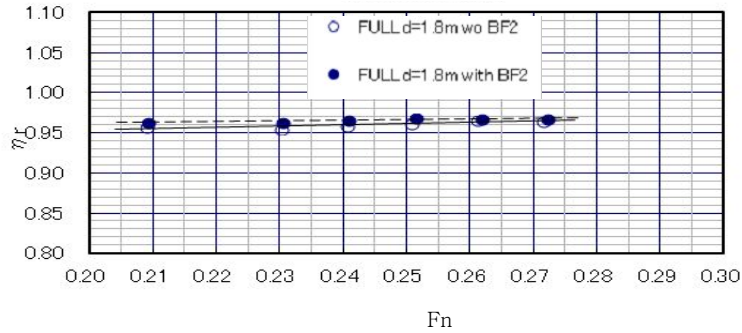


Fig. 5-14 η_r vs F_n for Without BF2 and With BF2 condition

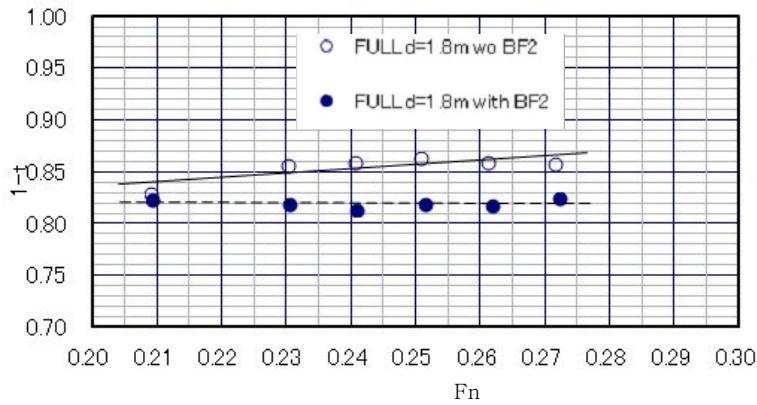


Fig. 5-15 $1-t$ vs F_n for Without BF2 and With BF2 condition

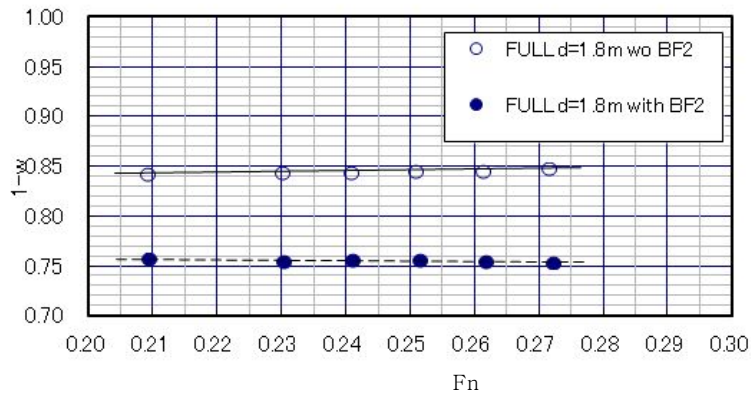


Fig. 5-16 $1-w$ vs F_n for Without BF2 and With BF2 condition

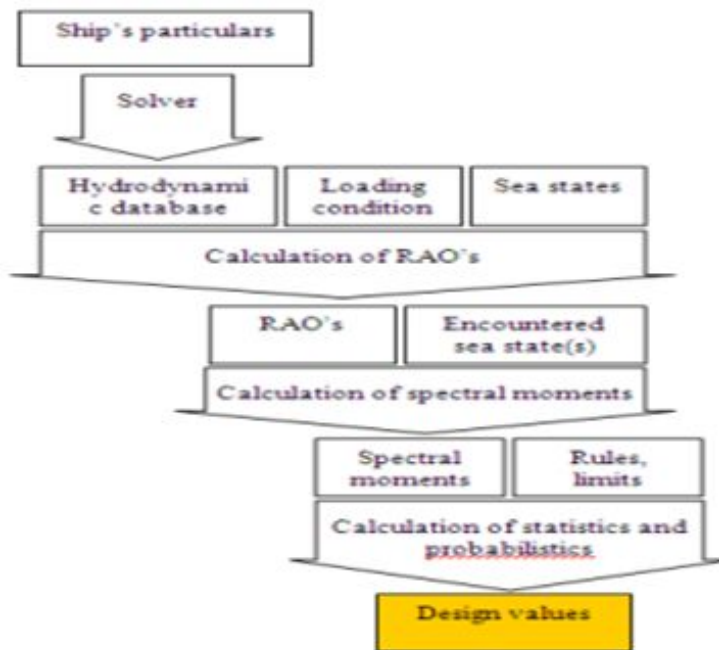
The results show the reduction of trust deduction coefficient(t) and wake fraction(w) for the case of appended hull by which hull efficiency(η_H)increased slightly. The relative rotative efficiency(η_R) decreased. It seems that this low η_R is the effect of relatively worse irregular wake field by the rotation of propeller.

VI. Check the seakeeping performance

Purpose of this study is predicting the responses of a ship in a particular sea state. 'Responses' being the motions of the ship: roll, pitch, yaw, surge, sway and heave; as well as the consequences of these motions such as bow slamming or Green water on deck, propeller emergence, crew and passengers suffering from motion sickness, loss of cargo, etc. The prediction of these responses is indispensable to determine how good a ship is with respect to sea-keeping. Poor performance in sea-keeping means different things for different vessels. Reduced fuel consumption and cargo capacity mean nothing if the ship cannot perform the task it was intended to in the oceans it was built for.

Objectives of this study are calculate the response amplitude operators of a ship for different loading conditions, configure the derived responses of a ship (slamming, propeller emergence, etc.), obtain a wave scatter diagram representative for the area/voyage share a ship operates and predict the responses of a ship in several sea states and understand what they mean for the ship's operability.

The analysis sequence of used software, Octopus is shown in following Figure. The obtained design values may serve as the criteria which should not be exceeded during the transport or operation. The calculated models and design values can be used in Octopus Onboard give onboard operational support using the same methods and results as used in design value calculation procedure.



This (statistical) data is specifically aimed at describing the wave environment. Either by means of a voyage, which can be matched in space and time with a wave climate database, or by a scatter diagram, or simply a set of design sea states.

A wave scatter diagram by calculation shows the probability of a wave combination of H_s and T_z .

Input of Loading Condition is as shown in Table and calculation result of Loading Condition is as shown in following Fig. 6-1.

Table 6-1 Dimension of ship

Name	Value
Mass[T]	1142.28
Draft Aft[m]	1.80
Draft Fwd[m]	1.80
LCG[m]	29.96
ZCG[m]	0.87
$R_{x,0}$ [m]	4.55
$R_{y,0}$ [m]	15.06
$R_{z,0}$ [m]	15.40
GM[m]	9.78
GG'[m]	0.0

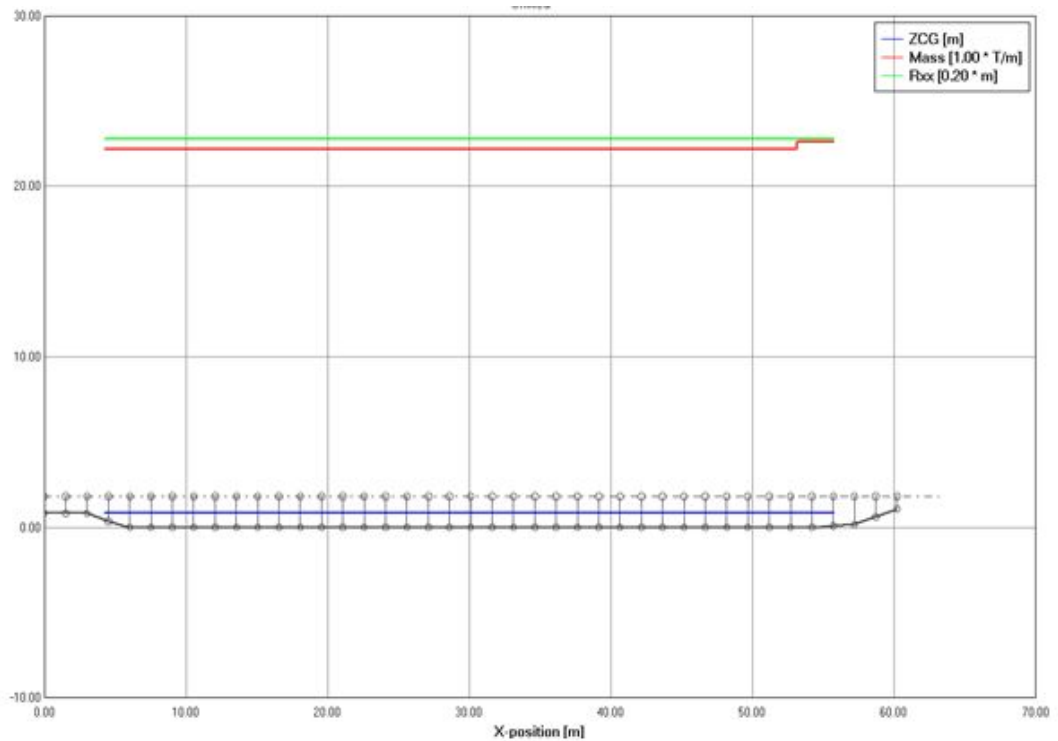


Fig. 6-1 Calculation result of Loading Condition

External condition can be defined in matrixes(6x6) for mass, added mass, damping and restoring coefficients. Added mass, damping and restoring coefficients matrixes can be defined for each combination of speed and encounter frequency. If an external condition is not defined relative to the coordinated system with 0 point at (APP,CL,BL) than is not necessary to recalculate all matrixes. The translation to (APP,CL,BL) can be given at the definition of the coordinate system.

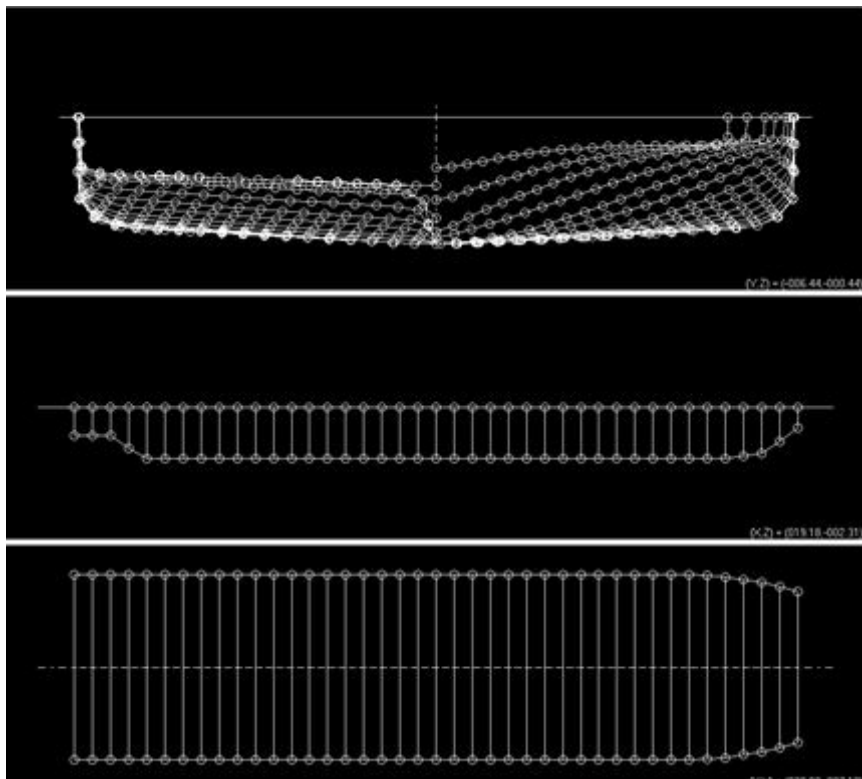


Fig. 6-2 Matrixes of ship

A hydrodynamic analysis starts with the calculation of a hydrodynamic database (HDB). The hydrodynamic database does not depend on parameters like ship mass, viscous damping or spring restoring parameters. These become important when RAO's are calculated.

RAO is an abbreviation of 'Response Amplitude Operators'. The RAO delivers the

response motion per unit wave height. Calculating a RAO requires a hydrodynamic database. In the Hydrodynamic database draft, speed, heading, and frequency dependent parameters were stored. The RAO requires that restoring parameters, viscous damping, and a load distribution are known. Basic responses are always required. The basic responses are motions of the motion reference point (surge, sway, heave, roll, pitch, yaw)

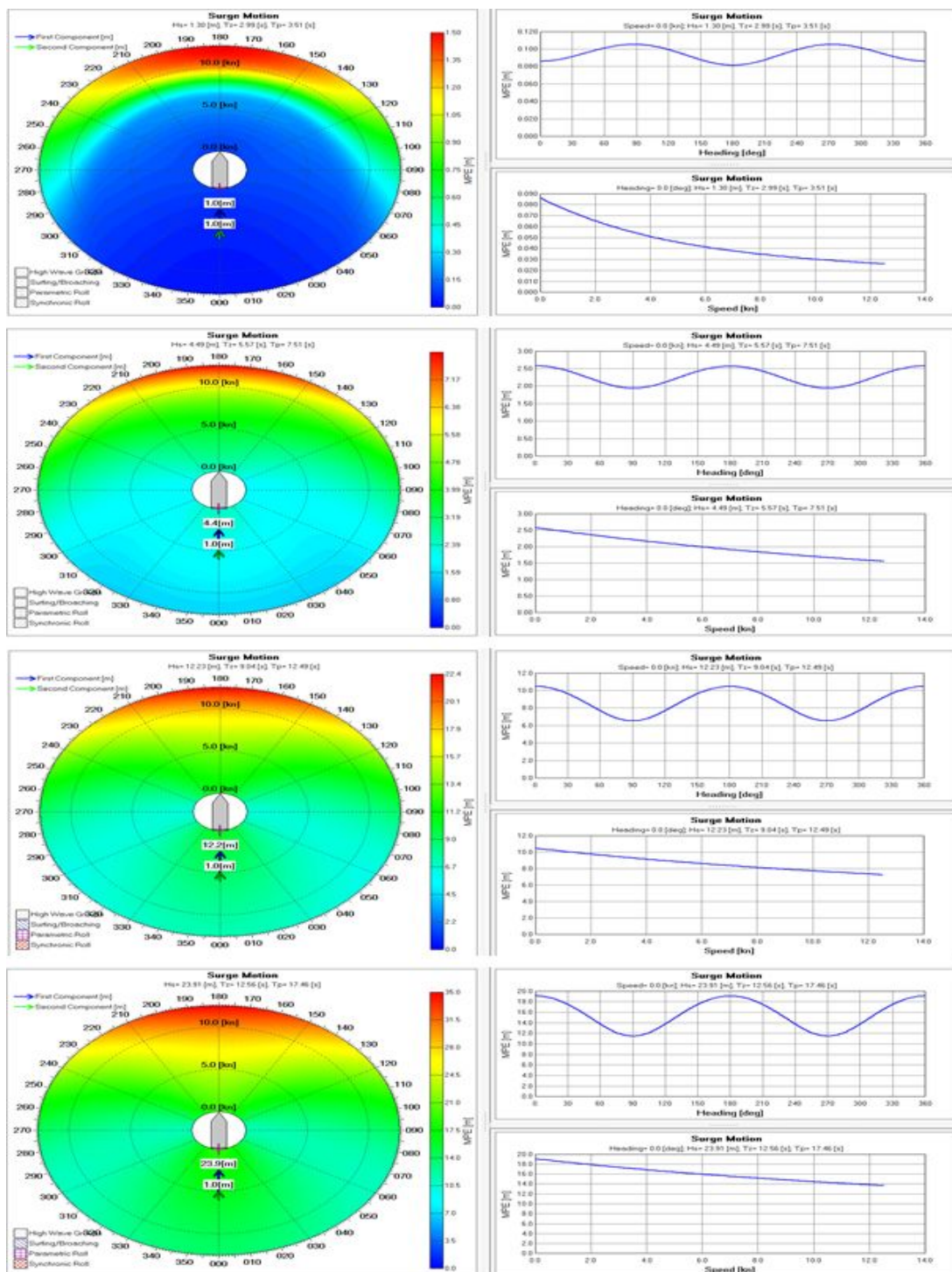
Input of RAO-response is as shown in following Table 6-2.

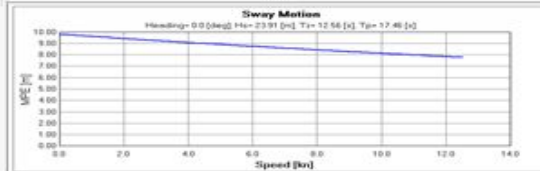
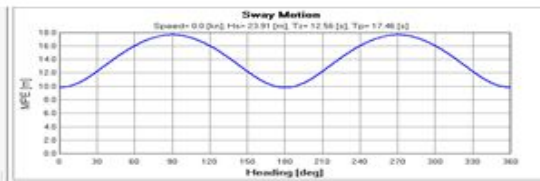
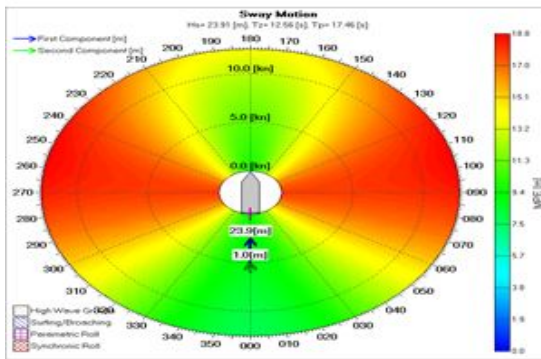
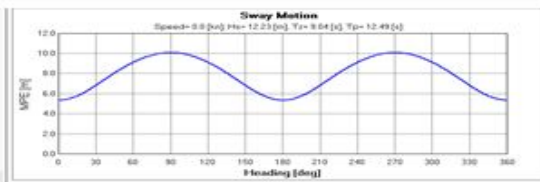
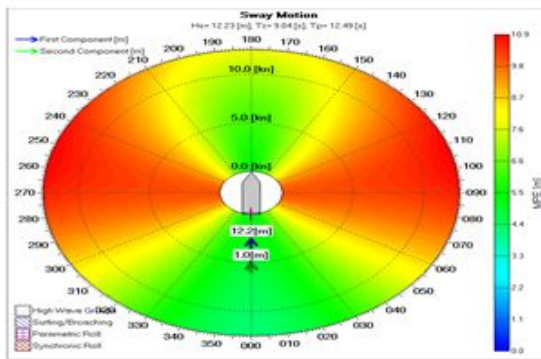
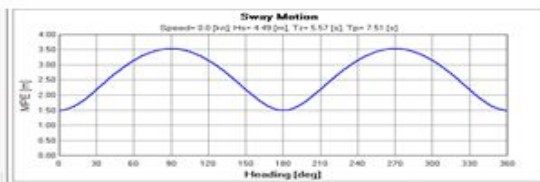
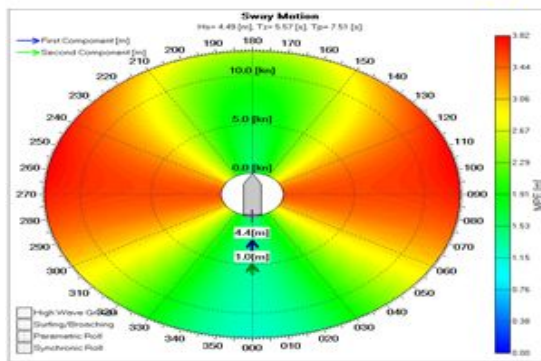
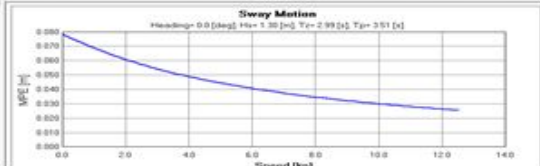
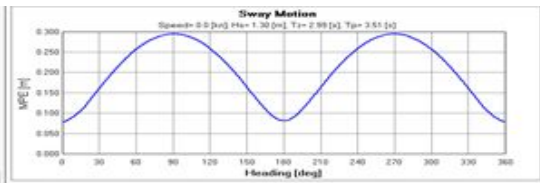
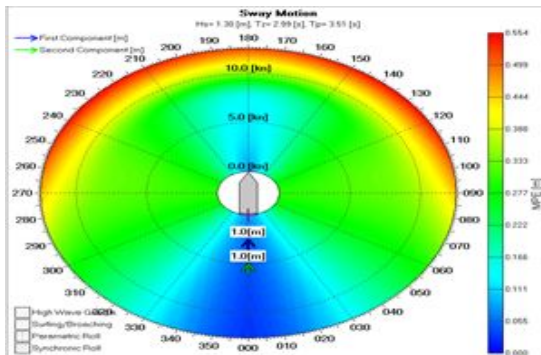
Table 6-2 Input of RAO-response

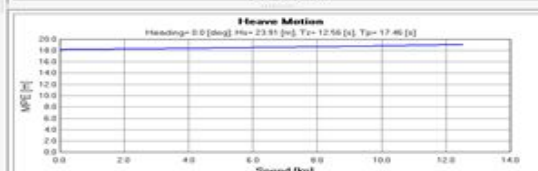
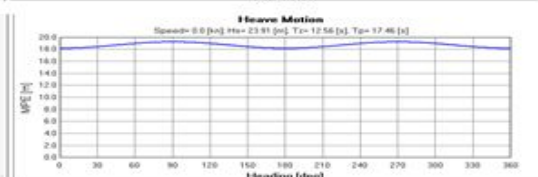
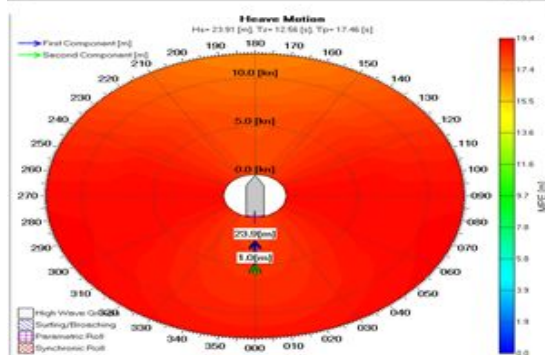
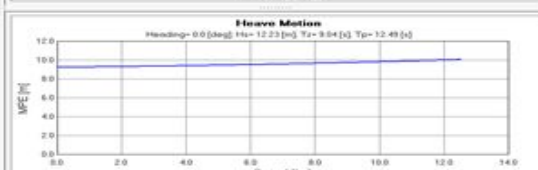
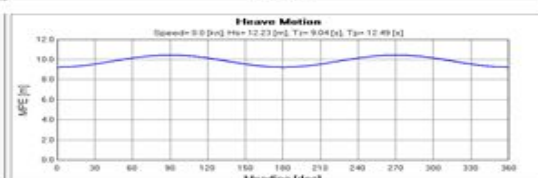
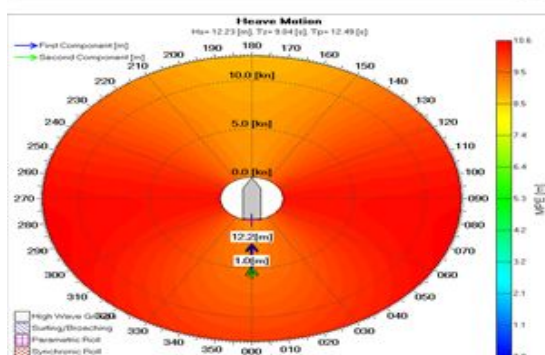
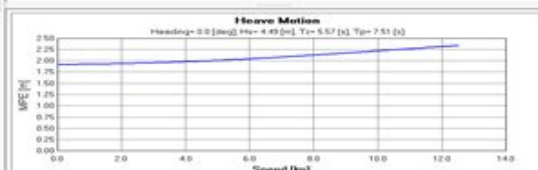
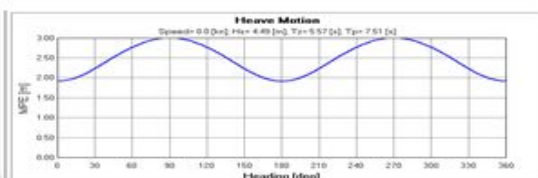
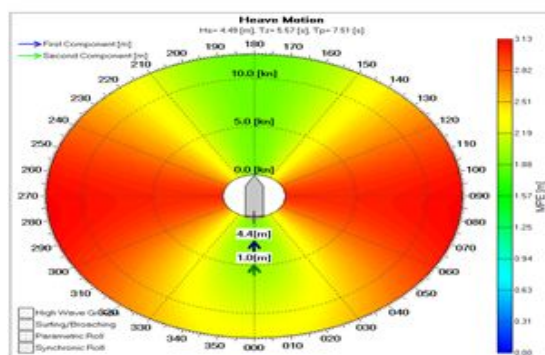
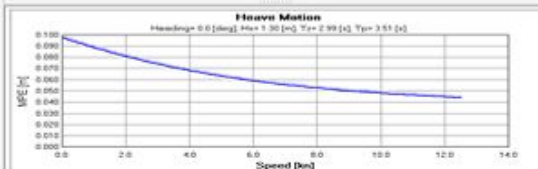
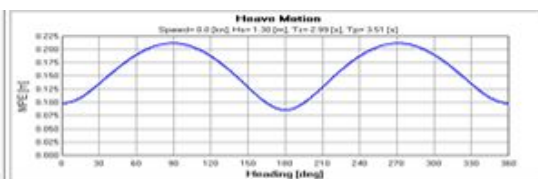
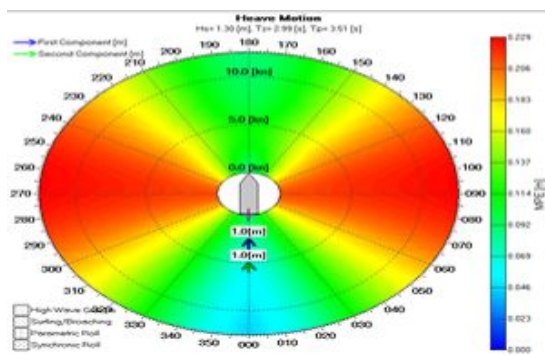
Name		Value		
S e c t i o n a l Loads	Plane	XZ-Plane		
	2.337		0	
Point response	(x , y , z) coordinates[m]	50	0	25
C o m b i n e d response	Unit	n/hr		
	Response	Factor	Derive	
	1	None		

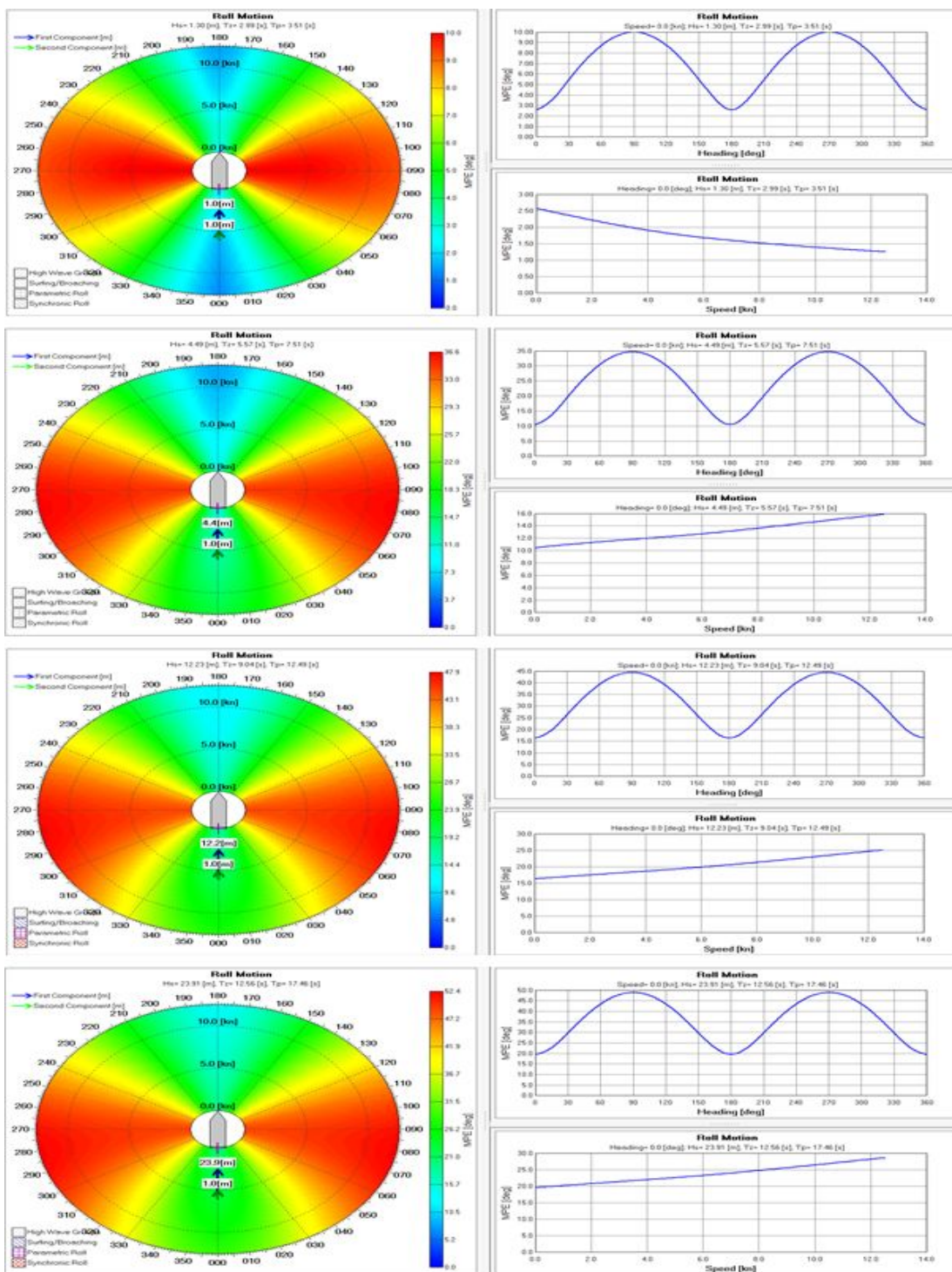
Short term statistics is calculated for the reference period give earlier when setting up the configurations and reponses. The values displayed in the plots will be different if another reference time is selected. MSI refers to the Motion Sickness Studies done by O'Hanlan and McCauly taken into ISO2631. Slamming criteria are defined according to the theory by Ochi. Note that when using the slamming operators, Slamming should also be inserted as a response in the response configurations including the relative motion at 0.90L. Level is used as a maximum value (criterion) for the diagram. By default level has the value of criterion as configured in Statistics Configuration.

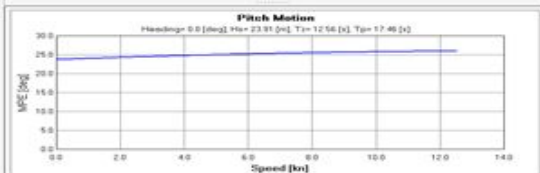
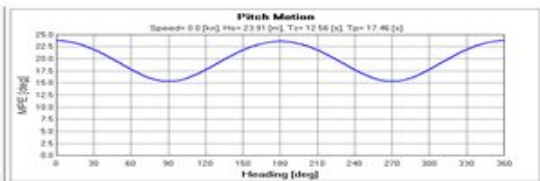
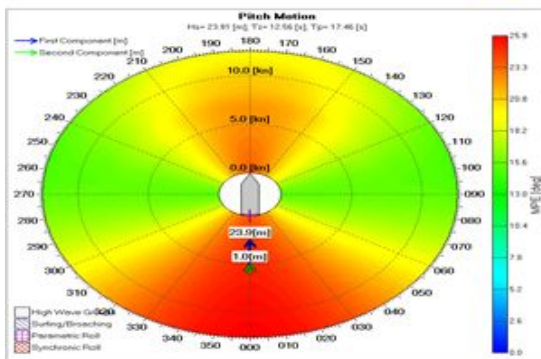
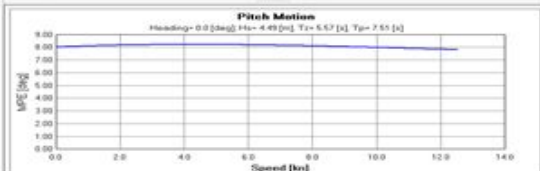
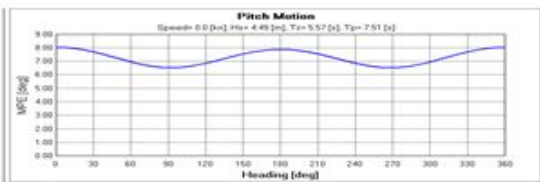
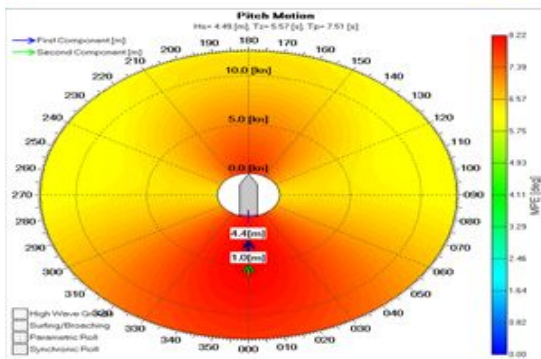
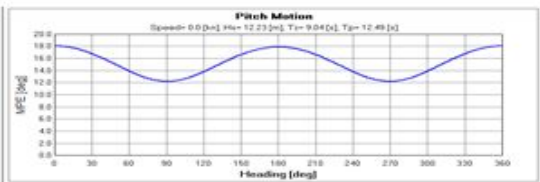
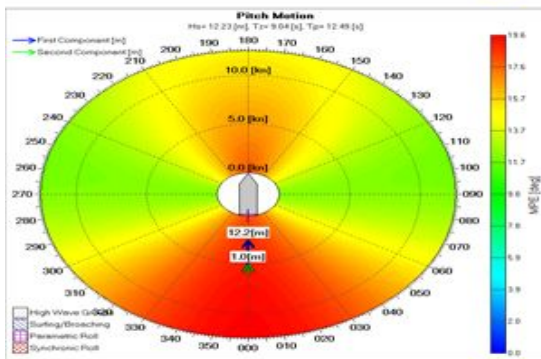
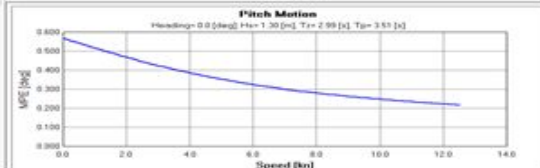
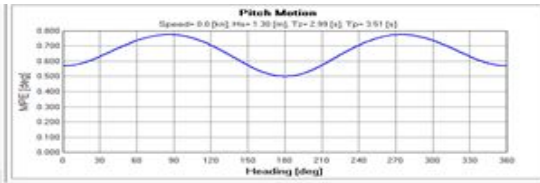
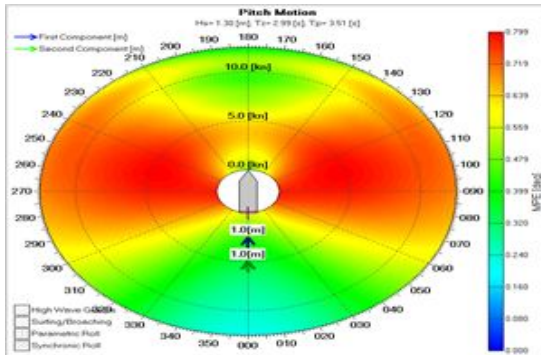
The calculated RAO is presented in a graphical way as shown in followng figures.











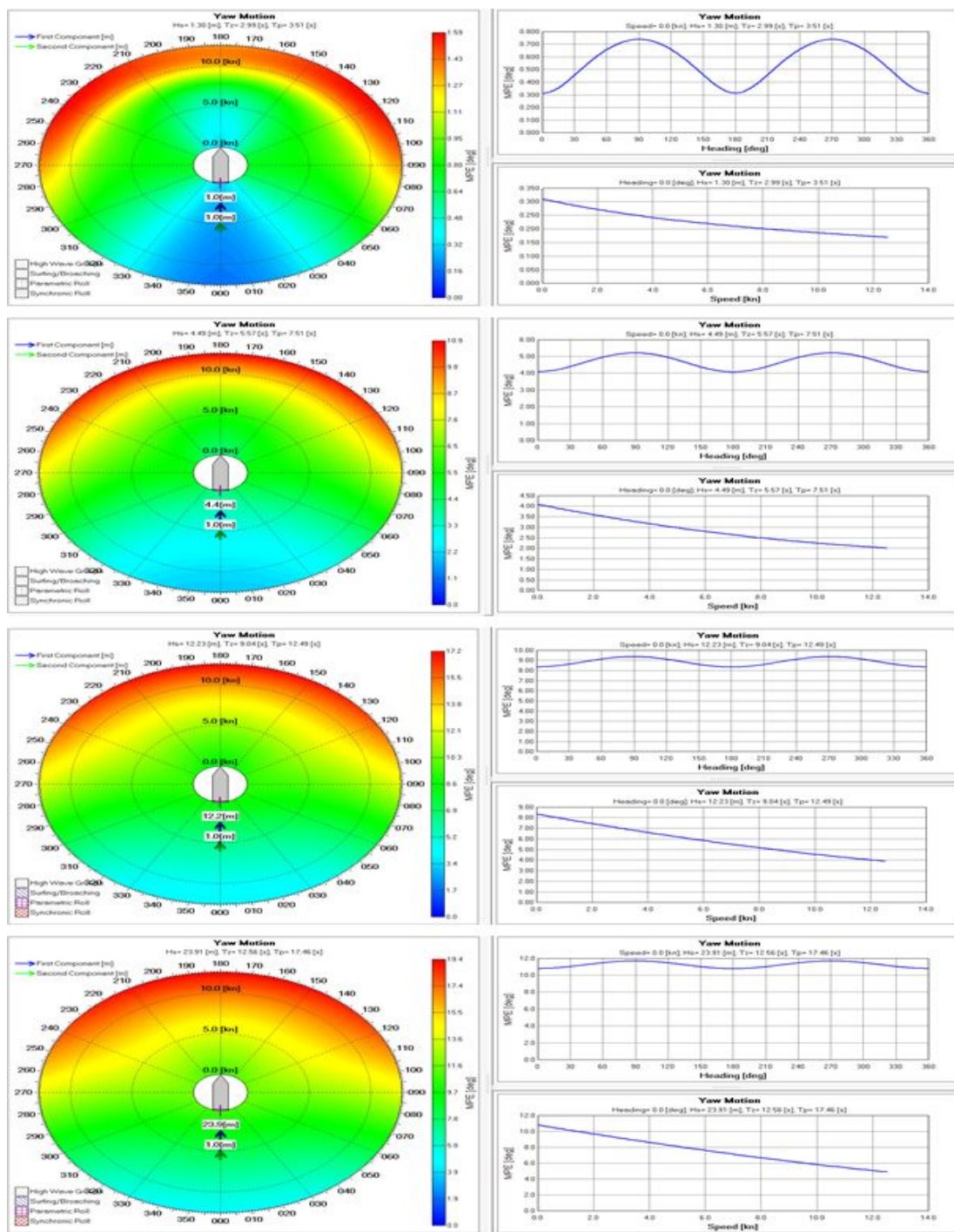
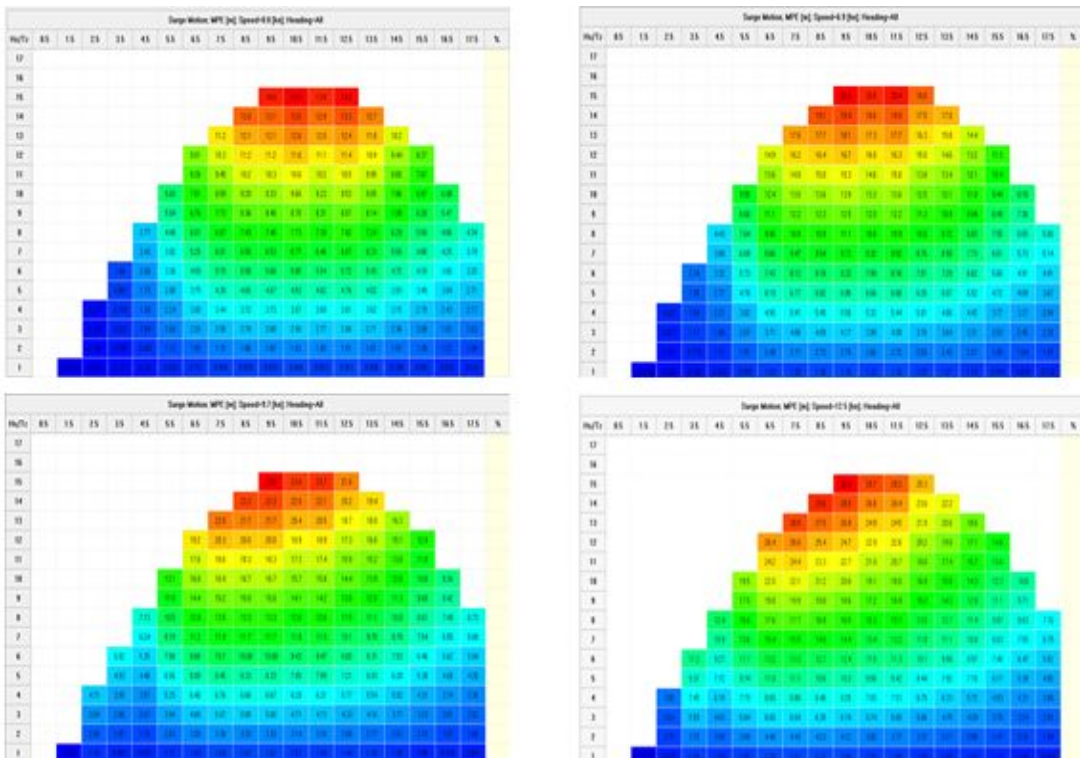
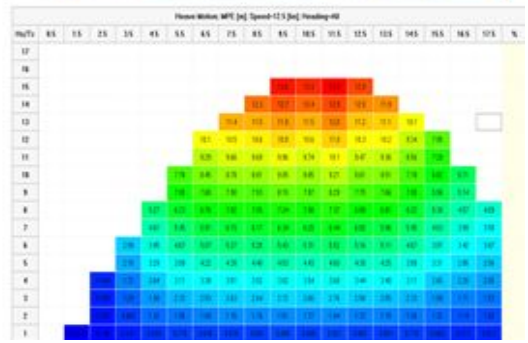
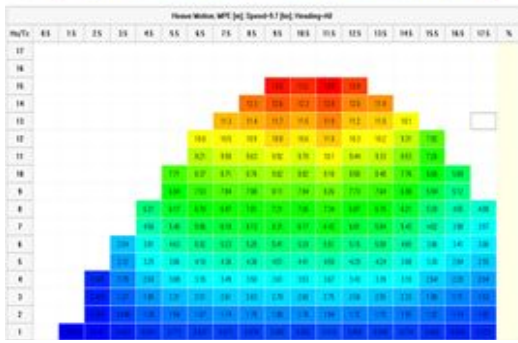
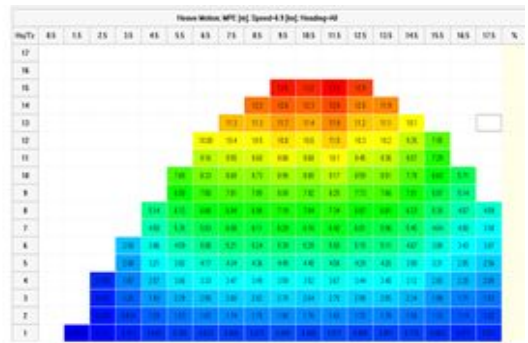
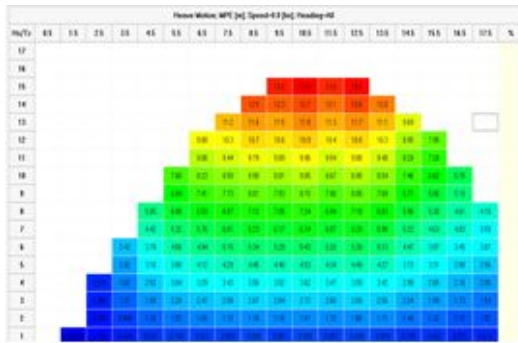
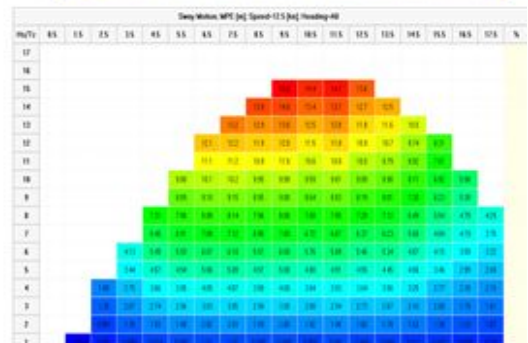
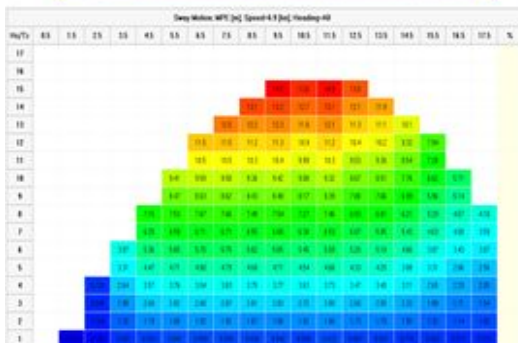
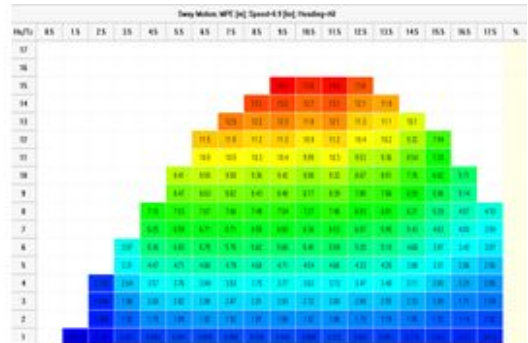
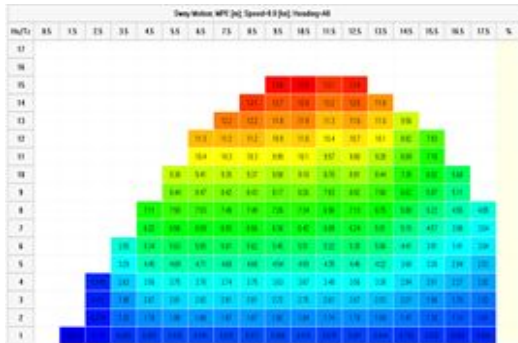


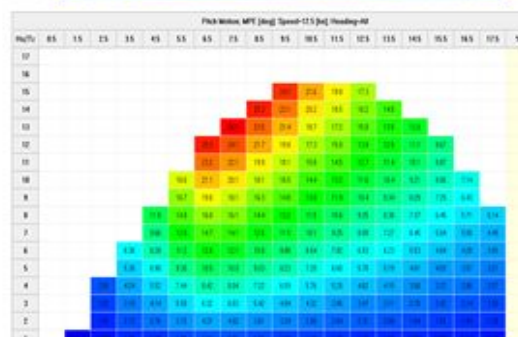
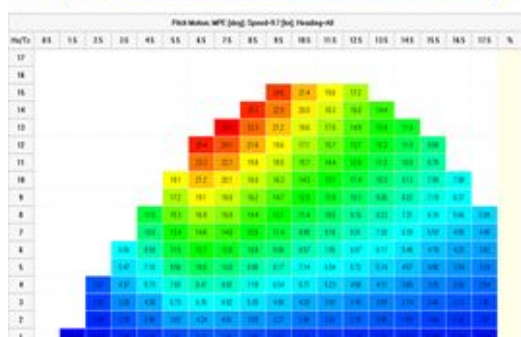
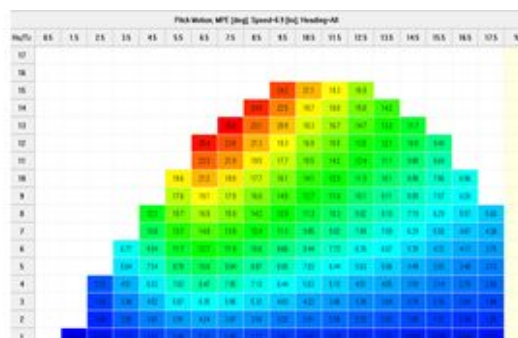
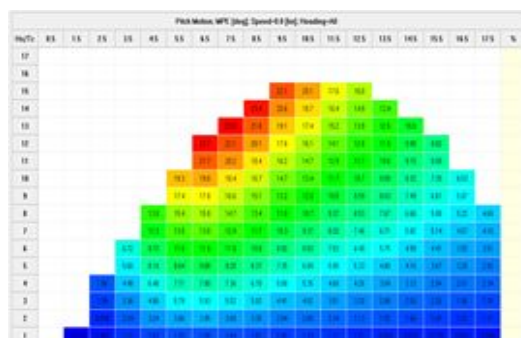
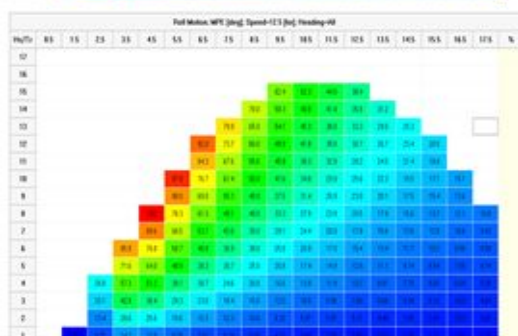
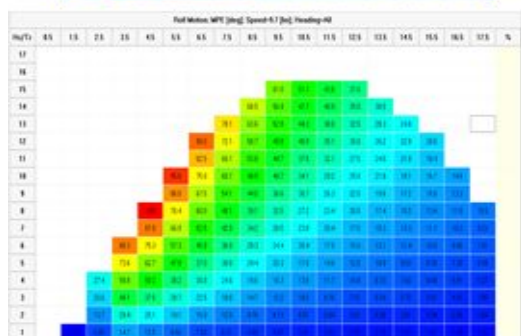
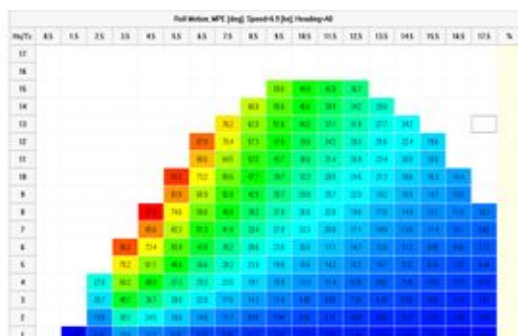
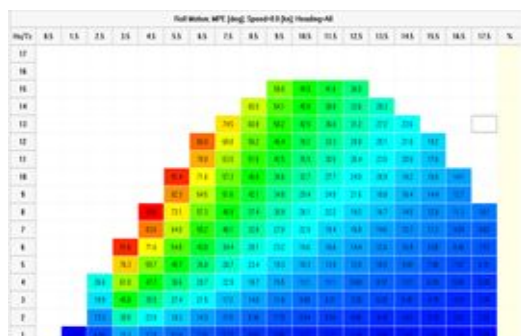
Fig. 6-3 Calculated RAO

SEAWAY is a strip theory based program to calculate the hydromechanical parameters, wave forces, Response Amplitude Operators, Statistics, and added resistance due to waves. These had to be investigated earlier by doing tank tests. Statistics enable a sea state to be properly modelled in a summation of a selection of random waves (frequency, height, etc). Via known RAO one can calculate the statistics of the response of the vessel, motion point, etc... Before statistical calculations can be performed, sea state should be modelled under Common in the project tree. Sea states can be modelled in a spectrum, scatter diagram, or can be imported from a 3rd party.

The results are visible in a numerical and graphical way, see tabs: General, Sea Condition, Short Term and Long Term as shown in Fig. 6-4.







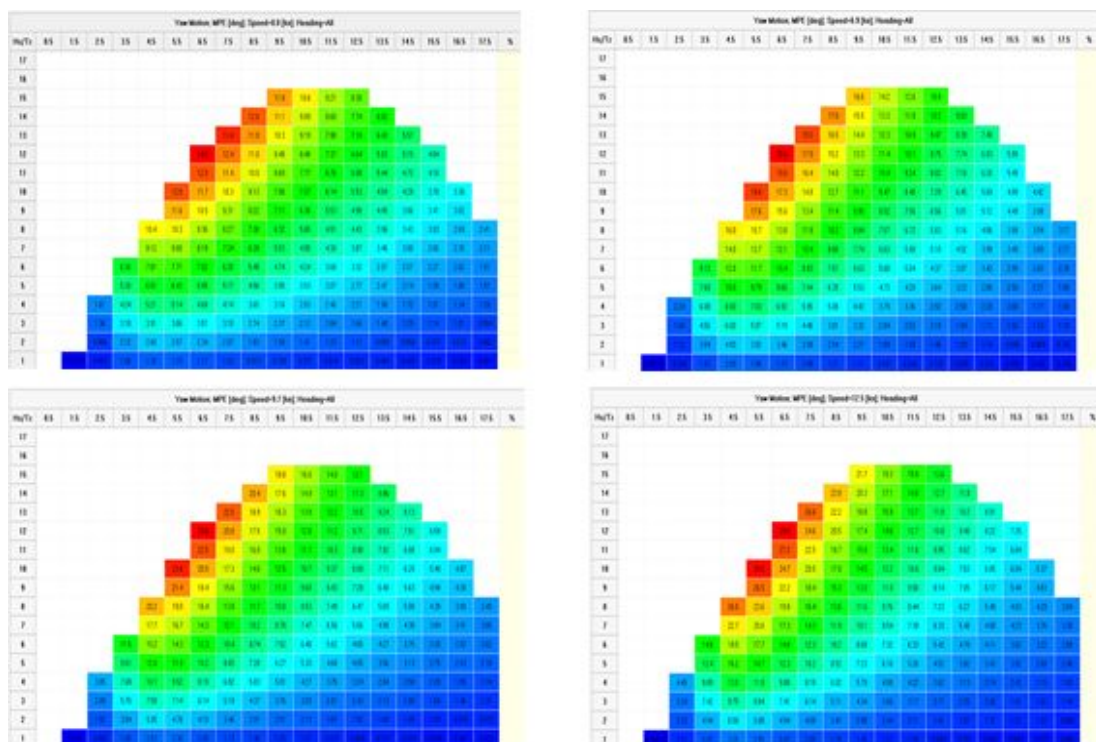
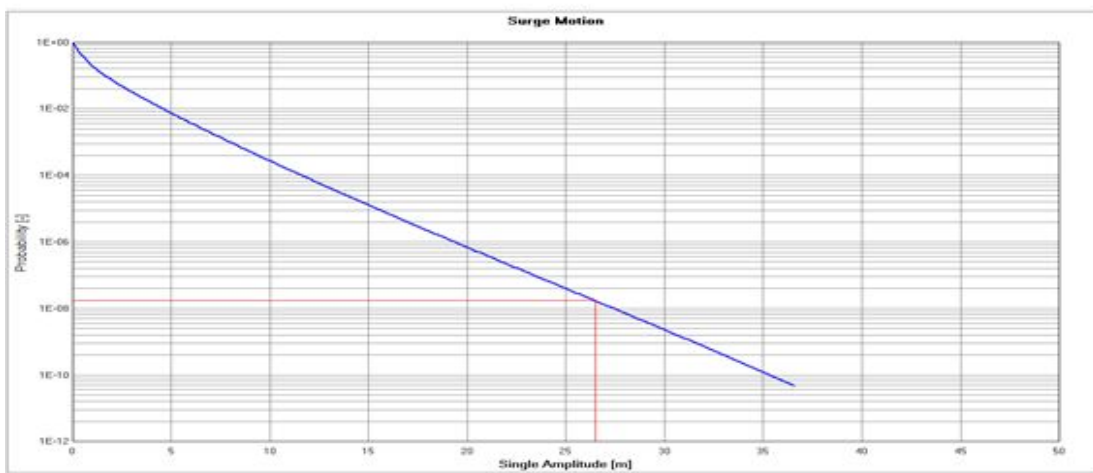
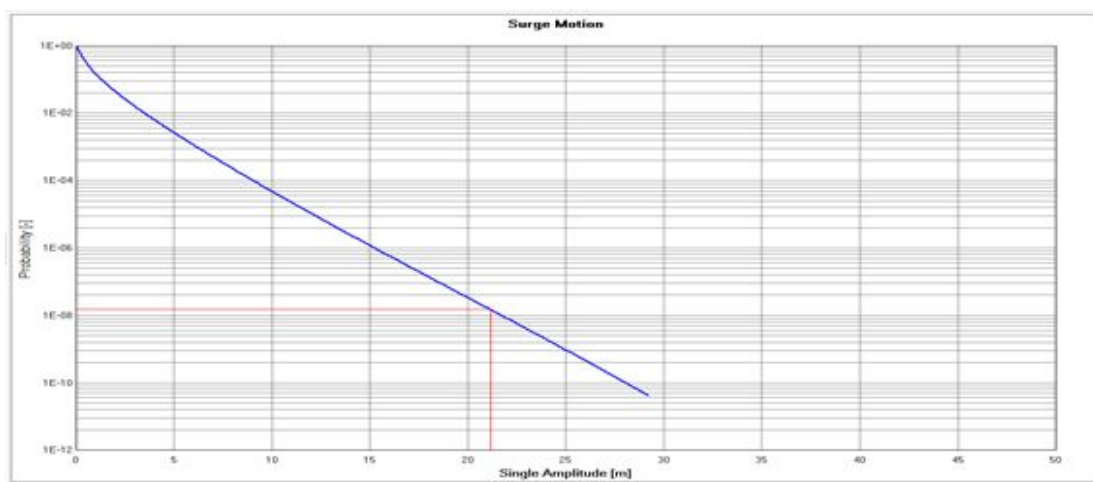
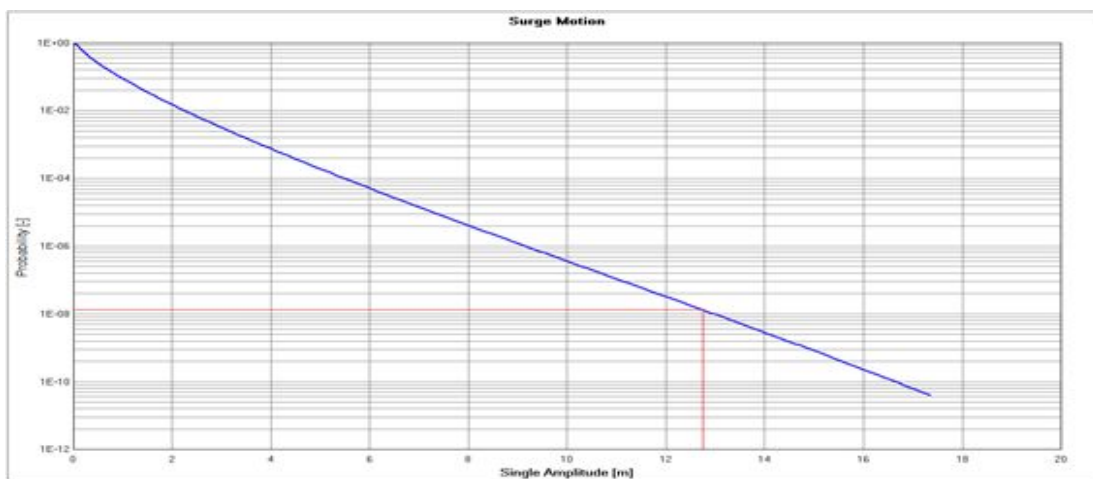
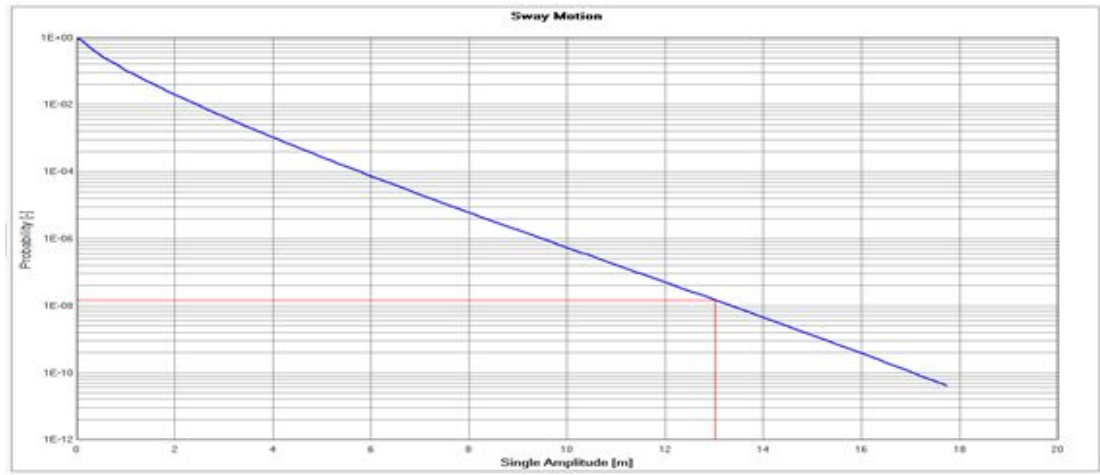
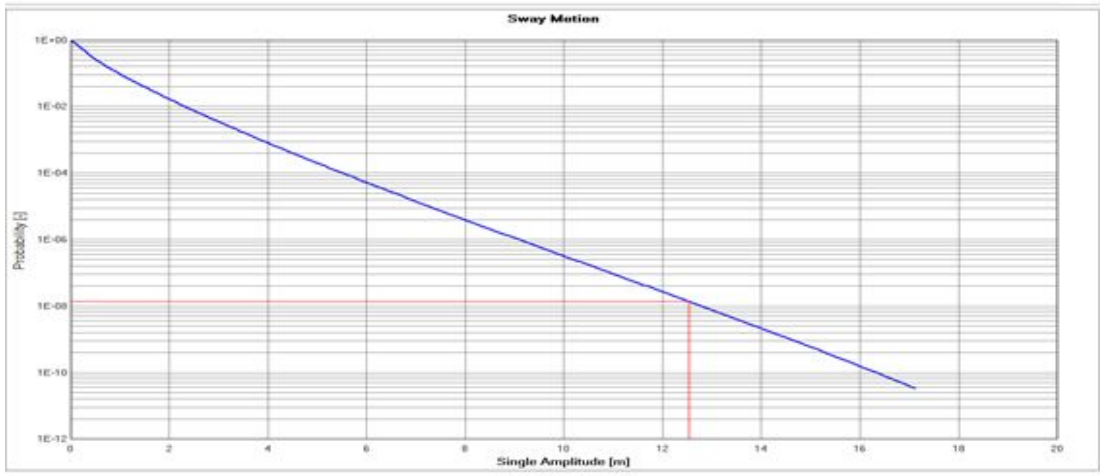
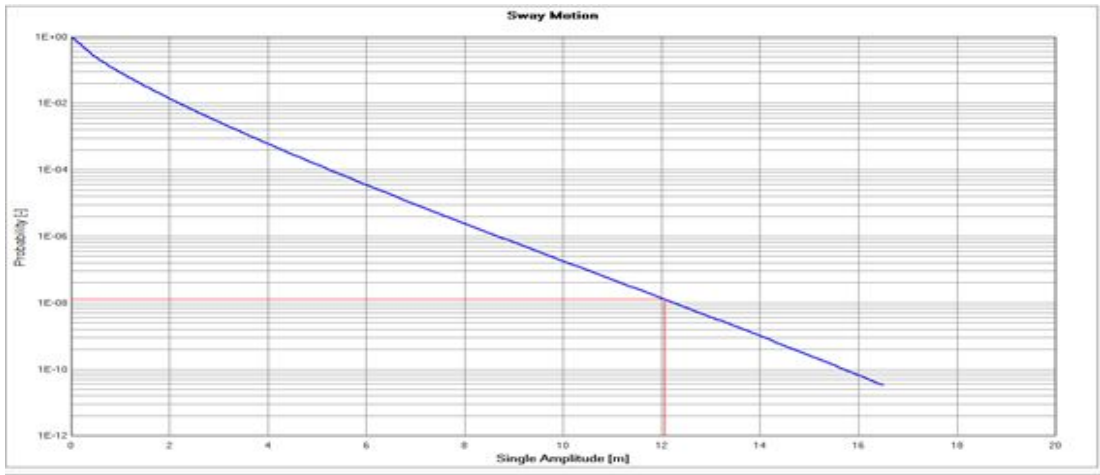
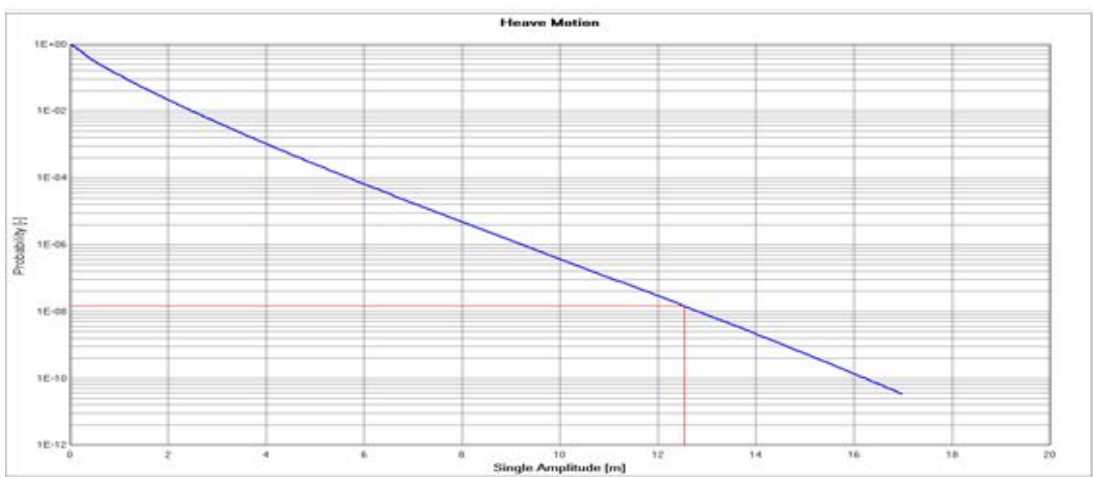
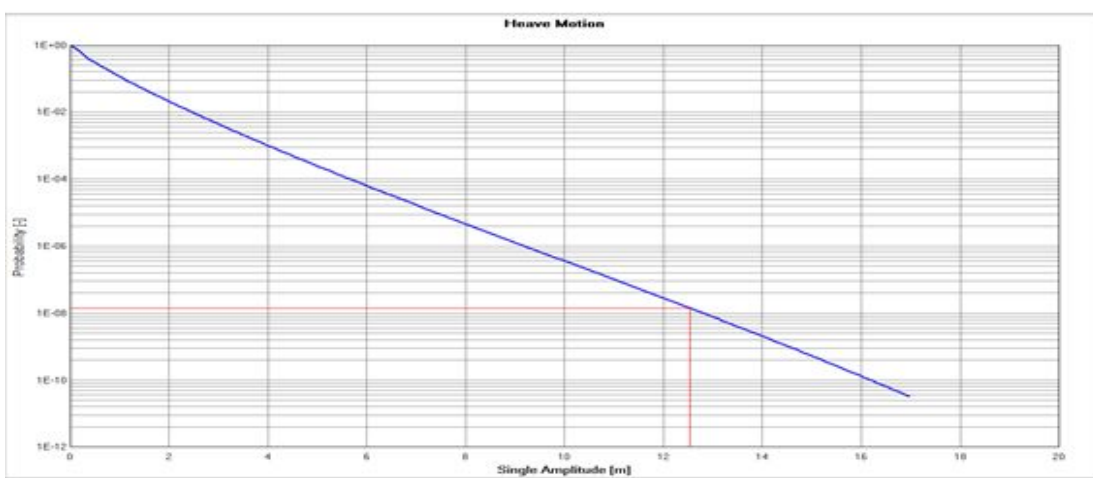
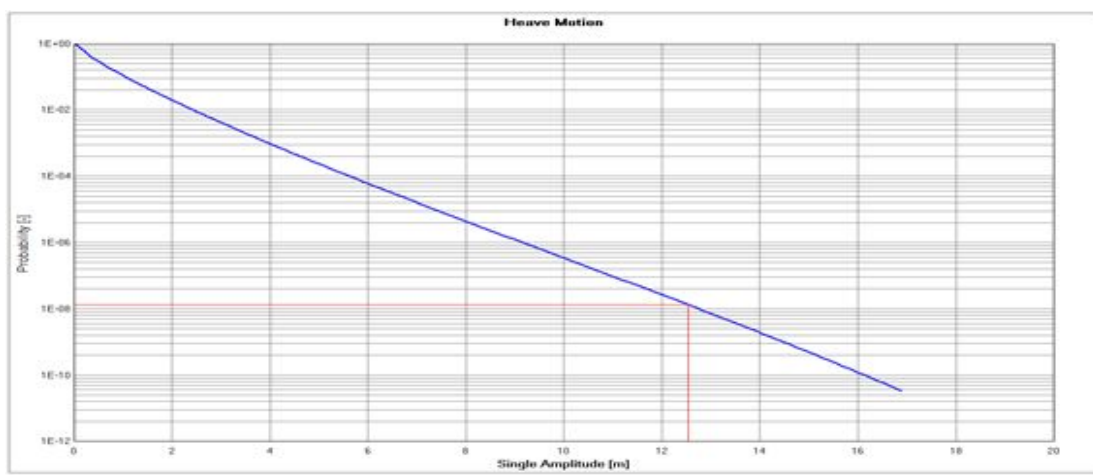
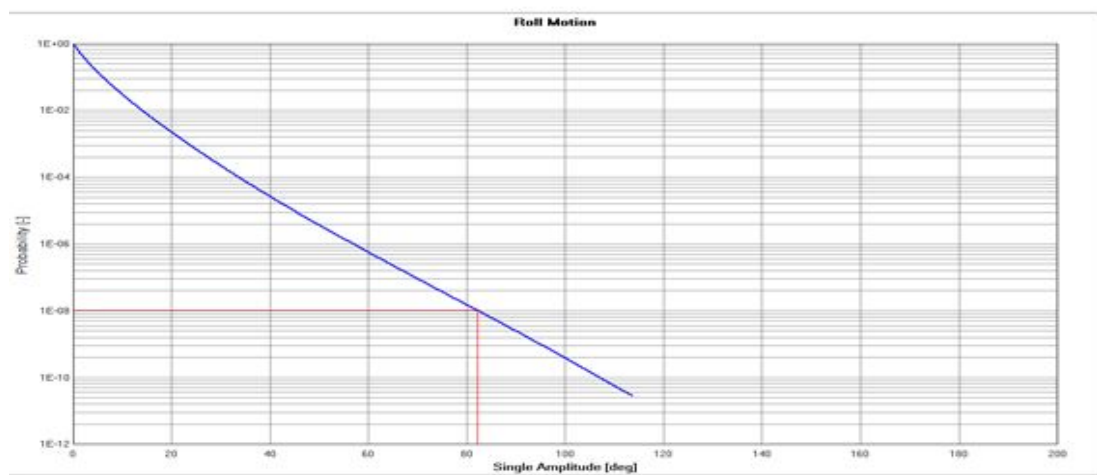
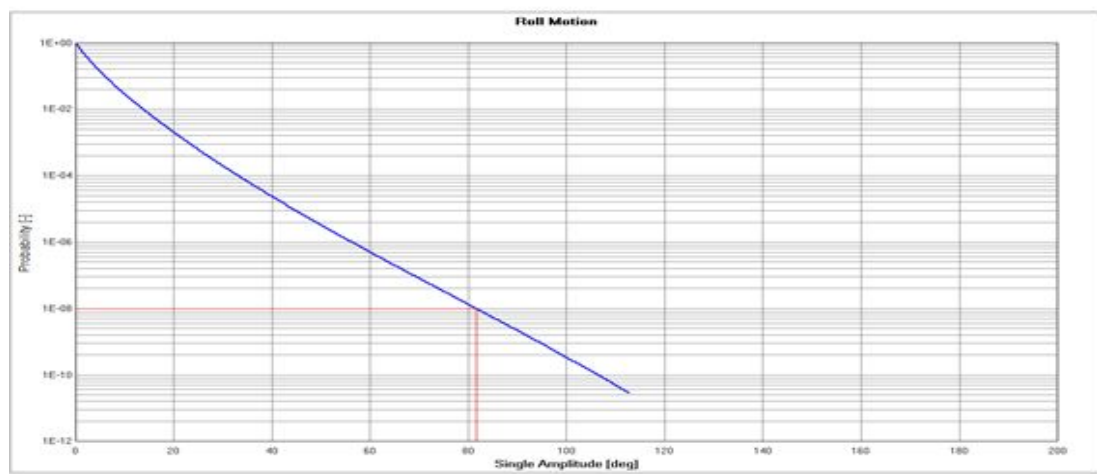
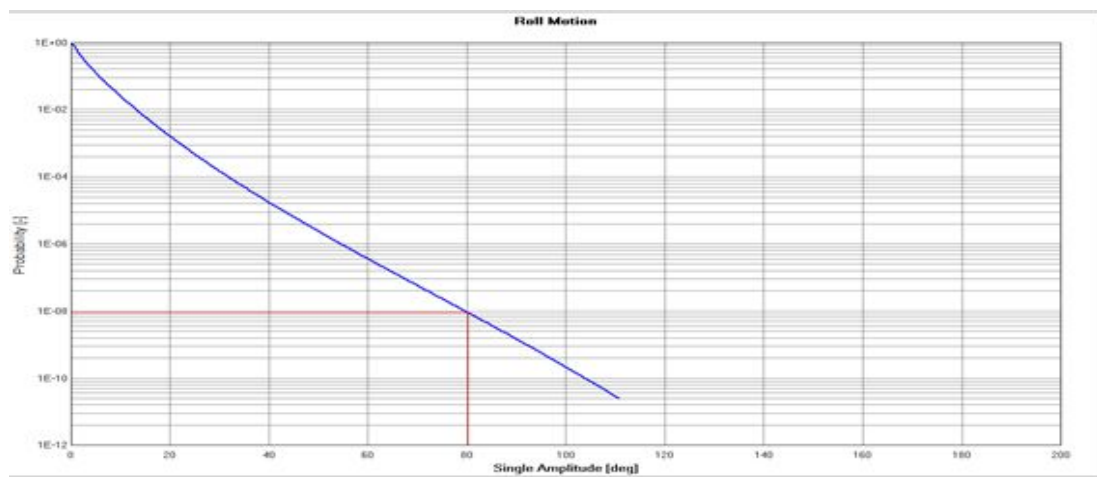


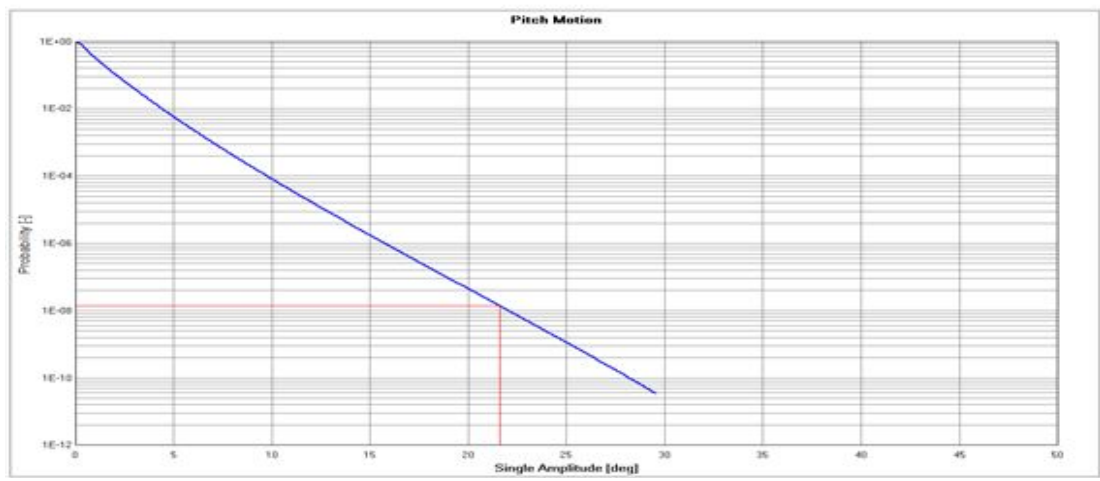
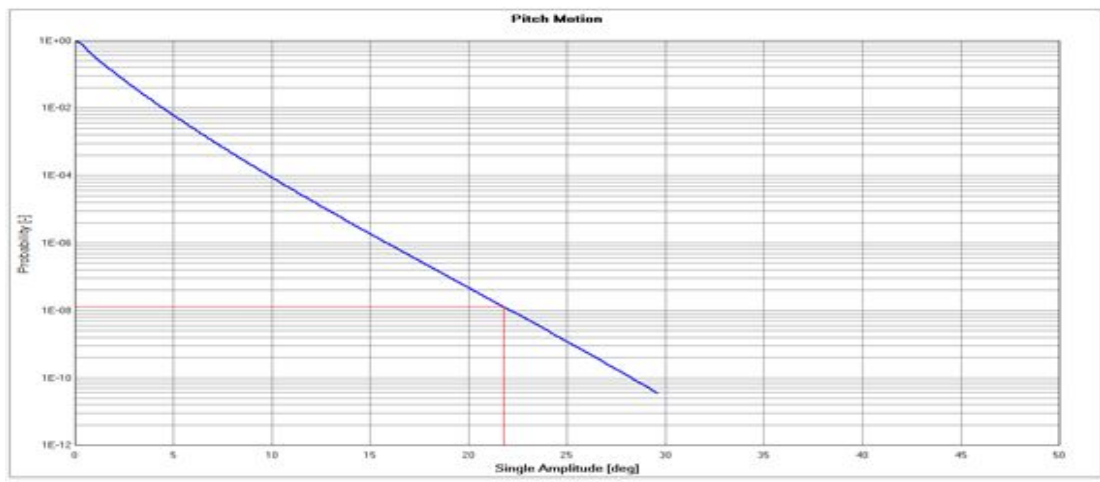
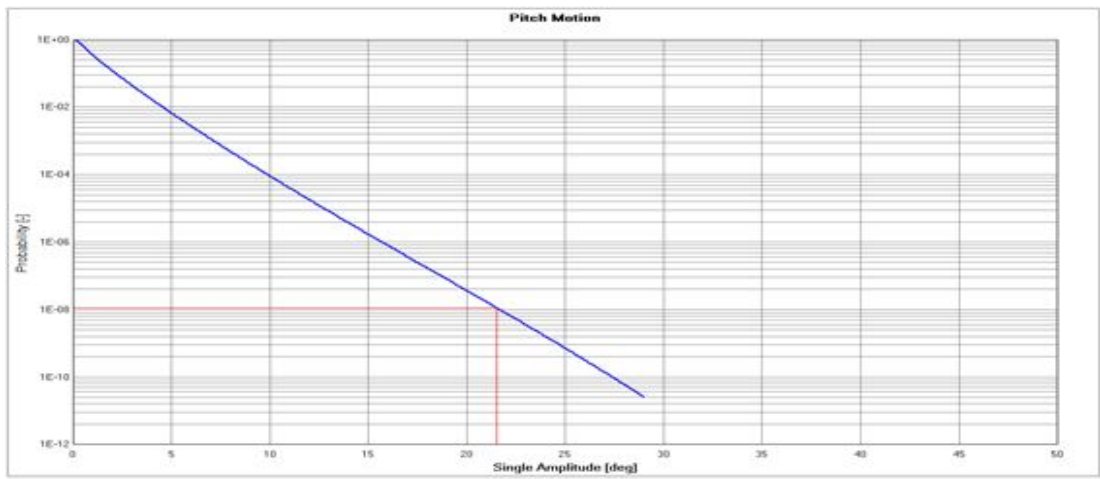
Fig. 6-4 Sea condition











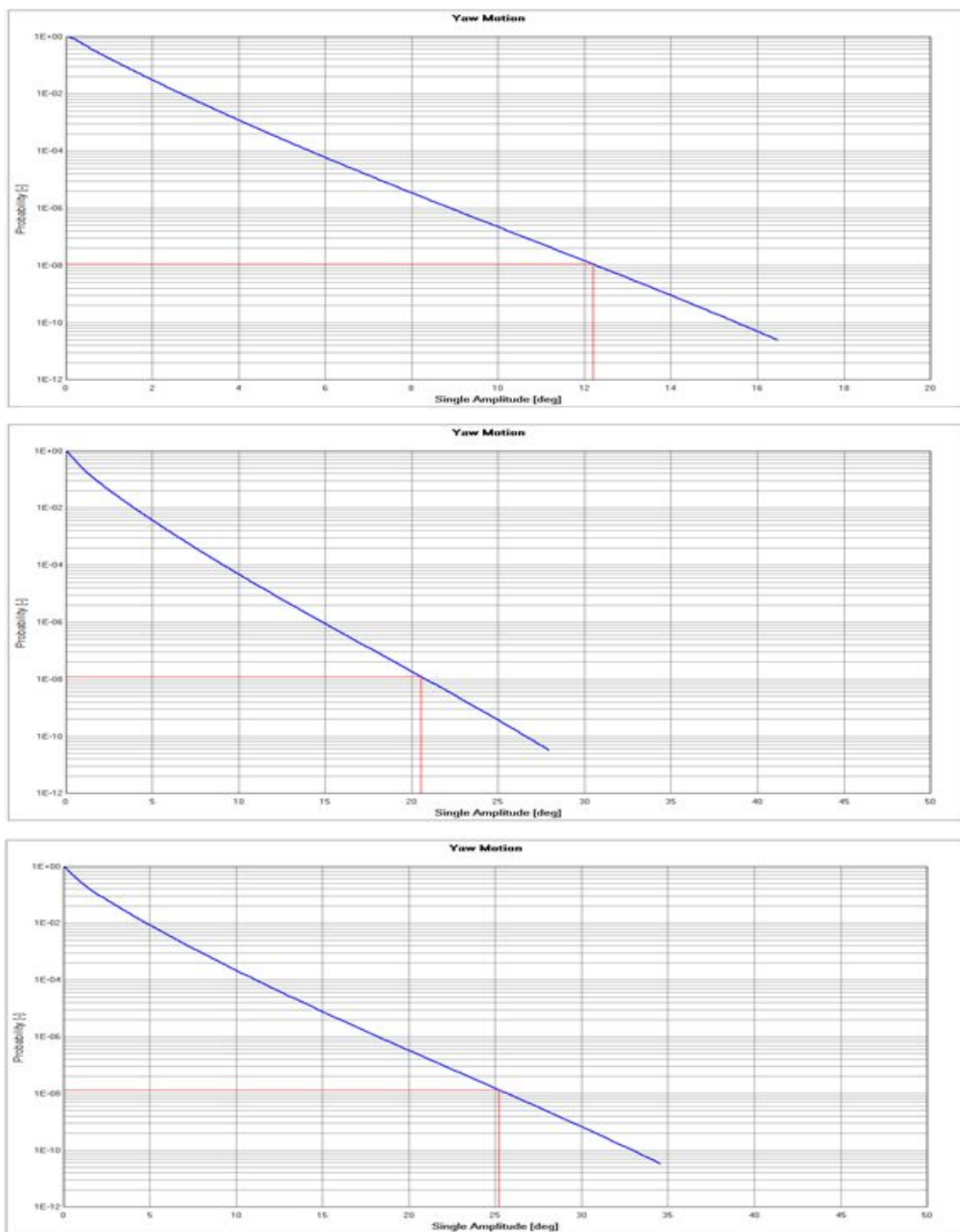


Fig. 6-5 Motion of ship

VII. Conclusions

The function of stern fin appended at the stern of ship is generally considered to equalize wake field at the propeller plane by both directing flow to propeller and reducing the wake peak at top position. When the propeller rotates in one direction, its performances of port and starboard sides are different and the center of pressure shifts to the side where the propeller blades downwards. This in turn leads to a non-symmetric pressure distribution on the hull in front of propeller, which influences the boundary layers of port and starboard differently.

The strut fin, which is designed to guide the flow for the equalization of wake field, showed 1.7% of DHP reduction at design speed.

References

1. L Broberg and M. Orych, 'An Efficient Numerical Technique to Simulate The Propeller Hull Interaction', FLOWTECH International AB, Sweden, 2012
2. MEPC, 'Interim Guidelines on the method of calculation of the EEDI for new ship', MEPC.1/Circ.681,2009.
3. Kwi-Joo Lee, Jung-Sun An and Sun-Hee Yang, 'A study on the Development of Energy-Saving Device "Crown Duct"', Dept. of Naval Architecture & Ocean Engineering, Chosun University, Gwangju, Korea and Basic Planning Department, SPP Shipbuilding Co., Ltd, Busan, Korea, 2012
4. JANSON, C.-E., 'Potential Flow Panel Method for the Calculation of Free-Surface Flows with Lift', Ph.D. Thesis, Chalmers University of Technology, 1997.
5. BROBERG. L., et. al., 'SHIPFLOW Users Manual', FLOWTECH International AB, Sweden, 2011
6. MENTER, F.R., 'Zonal Two Equation k- ω Turbulence Models for Aerodynamic Flows', 24th Fluid Dynamics Conference, Orlando, AIAA paper-93-2906, 1993
7. GATSKI, T., SPEZIALE, C.G., 'On Explicit Algebraic Stress Models for Complex Turbulent Flows', Journal of Fluid Mechanics, 254, 59-78, 1993
8. DENG, G.B., Queutey, P., Visonneau, M., 'Three Dimensional Flow Computation with Reynolds Stress and Algebraic Stress Models', Engineering Turbulence Modelling and Experiments 6, Rodi, W., Mulas, M., Editors, ELSEVIER, 389-398, 2005